

JPTM

Journal of Pathology
and Translational Medicine

May 2021
Vol. 55 / No.3
jpatholtm.org
pISSN: 2383-7837
eISSN: 2383-7845

*PD-L1 Assessment in
Urothelial Carcinoma*



Aims & Scope

The *Journal of Pathology and Translational Medicine* is an open venue for the rapid publication of major achievements in various fields of pathology, cytopathology, and biomedical and translational research. The Journal aims to share new insights into the molecular and cellular mechanisms of human diseases and to report major advances in both experimental and clinical medicine, with a particular emphasis on translational research. The investigations of human cells and tissues using high-dimensional biology techniques such as genomics and proteomics will be given a high priority. Articles on stem cell biology are also welcome. The categories of manuscript include original articles, review and perspective articles, case studies, brief case reports, and letters to the editor.

Subscription Information

To subscribe to this journal, please contact the Korean Society of Pathologists/the Korean Society for Cytopathology. Full text PDF files are also available at the official website (<https://jpatholm.org>). *Journal of Pathology and Translational Medicine* is indexed by Emerging Sources Citation Index (ESCI), PubMed, PubMed Central, Scopus, KoreaMed, KoMCI, WPRIM, Directory of Open Access Journals (DOAJ), and CrossRef. Circulation number per issue is 50.

Editors-in-Chief

Jung, Chan Kwon, MD (*The Catholic University of Korea, Korea*) <https://orcid.org/0000-0001-6843-3708>

Park, So Yeon, MD (*Seoul National University, Korea*) <https://orcid.org/0000-0002-0299-7268>

Associate Editors

Shin, Eunah, MD (*Yongin Severance Hospital, Yonsei University, Korea*) <https://orcid.org/0000-0001-5961-3563>

Kim, Haeryoung, MD (*Seoul National University, Korea*) <https://orcid.org/0000-0002-4205-9081>

Bychkov, Andrey, MD (*Kameda Medical Center, Japan; Nagasaki University Hospital, Japan*) <https://orcid.org/0000-0002-4203-5696>

Editorial Board

Avila-Casado, Maria del Carmen, MD (*University of Toronto, Toronto General Hospital UHN, Canada*)

Bae, Young Kyung, MD (*Yeungnam University, Korea*)

Bongiovanni, Massimo, MD (*Lausanne University Hospital, Switzerland*)

Bova, G. Steven, MD (*University of Tampere, Finland*)

Choi, Joon Hyuk, MD (*Yeungnam University, Korea*)

Chong, Yo Sep, MD (*The Catholic University of Korea, Korea*)

Chung, Jin-Haeng, MD (*Seoul National University, Korea*)

Fadda, Guido, MD (*Catholic University of Rome-Foundation Agostino Gemelli University Hospital, Italy*)

Fukushima, Noriyoshi, MD (*Fichi Medical University, Japan*)

Go, Heounjeong, MD (*University of Ulsan, Korea*)

Hong, Soon Won, MD (*Yonsei University, Korea*)

Jain, Deepali, MD (*All India Institute of Medical Sciences, India*)

Kakudo, Kennichi, MD (*Izumi City General Hospital, Japan*)

Kim, Jang-Hee, MD (*Ajou University, Korea*)

Kim, Jung Ho, MD (*Seoul National University, Korea*)

Kim, Se Hoon, MD (*Yonsei University, Korea*)

Komuta, Mina, MD (*Keio University, Tokyo, Japan*)

Kwon, Ji Eun, MD (*Ajou University, Korea*)

Lai, Chiung-Ru, MD (*Taipei Veterans General Hospital, Taiwan*)

Lee, C. Soon, MD (*University of Western Sydney, Australia*)

Lee, Hye Seung, MD (*Seoul National University, Korea*)

Lee, Sung Hak, MD (*The Catholic University, Korea*)

Liu, Zhiyan, MD (*Shanghai Jiao Tong University, China*)

Lkhagvadorj, Sayamaa, MD (*Mongolian National University of Medical Sciences, Mongolia*)

Moran, Cesar, MD (*MD Anderson Cancer Center, U.S.A.*)

Paik, Jin Ho, MD (*Seoul National University, Korea*)

Park, Jeong Hwan, MD (*Seoul National University, Korea*)

Ro, Jae Y., MD (*Cornell University, The Methodist Hospital, U.S.A.*)

Sakhuja, Puja, MD (*Govind Ballabh Pant Hospital, India*)

Shahid, Pervez, MD (*Aga Khan University, Pakistan*)

Song, Joon Seon, MD (*University of Ulsan, Korea*)

Tan, Puay Hoon, MD (*National University of Singapore, Singapore*)

Than, Nandor Gabor, MD (*Semmelweis University, Hungary*)

Tse, Gary M., MD (*The Chinese University of Hong Kong, Hong Kong*)

Yatabe, Yasushi, MD (*Aichi Cancer Center, Japan*)

Zhu, Yun, MD (*Jiangsu Institution of Nuclear Medicine, China*)

Ethic Editor

Choi, In-Hong, MD (*Yonsei University, Korea*)

Huh, Sun, MD (*Hallym University, Korea*)

Statistics Editors

Kim, Dong Wook (*National Health Insurance Service Ilsan Hospital, Korea*)

Lee, Hye Sun (*Yonsei University, Korea*)

Manuscript Editor

Chang, Soo-Hee (*InfoLumi Co., Korea*)

Layout Editor

Kim, Haeja (*iMiS Company Co., Ltd., Korea*)

Website and JATS XML File Producers

Cho, Yoosang (*M2Community Co., Korea*)

Im, Jeonghee (*M2Community Co., Korea*)

Administrative Assistants

Jung, Ji Young (*The Korean Society of Pathologists*)

Jeon, Annmi (*The Korean Society for Cytopathology*)

Contact the Korean Society of Pathologists/the Korean Society for Cytopathology

Publishers: Cho, Nam Hoon, MD, Gong, Gyungyub, MD

Editors-in-Chief: Jung, Chan Kwon, MD, Park, So Yeon, MD

Published by the Korean Society of Pathologists/the Korean Society for Cytopathology

Editorial Office

Room 1209 Gwanghwamun Officia, 92 Saemunan-ro, Jongno-gu, Seoul 03186, Korea

Tel: +82-2-795-3094 Fax: +82-2-790-6635 E-mail: office@jpatholm.org

#1508 Renaissancetower, 14 Mallijae-ro, Mapo-gu, Seoul 04195, Korea

Tel: +82-2-593-6943 Fax: +82-2-593-6944 E-mail: office@jpatholm.org

Printed by iMiS Company Co., Ltd. (JMC)

Jungang Bldg. 18-8 Wonhyo-ro 89-gil, Yongsan-gu, Seoul 04314, Korea

Tel: +82-2-717-5511 Fax: +82-2-717-5515 E-mail: ml@smileml.com

Manuscript Editing by InfoLumi Co.

210-202, 421 Pangyo-ro, Bundang-gu, Seongnam 13522, Korea

Tel: +82-70-8839-8800 E-mail: infolumi.chang@gmail.com

Front cover image: Differences in scoring algorithm and heterogeneous results of various PD-L1 arrays in urothelial carcinoma (p165, 168).

© Copyright 2021 by the Korean Society of Pathologists/the Korean Society for Cytopathology

© Journal of Pathology and Translational Medicine is an Open Access journal under the terms of the Creative Commons Attribution Non-Commercial License (<https://creativecommons.org/licenses/by-nc/4.0>).

© This paper meets the requirements of KS X ISO 9706, ISO 9706-1994 and ANSI/NISO Z.39.48-1992 (Permanence of Paper).

CONTENTS

REVIEWS

- 163 Programmed cell death-ligand 1 assessment in urothelial carcinoma: prospect and limitation
Kyu Sang Lee, Gheeyoung Choe
- 171 Hepatocellular adenomas: recent updates
Haeryoung Kim, Young Nyun Park
- 181 Molecular biomarker testing for non-small cell lung cancer: consensus statement of the Korean Cardiopulmonary Pathology Study Group
Sunhee Chang, Hyo Sup Shim, Tae Jung Kim, Yoon-La Choi, Wan Seop Kim, Dong Hoon Shin, Lucia Kim, Heae Surng Park, Geon Kook Lee, Chang Hun Lee, Korean Cardiopulmonary Pathology Study Group

ORIGINAL ARTICLES

- 192 Identification of PI3K-AKT signaling as the dominant altered pathway in intestinal type ampullary cancers through whole-exome sequencing
Niraj Kumari, Rajneesh K. Singh, Shravan K. Mishra, Narendra Krishnani, Samir Mohindra, Raghvendra L.
- 202 Mismatch repair deficiency and clinicopathological characteristics in endometrial carcinoma: a systematic review and meta-analysis
Alaa Salah Jumaah, Hawraa Sahib Al-Haddad, Mais Muhammed Salem, Katherine Ann McAllister, Akeel Abed Yasseen
- 212 Prognostic role of ALK-1 and h-TERT expression in glioblastoma multiforme: correlation with ALK gene alterations
Dalia ElSers, Doaa F. Temerik, Alia M. Attia, A. Hadia, Marwa T. Hussien

CASE REPORTS

- 225 Spindle cell oncocytoma of the sella turcica with anaplastic features and rapid progression in short-term follow-up: a case report with proposal of distinctive radiologic features
Dong Ja Kim, SangHan Lee, Mee-seon Kim, Jeong-Hyun Hwang, Myong Hun Hahm

-
- 230 Hepatoid thymic carcinoma: a case report of a rare subtype of thymic carcinoma
Ji-Seon Jeong, Hyo Jeong Kang, Uiree Jo, Min Jeong Song, Soon Yeol Nam, Joon Seon Song

EDITORIALS

- 235 Histologic subtyping of ampullary carcinoma for targeted therapy
Seung-Mo Hong
- 236 Prognostic and predictive markers in glioblastoma and ALK overexpression
Jang-Hee Kim

Instructions for Authors for *Journal of Pathology and Translational Medicine* are available at <http://jpatholm.org/authors/authors.php>

Programmed cell death-ligand 1 assessment in urothelial carcinoma: prospect and limitation

Kyu Sang Lee^{1,2}, Gheeyoung Choe^{1,2}

¹Department of Pathology, Seoul National University Bundang Hospital, Seongnam;

²Department of Pathology, Seoul National University College of Medicine, Seoul, Korea

Programmed cell death protein 1/programmed death-ligand 1 (PD-1/PD-L1) inhibition has revolutionized the treatment paradigm of urothelial carcinoma (UC). Several PD-L1 assays are conducted to formulate appropriate treatment decisions for PD-1/PD-L1 target therapy in UC. However, each assay has its own specific requirement of antibody clones, staining platforms, scoring algorithms, and cutoffs for the determination of PD-L1 status. These prove to be challenging constraints to pathology laboratories and pathologists. Thus, the present article comprehensively demonstrates the scoring algorithm used and differences observed in each assay (22C3, SP142, and SP263). Interestingly, the SP142 score algorithm considers only immune cells and not tumor cells (TCs). It remains controversial whether SP142 expressed only in TCs truly accounts for a negative PD-L1 case. Moreover, the scoring algorithm of each assay is complex and divergent, which can result in inter-observer heterogeneity. In this regard, the development of artificial intelligence for providing assistance to pathologists in obtaining more accurate and objective results has been actively researched. To facilitate efficiency of PD-L1 testing, several previous studies attempted to integrate and harmonize each assay in UC. The performance comparison of the various PD-L1 assays demonstrated in previous studies was encouraging, the exceptional concordance rate reported between 22C3 and SP263. Although these two assays may be used interchangeably, a clinically validated algorithm for each agent must be applied.

Key Words: Urothelial carcinoma; Programmed cell death-ligand 1; 22C3; SP142; SP263; Immunotherapy

Received: January 26, 2021 **Accepted:** February 22, 2021

Corresponding Author: Gheeyoung Choe, MD, PhD, Department of Pathology, Seoul National University Bundang Hospital, 82 Gumi-ro 173beon-gil, Bundang-gu, Seongnam 13620, Korea

Tel: +82-31-787-7711, Fax: +82-31-787-4012, E-mail: gychoe@snu.ac.kr

The U.S. Food and Drug Administration (FDA) has approved the use of programmed cell death protein 1/programmed death-ligand 1 (PD-1/PD-L1) inhibitors (pembrolizumab, nivolumab, atezolizumab, and durvalumab) in the treatment of various cancers. PD-1/PD-L1 target therapies are no longer limited to tumor subtypes or origins. The interesting emerging concept of 'PD-Loma' refers to tumors that respond to PD-1/PD-L1 target therapy [1]. Urothelial carcinoma (UC) is one of the most significant PD-Lomas. Particularly, pembrolizumab and atezolizumab are indicated as first-line treatments in patients with locally advanced or metastatic UC who are not eligible for cisplatin-containing chemotherapy and whose tumors are PD-L1 immunohistochemistry (IHC)-positive. PD-L1 IHC is a pivotal diagnostic technique used for determining the necessity of PD-1/PD-L1 target therapy. All agents are FDA-approved, used in conjunction with one of the PD-L1 assays available (22C3, 28-8, SP263,

and SP142)—each of which involves different antibody clones, autostainers, scoring algorithms, and cutoffs [2,3]. This complexity implicated in the usage of PD-L1 assays has raised questions on their comparability and interchangeability. Although previous studies have attempted to integrate and harmonize the PD-L1 assays in non-small cell lung cancer (NSCLC), discordant PD-L1 expression was observed across the results of various assays [4-6]. Similarly, in UC, although a good correlation between each assay was observed, none exhibited a perfect agreement [3,7-9].

Diagnostic assays can be essential for the use of therapeutics (companion diagnostics) or may inform on improving the benefit without restricting drug access (complementary diagnostics) [10]. Notably, 22C3 and SP142 were companion diagnostics in the first-line use of pembrolizumab and atezolizumab, respectively [11,12]. However, 28-8 and SP263 have not been used as com-

panion diagnostics for nivolumab and durvalumab in advanced UC patients [13,14]. Thus, the interpretation of 22C3 and SP142 may be crucial in practice and should be carefully assessed by pathologists. PD-L1 expression in immune cells (ICs) is comparatively as significant as that in tumor cells (TCs) in UC. The correlation between IC PD-L1 expression and treatment response has been demonstrated in all clinical studies conducted on UC, except in the case of nivolumab/28-8 [14].

In this review, we have discussed the scoring algorithm and differences in each PD-L1 assay in detail (Table 1) and assessed the current issues posed by PD-L1 testing in UC. Since the 28-8 assay is rarely used in most countries, including South Korea, 22C3, SP142, and SP263 in UC were evaluated.

COMPARISON OF PD-L1 ASSAY INTERPRETATION IN UROTHELIAL CARCINOMA

Agilent 22C3

According to the 22C3 (pharmDx) interpretation manual, PD-L1 expression was determined by using the combined positive score (CPS) in UC, which is the number of PD-L1–stained cells (TC + IC) divided by the total number of viable TCs, and multiplied by 100 (Table 1, Fig. 1) [15]. The result of the calculation can exceed 100; however, the maximum score is defined as CPS 100. The CPS is defined accordingly:

$$\text{CPS} = \frac{\text{Number of PD-L1 staining cells (TCs + ICs)}}{\text{Total number of viable TCs}} \times 100$$

ICs include lymphocytes and macrophages, but do not include plasma cells, neutrophils, and eosinophils. TCs with partial or complete linear membrane staining (at any intensity) were considered ‘TC-positive.’ ICs within the tumor nests and/or the immediately adjacent supporting stroma with convincing membrane

and/or cytoplasmic staining (at any intensity) were considered ‘IC-positive.’ PD-L1 expression and CPS are suggested to be evaluated at higher magnification (20×). Infiltrating UC, high-grade papillary UC, carcinoma in situ, and metastatic UC are included under CPS, whereas low-grade papillary UC and tumor necrotic area should be excluded. Finally, 22C3 is defined as positive if CPS ≥ 10 in UC.

Ventana SP142

SP142 is scored as the proportion of tumor area that is occupied by PD-L1–expressing ICs at any intensity (Table 1, Fig. 1). Unlike 22C3, SP142 measures the area occupied instead of the number of stained cells. ICs include lymphocytes, macrophages, dendritic cells, and granulocytes, wherein stained ICs can be found as aggregates in intratumoral or contiguous peritumoral stroma, or as single cell spread among TCs. Tumor area for PD-L1 scoring is defined as the area occupied by viable TCs and their associated intratumoral and contiguous peritumoral stroma. In papillary UC, the stroma in fibrovascular cores is considered intratumoral stroma. Tumor necrosis should be excluded for scoring. SP142 staining at any intensity of tumor-infiltrating ICs covering ≥ 5% of the tumor area is considered positive.

Ventana SP263

According to the manufacturer’s manual, SP263 status is determined by the percentage of TCs with any membrane staining, or by the percentage of tumor-associated ICs with staining at any intensity (Table 1, Fig. 1). Similar to SP142, SP263 expresses the area proportionate to the tumor area measured. The percentage of tumor area occupied by any tumor-associated ICs (Immune Cells Present, ICP) is used to determine IC expression, which is defined as the percentage area of ICP exhibiting PD-L1–positive IC staining. SP263 status is considered positive if any of the following criteria are met:

- ≥ 25% of the TCs exhibit membrane staining; or,

Table 1. Comparison of PD-L1 assays for UC and difference in scoring algorithm

	22C3	SP142	SP263
Manufacturer	Agilent	Ventana	Ventana
Drug	Pembrolizumab	Atezolizumab	Durvalumab
Status	Companion diagnostic	Companion diagnostic	Complementary diagnostic
Scoring algorithm	CPS = #TC+ and #IC+/Total #TC × 100 ≥ 10	IC+/tumor area ≥ 5%	TC+/tumor area or ≥ 25% ICP > 1%: IC+/ICP ≥ 25% or ICP = 1%: IC+/ICP = 100%
Algorithm based on	Positive cell number	Positive cell area	Positive cell area
Cell type	Tumor cells, lymphocytes, and macrophages	Lymphocytes, macrophages, dendritic cells and granulocytes	Tumor cells, lymphocytes, macrophages, histiocytes, plasma cells, and neutrophils

PD-L1, programmed cell death-ligand 1; UC, urothelial carcinoma; CPS, combined positive score; TC, tumor cell; IC, immune cell; ICP, immune cells present.

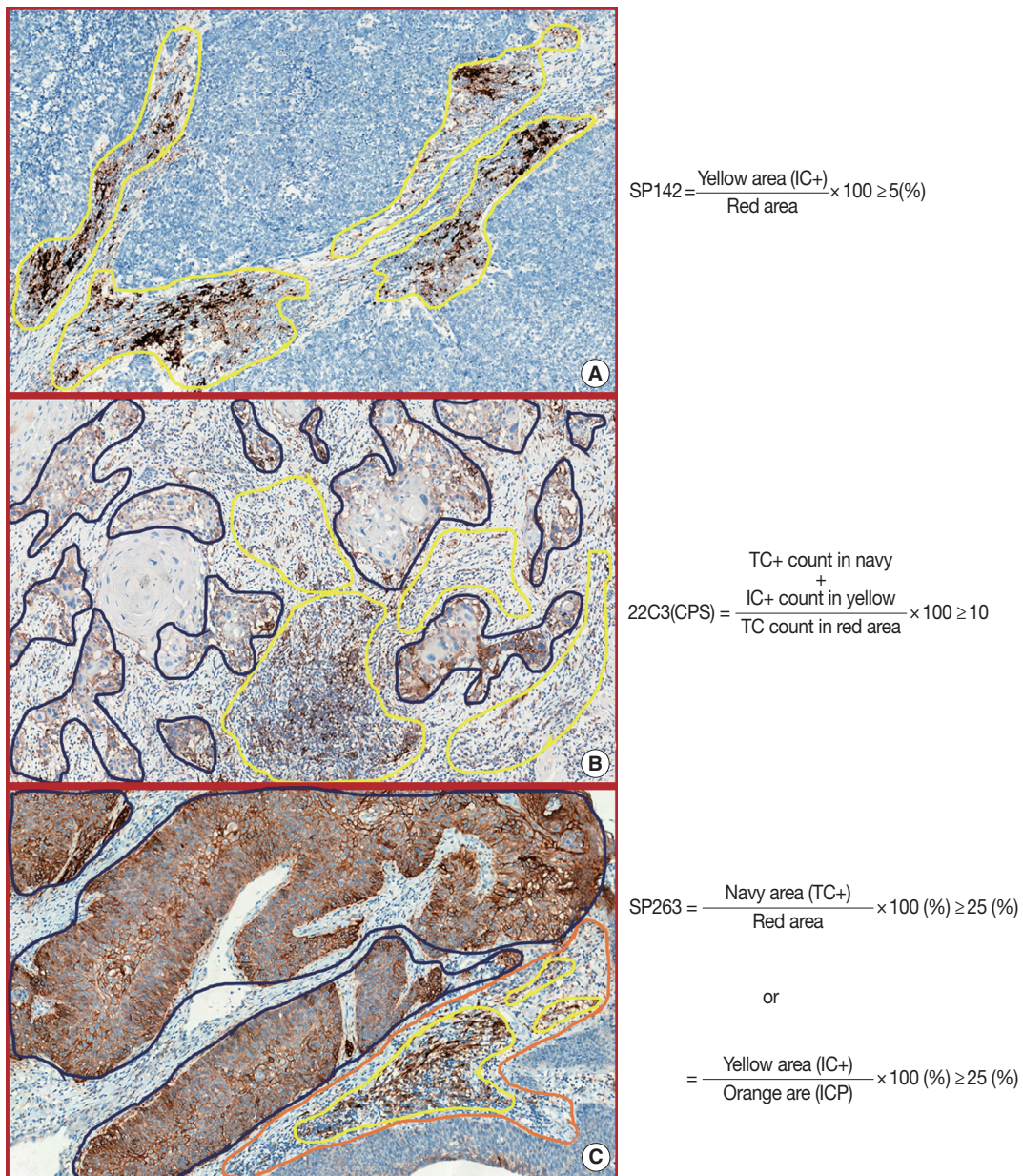


Fig. 1. Representative pictures for the comparison of programmed death-ligand 1 (PD-L1) assays and differences in scoring algorithm of urothelial carcinoma (UC). (A) Scoring algorithm of SP142 is based on the proportion of tumor area that is occupied by PD-L1-expressed immune cells (ICs) at any intensity. (B) Scoring algorithm of 22C3 is determined by using the combined positive score (CPS) in UC, which is the number of PD-L1–stained cells (tumor cell [TC] plus IC) divided by the total number of viable TCs, multiplied by 100. (C) SP263 status is determined by the percentage of TCs obtained by performing any membrane staining or by the percentage of tumor-associated ICs obtained by staining at any intensity. SP263-expressed TC area proportion of the tumor area is determined. Also, the percentage of tumor area occupied by any tumor-associated IC (Immune Cells Present, ICP) is used to determine IC expression, and IC positivity is defined as the percentage of PD-L1–positive IC area in ICP.

- ICP > 1% and IC+ ≥ 25%; or,
- ICP = 1% and IC+ = 100%.

The manufacturer’s manual suggests that an expression level greater than or equal to 25% of the TCs or ICs should be considered significant. Membrane staining of TCs can exhibit a partial

or complete circumferential pattern. TC cytoplasmic staining is disregarded when determining PD-L1 expression. The percentage of tumor-associated IC with staining is evaluated in addition to TC staining. Interestingly, IC scoring includes lymphocytes, macrophages, histiocytes, plasma cells, and neutrophils. IC staining is

assessed by initially reviewing the entire tumor area and by determining the ICP. Subsequently, the percentage of PD-L1 expressing ICs within the ICP is visually estimated (IC+). Additionally, in cases where the percentage of ICP in the tumor area is 1%, it is considered positive only when 100% of the ICs are stained.

INTERCHANGEABILITY OF PD-L1 ASSAYS IN UROTHELIAL CARCINOMA

The use of different expensive autostainers and various assays is neither economical nor reasonable for pathology laboratories. Interchangeability of different assays may enable the usage of only one standardized PD-L1 assay in laboratories. In NSCLC, Adam et al. [16] showed that 28-8, 22C3, and SP263 assays demonstrated close analytical performance for TC staining across seven centers. However, a significant discrepancy was observed between SP142 and the other three assays for TC staining, whereas IC staining results were similar [17-19]. Moreover, the SP142 assay was an outlier that detected markedly less PD-L1 expression in both TCs and ICs [5].

Rijnders et al. [3] have suggested that agreement in the PD-L1 status in UC between 22C3, 28-8, SP142, and SP263 is substantial (80%–90%), implying that these assays may be interchangeable in clinical practice. Moreover, a collaborative study conducted by the Russian Society of Clinical Oncology and the Russian Society of Pathology found that a patient with UC classified as negative by one of the three tests (22C3, SP142, and SP263) using the corresponding cutoff rule was highly likely (91%–100%) to be classified as negative based on the results of any other test performed, therefore avoiding the need for repeated testing [8]. Furthermore, Zajac et al. [9] reported a high level of analytical concordance among the SP263, 22C3, and 28-8 assays for TC and IC staining; however, such a level of concordance was not observed for SP142. Additionally, Hodgson et al. [7] demonstrated that SP142 TC staining intensity was lower in UC and hypopharyngeal squamous cell carcinoma samples, although there existed adequate analytic comparability between 22C3 and SP263. Another recent study has highlighted greater differences in the assays used for the analysis of PD-L1–stained TCs, particularly between SP142 and other assays [20]. These analytical findings were consistent with other studies conducted using NSCLC samples, which suggested that SP142 did not exhibit sufficient concordance with the other three assays. While 22C3 and SP263 have a high concordance rate and can be used interchangeably, clinical validation for each immune-therapy remains a necessity [9]. The interchangeability of PD-L1 assay must be considered

carefully so as to ensure that no patient is devoid of treatment opportunity.

INTER-OBSERVER HETEROGENEITY

Inter-observer variability may lead to the obtainment of discordant results for PD-L1, which can consequentially impact therapy decisions. A recent study demonstrated that inter-observer agreement for each assay is moderate to high for IC staining (0.532–0.729) as well as TC staining (0.609–0.883) based on intra-class correlation coefficient obtained for UC [20]. However, 22C3 and 28-8 exhibited low inter-observer correlation in IC staining, while SP142 showed low inter-observer correlation in TC staining [20]. Downes et al. [21] suggested that excellent inter-observer agreement could be found using SP263 and 22C3, whereas PD-L1 scoring using SP142 was associated with a higher level of subjectivity in head and neck squamous cell carcinoma, breast carcinoma, and UC. The study of inter-observer heterogeneity of PD-L1 assays has also been well conducted using NSCLC samples. According to Cooper et al. [22], 10 pathologists reported good reproducibility at both 1% cutoffs of 22C3, whereas agreement was slightly lower for the 50% cutoff. Moreover, the Cardiopulmonary Pathology Study Group of the Korean Society of Pathologists investigated the inter-observer heterogeneity of PD-L1 staining with 22C3 using NSCLC samples [23]. Inter-observer reproducibility for the 1% cutoff was found to be relatively lower than the 50% cutoff, in contrast to the results reported by Cooper et al. [22]. Similarly, Rimm et al. [5] indicated that 13 pathologists reported excellent concordance when scoring TCs stained with any antibody (22C3, 28-8, SP142, and E1L3N) but reported poor concordance when scoring ICs stained with any antibody using NSCLC samples [16]. Although differing results were reported in previous studies of both UC and NSCLC, inter-observer heterogeneity of PD-L1 seems to occur.

CORRELATION BETWEEN PD-L1 EXPRESSION AND HISTOLOGIC SUBTYPES

UC is among the most histologically diverse cancers. A previous study found that infiltrating UC exhibits significantly higher T cell infiltration and PD-L1 expression than non-invasive papillary UC and UC in situ [24]. In addition to the conventional morphology observed, UC can contain elements of squamous differentiation, glandular differentiation, nested, plasmacytoid, sarcomatoid, and/or rarer variants. UC patients with histologic variants account for up to one-third of advanced cases. Li et al.

[24] found that PD-L1 was expressed in a significant percentage of histologic variant of UC cases (cutoff 1% TC, 37% to 54%; cutoff 5% TC, 23% to 37%), while the highest PD-L1 expression was observed in patients with UC exhibiting squamous differentiation [25]. These results suggest that patients with histologic variants of UC may benefit more from anti-PD-1/PD-L1 therapy.

DISCUSSION

PD-1/PD-L1 target therapy has garnered considerable attention as a potential treatment strategy for patients with advanced UC. These agents are approved by the U.S. Food and Drug Administration for the treatment of patients with locally advanced or metastatic UC, with disease progression during or following platinum-containing chemotherapy, or disease progression within 12 months of neoadjuvant or adjuvant treatment with platinum-containing chemotherapy. Moreover, pembrolizumab and atezolizumab have received approval for first-line treatment of locally advanced or metastatic UC in patients ineligible for cisplatin-containing chemotherapy. PD-L1 expression levels in UC can thus effectively aid physicians in identifying patients who are more likely to benefit from anti-PD-1/PD-L1 therapy.

However, every single agent is tested in conjunction with a specific PD-L1 assay, which must be performed on a specific staining platform. Moreover, the PD-L1 scoring algorithm is heterogeneous and unique for each assay. These aspects have encouraged pathologists to consider assay interchangeability. Several studies have attempted to harmonize PD-L1 assays conducted for NSCLC and UC samples. However, SP142 was an outlier that detected markedly less PD-L1 expression in TC (Fig. 2A–C) [5-7,9,18,20]. In contrast, relatively high concordance was observed between SP263 and 22C3. As each assay is performed using different immunogens, and thus a unique epitope, different PD-L1 conformations or isoforms may lead to the obtainment of heterogeneous results. Moreover, the location of the antibody-binding domain has been known to affect the staining pattern, resulting in increased variability [26]. This discordance in the results suggests that the prospects for interchangeability of the assays is not optimistic. Although the discordance rate between SP263 and 22C3 is low, there is no scientific evidence to prove that two assays can be used interchangeably. It is of utmost priority that all patients should receive proper treatment, without any exceptions arising due to assay discordance.

The scoring algorithm for each PD-L1 assay in UC is described in Table 1 and Fig. 1. There are several common practical diffi-

culties in analyses performed using PD-L1 assays. First, it is difficult to distinguish between TC and IC positivity. Representatively, distinguishing between TCs and macrophages proves burdensome when PD-L1 is stained, because macrophages are of comparative size to the TCs (Fig. 2H). Reviewing the hematoxylin and eosin-stained slides can be helpful in this respect. 22C3 should be used to count both ICs and TCs, which may not be problematic; however, SP142 should be excluded PD-L1-positive TCs. Moreover, ICs commonly include lymphocytes and macrophages. However, the ICs of SP263 additionally include plasma cells and neutrophils. Although this can also prove to be beneficial if we compare the hematoxylin and eosin-stained slides with PD-L1-stained slides, it remains uncertain whether PD-L1-positive neutrophils, plasma cells, and lymphocytes can be distinguished effectively (Fig. 2I). Lastly, the lamina propria at the base of the papillary lesion may contain lymphoid aggregates that show PD-L1 positivity, whereas only the lamina propria contiguous to the base of the tumor is considered part of the tumor area. Moreover, in fragmented tissue samples, including transurethral resection or biopsies—where distinction of intra- or peritumoral stroma cannot be ascertained—only stroma that is contiguous to individual tumor nests is included in the tumor area definition (Fig. 2G). However, the meaning of ‘contiguous’ is ambiguous and subjective.

The 22C3 scoring system uses the CPS algorithm. Theoretically, regardless of whether the number of TCs is large or small, 22C3 should be used to count all TCs present in the tumor area for the denominator. Additionally, all PD-L1-positive TCs and ICs should be counted in the tumor area for obtaining values for the numerator. This scoring algorithm is labor-intensive and an accurate calculation is practically impossible for the whole tumor area. Thus, the 22C3 manufacturer (Agilent) suggests that a partial portion of the tumor can be selected and scored. However, these results may be inconsistent due to intratumoral heterogeneity of 22C3 expression.

A comparatively higher positive cutoff ($\geq 25\%$ of TC) is required for SP263. If the test results do not meet the TC cutoff, the IC cutoff ($\geq 25\%$ of IC) can be evaluated subsequently. Unlike SP142, the total tumor area is not evaluated for IC scoring. IC positivity is only evaluated in the ICP. Therefore, SP263 results may easily meet the cutoff ($\geq 25\%$ of IC) because ICP is relatively smaller than the total tumor area values used as a denominator. However, the evaluation of complex geographic ICP may pose challenges. For accurate evaluation, one must physically draw and cut out the ICP—which lies beyond the confines of plausibility. Hence, advances in artificial intelligence and digital pathology are nec-

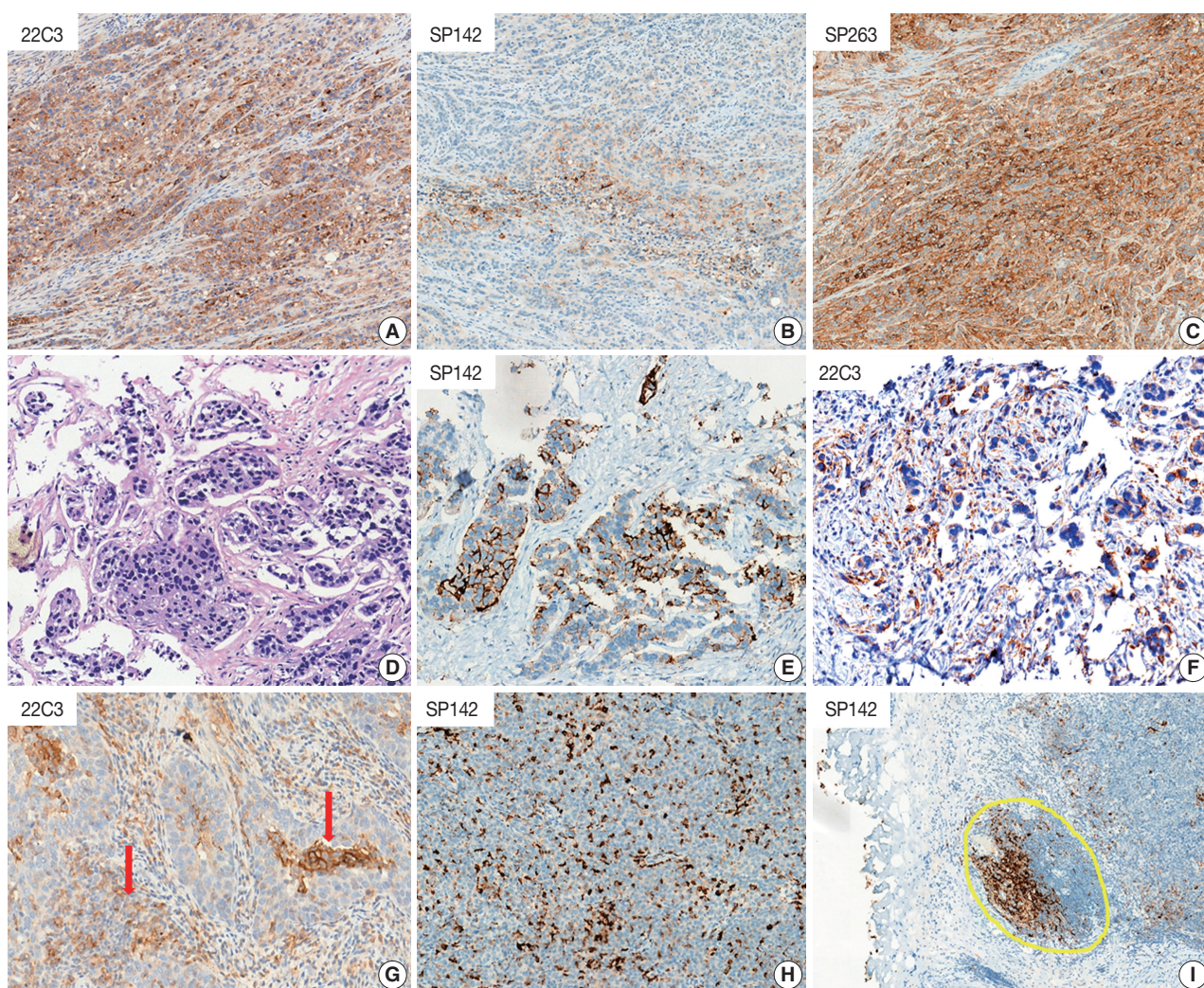


Fig. 2. (A–C) Representative pictures of heterogeneity observed in programmed death-ligand 1 (PD-L1) assay results (22C3, SP142, and SP263). SP142 was an outlier that detected markedly less PD-L1 expression in tumor cells (TCs). (D–F) Biopsy sample of metastatic urothelial carcinoma with PD-L1 expression observed only in TCs. Although SP142 was expressed in TCs, the result obtained was negative. However, the result for 22C3 was positive. This patient may be administered with pembrolizumab, but not with atezolizumab, as first-line therapy. (G) It is difficult to distinguish between the various subtypes of immune cells. If the regions indicated by the red arrows are plasma cells, they should be excluded from the 22C3 score. (H) Investigation may be necessary to ascertain whether the SP142-stained cells are TCs or ICs. This picture shows SP142 expression on intra-tumoral macrophages. (I) In fragmented tissue samples, including transurethral resection or biopsy samples, where the distinction between intratumoral or peritumoral stroma cannot be clearly observed. The yellow area contiguous to the base of the tumor is considered part of the tumor area.

essary for the precise assessment of SP263 expression. At present, SP263 is not clinically used as a companion diagnostic for durvalumab in UC.

SP142 evaluation for the determination of the IC-positive area and score seems relatively simpler than performing other assays. However, exclusion of SP142 TC positivity information from scoring may not be an appropriate approach. We analyzed three UC biopsy cases (unpublished data), which showed only strong PD-L1 positivity in TCs and not in ICs, with negative SP142 results (Fig. 2D–F). Although all the UC cases studied

herein were SP142-negative, these patients demonstrated a complete response to atezolizumab. Whilst these results were obtained for only a limited number of cases, it should nonetheless be considered whether the exclusion of positive TCs from the scoring algorithm is a reasonable methodology. The ability of SP142 to detect TC expression is low, which may lead to the generation of statistical bias in clinical trials of atezolizumab in UC. This is probably main reason that TC were not included in the scoring algorithm of the SP142. Re-evaluation of SP142 TC expression may thus be necessary in a novel clinical study to assess anti-PD-1/

PD-L1 therapy in UC. Furthermore, in cases where SP142 expression is observed only in TCs, it is recommended to adopt the 22C3 test to determine the applicability of pembrolizumab as first-line treatment.

These complex score algorithms and intratumoral heterogeneity of PD-L1 expression can result in inter-observer heterogeneity, particularly in scoring the SP142 of UC [20,21]. It is not difficult to score definite PD-L1 positive or negative cases; however, inter-observer heterogeneity must be observed in cases with approximate cutoff scores (e.g., 22C3 CPS, 5%–15%; SP142, 3%–10%, and so on). Providing training to the pathologist in these aspects as well as in the use of artificial intelligence may be a possible method for reduction of the inter-observer PD-L1 discordance.

Several studies have suggested the prognostic significance of PD-L1 expression in various malignancies; PD-L1-expressing tumors tend to exhibit poor prognosis [27]. Previous meta-analyses have demonstrated that PD-L1 expression is correlated with worse prognosis and advanced clinicopathological features in UC [28,29]. Moreover, Kawahara et al. indicated that UC with high-grade features exhibited higher PD-L1 expression [30]. A recent study has reported that the increased expression of PD-L1 is correlated with histologic variants of UC, including squamous, glandular, plasmacytoid, and sarcomatoid differentiation [25]. Histologic variants of UC constitute a high-grade feature that tends to be associated with PD-L1 expression. In this regard, PD-1/PD-L1 target therapy may be more effective for the treatment of histologic variants of UC. Although PD-L1 positivity is an important predictor of anti-PD-1/PD-L1 treatment response, PD-L1 expression status alone is insufficient to determine prognosis in any cancer subtype.

CONCLUSION

We reviewed the prospect and existing limitations of PD-L1 assays performed using samples from patients with UC. Discordance of PD-L1 positivity was observed, depending on the results of each assay. Notably, the inter-assay and inter-observer discordance were primarily observed in scoring SP142. Thus far, there exists no scientific evidence for the interchangeability of PD-L1 assays. If atezolizumab cannot be used as first-line therapy due to SP142 positivity observed only in TCs, and not in ICs, we recommend adopting the use of 22C3 in conjunction with pembrolizumab. The complex scoring algorithm of each assay is challenging for pathologists and also results in inter-observer heterogeneity. Providing suitable training to pathologists may be the only ap-

proach to overcome these challenges. Moreover, in the future, digital pathology and artificial intelligence may assist PD-L1 evaluation with greater accuracy.

Ethics Statement

Not applicable.

Availability of Data and Material

Data sharing not applicable to this article as no datasets were generated or analyzed during the study.

Code Availability

Not applicable.

ORCID

Kyu Sang Lee <https://orcid.org/0000-0003-2801-9072>
Gheeyoung Choe <https://orcid.org/0000-0001-6547-5603>

Author Contributions

Conceptualization: KSL, GC. Data curation: KSL. Formal analysis: KSL. Investigation: KSL. Methodology: KSL. Supervision: GC. Writing—original draft: KSL. Writing—review & editing: KSL, GC. Approval of final manuscript: all authors.

Conflicts of Interest

The authors declare that they have no potential conflicts of interest.

Funding Statement

No funding to declare.

References

- Hirsch L, Zitvogel L, Eggermont A, Marabelle A. PD-Loma: a cancer entity with a shared sensitivity to the PD-1/PD-L1 pathway blockade. *Br J Cancer* 2019; 120: 3-5.
- Kerr KM, Tsao MS, Nicholson AG, et al. Programmed death-ligand 1 immunohistochemistry in lung cancer: in what state is this art? *J Thorac Oncol* 2015; 10: 985-9.
- Rijnders M, van der Veldt AA, Zuiverloon TC, et al. PD-L1 antibody comparison in urothelial carcinoma. *Eur Urol* 2019; 75: 538-40.
- Ratcliffe MJ, Sharpe A, Midha A, et al. Agreement between programmed cell death ligand-1 diagnostic assays across multiple protein expression cutoffs in non-small cell lung cancer. *Clin Cancer Res* 2017; 23: 3585-91.
- Rimm DL, Han G, Taube JM, et al. A prospective, multi-institutional, pathologist-based assessment of 4 immunohistochemistry assays for PD-L1 expression in non-small cell lung cancer. *JAMA Oncol* 2017; 3: 1051-8.
- Scheel AH, Dietel M, Heukamp LC, et al. Harmonized PD-L1 immunohistochemistry for pulmonary squamous-cell and adenocarcinomas. *Mod Pathol* 2016; 29: 1165-72.
- Hodgson A, Slodkowska E, Jungbluth A, et al. PD-L1 immunohistochemistry assay concordance in urothelial carcinoma of the bladder and hypopharyngeal squamous cell carcinoma. *Am J Surg Pathol* 2018; 42: 1059-66.
- Zavalishina L, Tsimafeyu I, Povilaitis P, et al. RUSSCO-RSP comparative study of immunohistochemistry diagnostic assays for PD-L1 expression in urothelial bladder cancer. *Virchows Arch* 2018;

- 473: 719-24.
9. Zajac M, Scott M, Ratcliffe M, et al. Concordance among four commercially available, validated programmed cell death ligand-1 assays in urothelial carcinoma. *Diagn Pathol* 2019; 14: 99.
 10. Scheerens H, Malong A, Bassett K, et al. Current status of companion and complementary diagnostics: strategic considerations for development and launch. *Clin Transl Sci* 2017; 10: 84-92.
 11. Rosenberg JE, Hoffman-Censits J, Powles T, et al. Atezolizumab in patients with locally advanced and metastatic urothelial carcinoma who have progressed following treatment with platinum-based chemotherapy: a single-arm, multicentre, phase 2 trial. *Lancet* 2016; 387: 1909-20.
 12. Balar AV, Castellano D, O'Donnell PH, et al. First-line pembrolizumab in cisplatin-ineligible patients with locally advanced and unresectable or metastatic urothelial cancer (KEYNOTE-052): a multicentre, single-arm, phase 2 study. *Lancet Oncol* 2017; 18: 1483-92.
 13. Powles T, O'Donnell PH, Massard C, et al. Efficacy and safety of durvalumab in locally advanced or metastatic urothelial carcinoma: updated results from a phase 1/2 open-label study. *JAMA Oncol* 2017; 3: e172411.
 14. Sharma P, Retz M, Siefker-Radtke A, et al. Nivolumab in metastatic urothelial carcinoma after platinum therapy (CheckMate 275): a multicentre, single-arm, phase 2 trial. *Lancet Oncol* 2017; 18: 312-22.
 15. Kulangara K, Zhang N, Corigliano E, et al. Clinical utility of the combined positive score for programmed death ligand-1 expression and the approval of pembrolizumab for treatment of gastric cancer. *Arch Pathol Lab Med* 2019; 143: 330-7.
 16. Adam J, Le Stang N, Rouquette I, et al. Multicenter harmonization study for PD-L1 IHC testing in non-small-cell lung cancer. *Ann Oncol* 2018; 29: 953-8.
 17. Torlakovic E, Lim HJ, Adam J, et al. "Interchangeability" of PD-L1 immunohistochemistry assays: a meta-analysis of diagnostic accuracy. *Mod Pathol* 2020; 33: 4-17.
 18. Hirsch FR, McElhinny A, Stanforth D, et al. PD-L1 immunohistochemistry assays for lung cancer: results from phase 1 of the Blueprint PD-L1 IHC assay comparison project. *J Thorac Oncol* 2017; 12: 208-22.
 19. Buttner R, Gosney JR, Skov BG, et al. Programmed death-ligand 1 immunohistochemistry testing: a review of analytical assays and clinical implementation in non-small-cell lung cancer. *J Clin Oncol* 2017; 35: 3867-76.
 20. Schwamborn K, Ammann JU, Knuchel R, et al. Multicentric analytical comparability study of programmed death-ligand 1 expression on tumor-infiltrating immune cells and tumor cells in urothelial bladder cancer using four clinically developed immunohistochemistry assays. *Virchows Arch* 2019; 475: 599-608.
 21. Downes MR, Slodkowska E, Katabi N, Jungbluth AA, Xu B. Inter- and intraobserver agreement of programmed death ligand 1 scoring in head and neck squamous cell carcinoma, urothelial carcinoma and breast carcinoma. *Histopathology* 2020; 76: 191-200.
 22. Cooper WA, Russell PA, Cherian M, et al. Intra- and interobserver reproducibility assessment of PD-L1 biomarker in non-small cell lung cancer. *Clin Cancer Res* 2017; 23: 4569-77.
 23. Chang S, Park HK, Choi YL, Jang SJ. Interobserver reproducibility of PD-L1 biomarker in non-small cell lung cancer: a multi-institutional study by 27 pathologists. *J Pathol Transl Med* 2019; 53: 347-53.
 24. Li H, Zhang Q, Shuman L, et al. Evaluation of PD-L1 and other immune markers in bladder urothelial carcinoma stratified by histologic variants and molecular subtypes. *Sci Rep* 2020; 10: 1439.
 25. Reis H, Serrette R, Posada J, et al. PD-L1 expression in urothelial carcinoma with predominant or pure variant histology: concordance among 3 commonly used and commercially available antibodies. *Am J Surg Pathol* 2019; 43: 920-7.
 26. Mahoney KM, Sun H, Liao X, et al. PD-L1 antibodies to its cytoplasmic domain most clearly delineate cell membranes in immunohistochemical staining of tumor cells. *Cancer Immunol Res* 2015; 3: 1308-15.
 27. Wu P, Wu D, Li L, Chai Y, Huang J. PD-L1 and survival in solid tumors: a meta-analysis. *PLoS One* 2015; 10: e0131403.
 28. Ding X, Chen Q, Yang Z, et al. Clinicopathological and prognostic value of PD-L1 in urothelial carcinoma: a meta-analysis. *Cancer Manag Res* 2019; 11: 4171-84.
 29. Wen Y, Chen Y, Duan X, et al. The clinicopathological and prognostic value of PD-L1 in urothelial carcinoma: a meta-analysis. *Clin Exp Med* 2019; 19: 407-16.
 30. Kawahara T, Ishiguro Y, Ohtake S, et al. PD-1 and PD-L1 are more highly expressed in high-grade bladder cancer than in low-grade cases: PD-L1 might function as a mediator of stage progression in bladder cancer. *BMC Urol* 2018; 18: 97.

Hepatocellular adenomas: recent updates

Haeryoung Kim¹, Young Nyun Park²

¹Department of Pathology, Seoul National University Hospital, Seoul National University College of Medicine, Seoul;

²Department of Pathology, Graduate School of Medical Science, Brain Korea 21 Project, Yonsei University College of Medicine, Seoul, Korea

Hepatocellular adenoma (HCA) is a heterogeneous entity, from both the histomorphological and molecular aspects, and the resultant subclassification has brought a strong translational impact for both pathologists and clinicians. In this review, we provide an overview of the recent updates on HCA from the pathologists' perspective and discuss several practical issues and pitfalls that may be useful for diagnostic practice.

Key Words: Hepatocellular adenoma; Classification; Pathology

Received: February 4, 2021 **Revised:** February 27, 2021 **Accepted:** February 28, 2021

Corresponding Author: Young Nyun Park, MD, PhD, Department of Pathology, Yonsei University College of Medicine, 50-1 Yonsei-ro, Seodaemun-gu, Seoul 03722, Korea
 Tel: +82-2-2228-1678, Fax: +82-2-362-0860, E-mail: young0608@yuhs.ac

Hepatocellular adenoma (HCA) is defined as a benign monoclonal proliferation of hepatocytes [1]. It is more prevalent in Western countries, with an incidence of 3–4 cases/100,000 in Europe and North America [1], and its incidence is much lower in Asian countries [2–6]. Since the first characterization of the molecular subtypes of HCAs in 2006 [7], HCA has now become an increasingly heterogeneous entity, and this has brought a strong translational impact for pathologists (Table 1) [8–10]. In this review, we will summarize the clinicopathological and molecular characteristics of the various subtypes of HCA, and discuss the various pitfalls in the pathological diagnosis of HCA.

GENERAL CLINICOPATHOLOGICAL FEATURES OF HEPATOCELLULAR ADENOMA

The typical patient is female and of reproductive age (15–50 years), while HCAs are relatively rare in men, children and elderly patients (> 65 years). The major risk factors for HCA include oral contraceptive use, obesity, metabolic syndrome, alcohol intake and use of anabolic steroids. Other conditions associated with HCA development include glycogen storage diseases (especially types 1 and 3), galactosemia, tyrosinemia, familial polyposis coli, polycystic ovary syndrome and β -thalassemia. Interestingly, a few series from Asian countries have demonstrated a higher inci-

dence of HCA in men, and the incidence of oral contraceptive use was lower in female patients [2,3,5]. The main clinical implications of HCA include the risk of bleeding, especially in larger tumors, and the risk of malignant transformation to hepatocellular carcinoma (HCC). The risk of HCC development depends on the subtype, being the highest in β -catenin-activated HCAs (B-HCAs). The general indications for surgical management of HCAs include male gender, large size (>5 cm), interval growth during follow up on imaging, and atypical pathological features (e.g., atypical cytoarchitectural features, presence of β -catenin activation).

In general, HCAs are grossly well demarcated but non-encapsulated, and the color varies from pale yellow-tan to bile-stained depending on the histology. Hemorrhage or peliosis may be present. HCAs are more frequently solitary lesions; however, multiple HCAs may occur, and the term “adenomatosis” is used when there are 10 or more HCAs. In cases of multiple HCAs, most cases demonstrate multiple HCAs of the same molecular subtype, although some tumors from the same patient may belong to different subgroups of HCA [11]. The size is variable, ranging from 1 cm to as large as 30 cm. Unlike HCCs, the background liver is typically non-cirrhotic, although advanced stage fibrosis may be present in the setting of alcoholic liver disease, metabolic syndrome or vascular disorders. Histologically, the tumor cells resemble he-

Table 1. Summary of the clinicopathological and molecular characteristics of different HCA subtypes

Subtype (frequency, %)	Characteristic features			
	Molecular	Clinical	Histopathological	Immunohistochemical
<i>HNF1A</i> -inactivated HCA (30%–40%)	<i>HNF1A</i> inactivating mutations (germline 10%, somatic 90%)	Female, obesity, MODY3, adenomatosis	Diffuse steatosis	LFABP expression loss
Inflammatory HCA (40%–50%)	gp130/ <i>IL6ST</i> , <i>FRK</i> , <i>STAT3</i> , <i>GNAS</i> , <i>JAK1</i> mutations	Obesity, metabolic syndrome, alcohol, oral contraceptives	Sinusoidal dilatation Vascular proliferation Inflammatory cell infiltration Ductular reaction Focal steatosis	SAA, CRP expression
β -catenin-activated HCA (10%)				
β -catenin (exon 3)-activated HCA (7%)	<i>CTNNB1</i> exon 3 activating mutations	Male, young age, anabolic steroids, glycogen storage disease, increased risk of HCC transformation	Cytological and architectural atypia	Nuclear β -catenin expression Diffuse strong GS expression
β -catenin (exon 7,8)-activated HCA (3%)	<i>CTNNB1</i> exon 7 or 8 activating mutations	Low risk of HCC transformation	-	Absent/rare nuclear β -catenin expression GS expression: absent/weak/patchy
β -catenin-activated inflammatory HCA (5%–10%)	gp130/ <i>IL6ST</i> , <i>STAT3</i> , <i>FRK</i> , <i>GNAS</i> , <i>JAK1</i> mutations + <i>CTNNB1</i> exon 3 or 7/8 mutations	Similar to inflammatory HCA Increased risk of HCC transformation (ex.3)	Similar to inflammatory HCA Cyoarchitectural atypia (ex.3)	SAA, CRP expression Nuclear β -catenin, diffuse strong GS expression (ex.3)
Sonic hedgehog-activated HCA (4%)	<i>INHBE-GLI1</i> fusion, resulting in sonic hedgehog pathway activation	Obesity, hemorrhage	Hemorrhage	PTGDS, ASS1
Unclassified HCA (<7%)	Unknown	-	-	-

HCA, hepatocellular adenoma; MODY3, maturity-onset diabetes type 3; LFABP, liver fatty acid binding protein; SAA, serum amyloid A; CRP, C-reactive protein; HCC, hepatocellular carcinoma; GS, glutamine synthetase; PTGDS, prostaglandin D2 synthase; ASS1, argininosuccinate synthase 1.

patocytes, demonstrating eosinophilic or clear cytoplasm, and they are arranged in thin trabeculae. Portal tracts are absent, and thin-walled vascular channels and small arteriolar structures are seen.

RECENT UPDATES ON THE CLASSIFICATION OF HEPATOCELLULAR ADENOMA

Inflammatory HCA

Inflammatory HCA (IHCA) is the most common subtype (40%–50%) of HCAs, and demonstrates constitutive activation of the interleukin-6/JAK/STAT pathway. Molecular alterations include mutations in gp130/*IL6ST* (50%), *FRK* (10%), *STAT3* (5%), *GNAS* (5%), *ROS1* (3%), and *JAK1* (1%). The main risk factors for IHCA include obesity, metabolic syndrome and alcohol intake.

The main histological features include foci of inflammation, thick arteries, and sinusoidal dilatation (Fig. 1). Congestion, hemorrhage and peliosis may be present. Portal tracts are absent; however, ductular reaction and pseudoportals are frequently seen. Steatosis may be observed and is usually focal. The background liver frequently demonstrates steatosis, which may be attributed to the patient's underlying risk factors (obesity, met-

abolic syndrome, alcoholic liver disease etc.).

Immunohistochemistry for serum amyloid A (SAA) and C-reactive protein (CRP) may provide important diagnostic clues, as IHCA is characterized by the overexpression of these acute phase reactants via *STAT3* activation. SAA and/or CRP expression in IHCA is usually diffuse and strong, and sharply demarcated from the surrounding liver parenchyme. However, it should be noted that the adjacent liver may be focally or even diffusely positive for SAA and/or CRP in some cases, especially when there is marked inflammation or hemorrhage in the background liver, and in the setting of previous embolization [12]. Therefore, the histological context should be taken into account when interpreting SAA/CRP stains and it is important that the staining results are compared with the background liver, preferably also with positive control tissues.

Importantly, about 10% of IHCA also demonstrate mutations in *CTNNB1* (B-IHCA, "mixed" HCA). Although the risk for HCC transformation is generally low in IHCA, the concurrence of strong β -catenin activation in HCAs increases the risk of HCC development. Therefore, the addition of β -catenin and glutamine synthetase (GS) immunohistochemistry is also necessary, in order to identify mixed HCAs (B-IHCA). B-HCAs

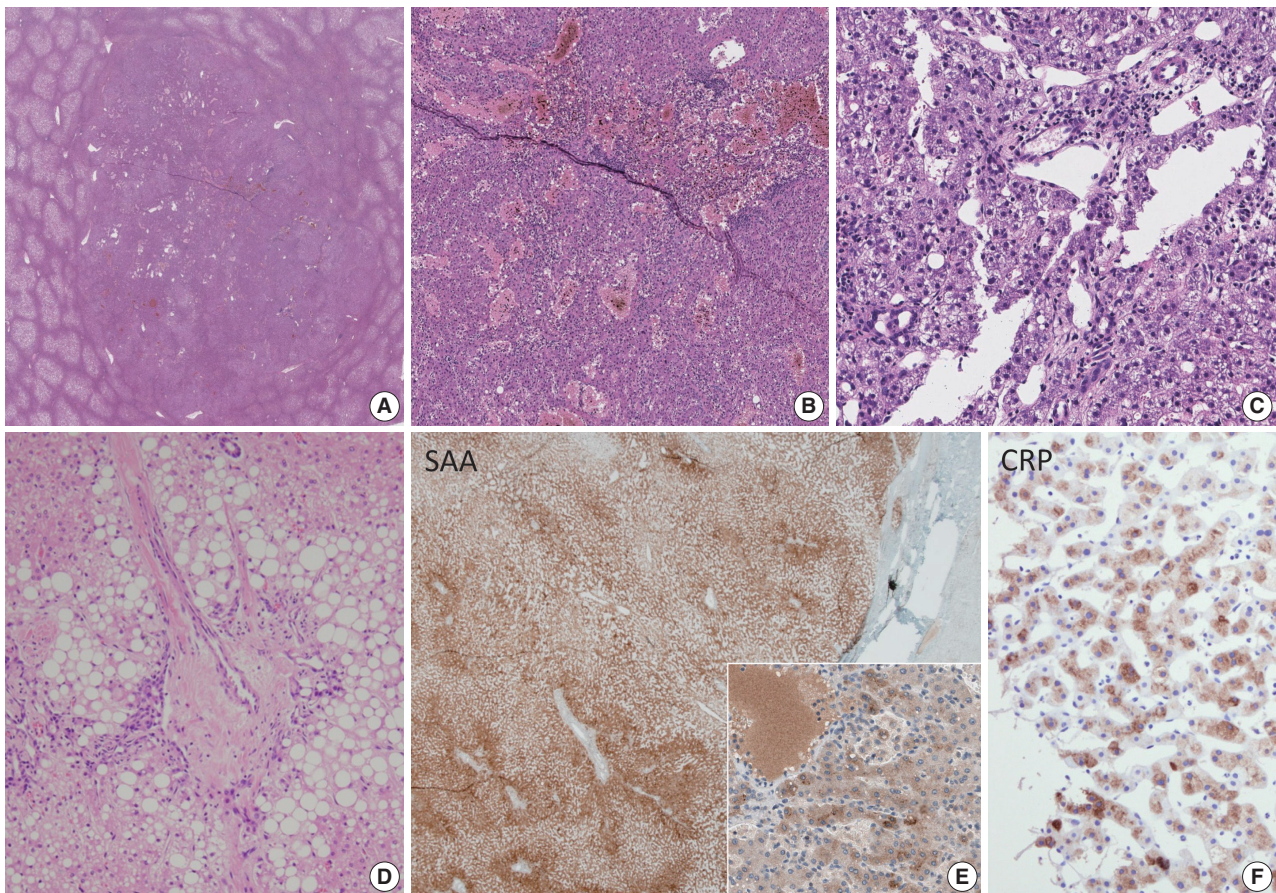


Fig. 1. Inflammatory hepatocellular adenoma. Sinusoidal dilatation, congestion and peliosis is seen in the tumor (A–C). Inflammatory cell infiltration (C), thick arteriolar structures with ductular reaction, resembling portal tracts (“pseudo-portal tracts”) and steatosis (D) may be seen in these tumors. Diffuse steatosis may be seen in the background liver (A). The tumor cells express serum amyloid A (E; inset: granular cytoplasmic staining in tumor cells) and C-reactive peptide (F).

are described in more detail in the following section.

β -catenin-activated HCA

Approximately 10% of HCAs demonstrate *CTNNB1* mutations/deletions leading to different levels of β -catenin pathway activation. These tumors are designated as B-HCA. *CTNNB1* alterations most often occur in exon 3 (7%, B^{ex3}-HCA) or in exons 7 and 8 (3%, B^{ex7,8}-HCA). Mutations or large deletions in exon 3 most frequently involve the β -Trcp consensus site (D32–S37, also known as the exon 3 hotspot) and these are associated with high levels of β -catenin activation and high risk of HCC transformation [13,14]. Outside of the β -Trcp consensus site, T41 and S45 mutations in exon 3 have also been frequently demonstrated, and these are associated with moderate to weak levels of β -catenin activation. In contrast, mutations in *CTNNB1* exon 7 (K335) and exon 8 (W383, R386, and N387) result in weak β -catenin activation. The clinical and histopathological features

of B^{ex7,8}-HCA are still unclear, although the risk of HCC development appear to be low in these tumors, unlike the B^{ex3}-HCAs [10,13,14]. *CTNNB1* alterations may also occur in a subset of IHCA (B-IHCA or “mixed” HCA, 5%–10%).

The characteristic clinical features associated with B^{ex3}-HCAs include male gender, a history of androgen administration and underlying glycogen storage disease. These tumors are usually solitary and rarely multiple. Mild cytological atypia may be observed in B^{ex3}-HCAs, and architectural atypia, including mild trabecular thickening, small cell change or pseudoglandular structures, is also frequently seen (Fig. 2). Bile or lipofuscin pigments are frequently observed in the tumor cells; the lipofuscin pigmentation may be very prominent in some HCAs [15]. Most importantly, as B^{ex3}-HCAs are associated with high risk of malignant transformation to HCC, the practical implication of this subtype of HCA is in excluding the possibility of well-differentiated HCC. This differential diagnosis is discussed later.

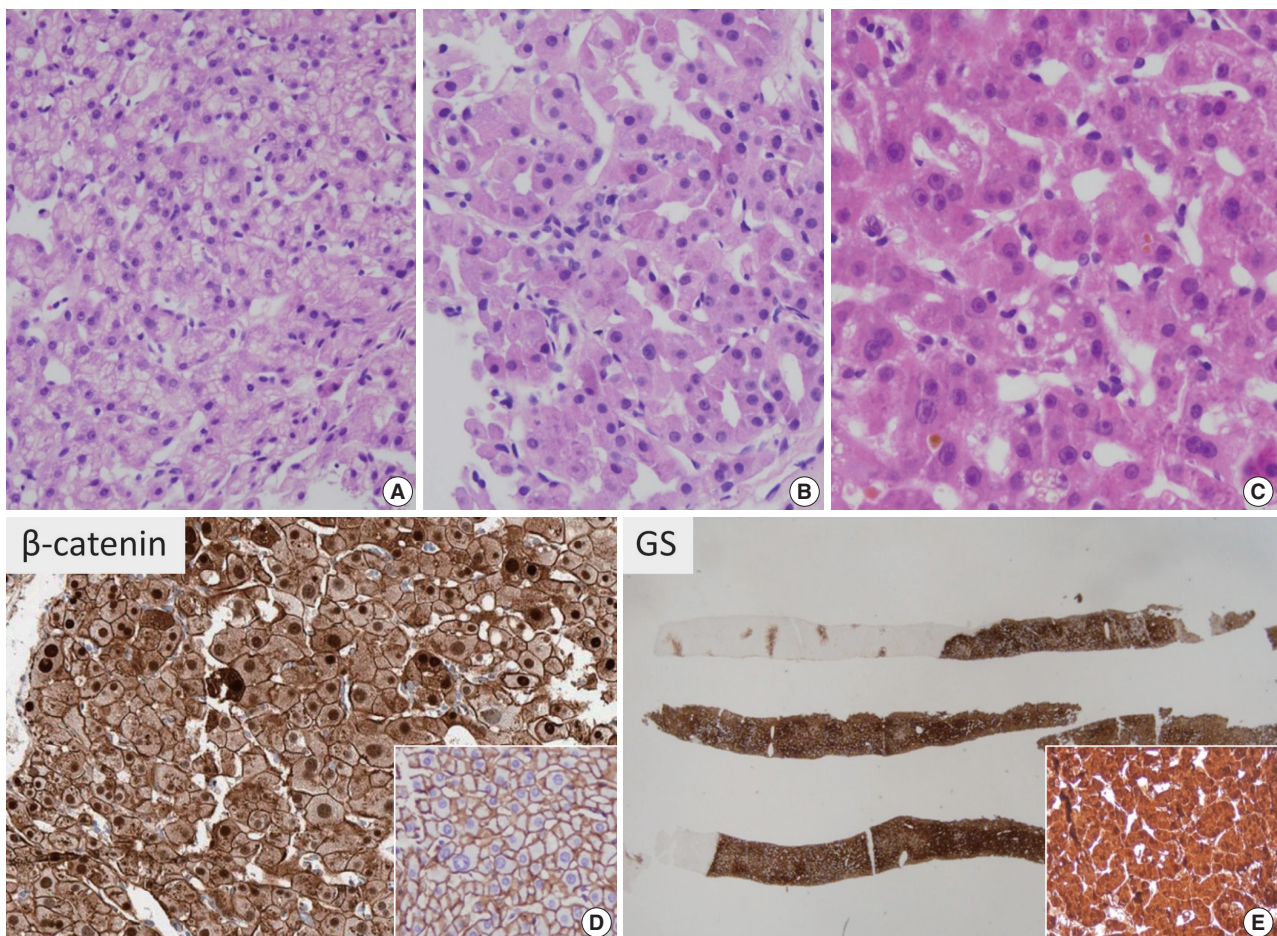


Fig. 2. β -catenin-activated hepatocellular adenoma (B-HCA). There is mild trabecular thickening (A) and pseudoglandular structures (B, C). Mild cytological atypia is present (A–C). Cholestasis may be seen (C). On immunohistochemistry, B-HCA with strong β -catenin activation (B $^{\text{ex3}}$ -HCA) demonstrates nuclear β -catenin expression (D), instead of the normal membranous pattern (inset), and diffuse homogeneous glutamine synthetase expression is seen in such tumors (E, inset: high-power view).

Although direct sequencing of the *CTNNB1* gene would be the most definitive means of characterizing the molecular subtype of a presumed B-HCA, this is not feasible in most clinical practices. Fortunately, immunohistochemical stains for β -catenin and GS have been demonstrated to be good surrogate markers reflecting *CTNNB1* status. Nuclear β -catenin expression and diffuse strong homogeneous GS expression are the typical immunohistochemical features of B-HCAs with strong β -catenin activation (non-S45 B $^{\text{ex3}}$ -HCA). Interestingly, GS expression patterns have been recently demonstrated to reflect the mutational status of *CTNNB1* (Fig. 3). Diffuse homogeneous expression (strong GS expression in > 90% of tumor cells) has been demonstrated in B $^{\text{ex3}}$ -HCAs with mutations or large deletions in the D32–S37 hotspot of *CTNNB1* exon 3 (β -Trcp consensus site). In contrast, B $^{\text{ex3}}$ -HCAs with *CTNNB1* exon 3 T41 or S45 mutations, which have been associated with moderate β -catenin activation, dem-

onstrate diffuse heterogeneous GS expression (50%–90% of tumor cells expressing GS in a starry-sky pattern). B $^{\text{ex7,8}}$ -HCAs lack the immunohistochemical features of strong β -catenin activation (i.e., diffuse strong GS expression, nuclear β -catenin). Weak patchy GS staining in addition to the “normal” perivenular pattern has been frequently seen in association with weak β -catenin activation (absent or rare nuclear β -catenin), which is common in B $^{\text{ex7,8}}$ -HCAs, but also rarely seen in B $^{\text{ex3}}$ -HCAs with S45 mutations. Interestingly, GS accentuation and discontinuous band-like GS staining at the tumor border has been described in B $^{\text{ex3}}$ -HCAs with S45 mutations and B $^{\text{ex7,8}}$ -HCAs, respectively [16,17]. These expression patterns are different from the “map-like” GS pattern of focal nodular hyperplasia (FNH), which is described later. In contrast, GS expression in the normal liver has a perivenular distribution (“normal” pattern), where GS expression is limited to 1 to 3 layers of hepatocytes around the central vein.

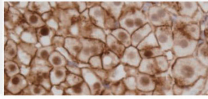
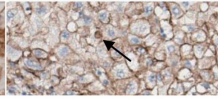
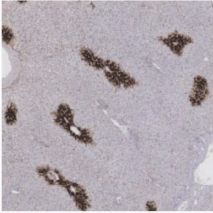
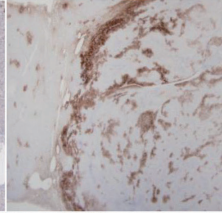
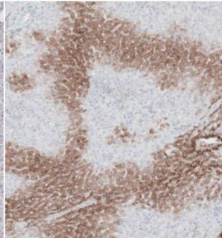
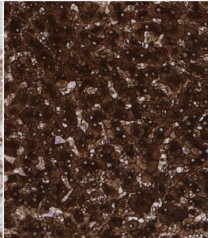
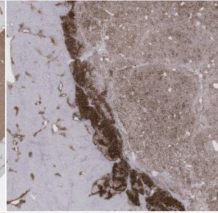
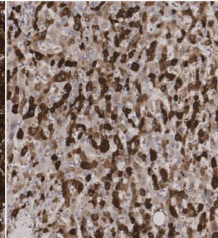
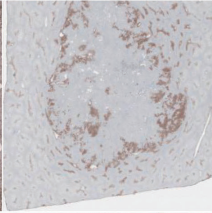
	Normal liver	FNH	β -catenin-activated HCA ^a		
<i>CTNNB1</i> gene alteration	None	None	Exon 3 D32–S37, T41 mutation or large deletion	Exon 3 S45 mutation	Exon 7, 8 mutation
Nuclear β -catenin expression	Absent	Absent	Present 	Focal or absent 	Absent
Glutamine synthetase expression	Perivenular (1–3 layers of hepatocytes)  	“Map-like”  	Diffuse strong homogeneous  	Diffuse heterogeneous or weak/patchy Strong band-like expression at border  	Weak/patchy perivenular pattern  

Fig. 3. Immunohistochemical correlates of *CTNNB1* alteration status in β -catenin-activated HCA, FNH and normal liver. FNH, focal nodular hyperplasia; HCA, hepatocellular adenoma. ^aSerum amyloid A and/or reactive peptide is additionally expressed in β -catenin-activated inflammatory HCA.

HNF1A-inactivated HCA

HNF1A-inactivated HCAs (H-HCA) constitute 30%–35% of HCAs and are characterized by inactivating mutations in *HNF1A*, which encodes hepatocyte nuclear factor 1 α . In the majority (90%) of H-HCAs, the *HNF1A* mutation is somatic and biallelic, while the remaining 10% comprise H-HCAs with germline *HNF1A* mutations. The latter is frequently associated with maturity-onset diabetes type 3 (MODY3) and the presence of adenomatosis. H-HCAs have also been reported in the background of vascular abnormalities and congenital hepatic fibrosis [18–20].

Histologically, H-HCAs typically demonstrate diffuse steatosis in the tumor cells (Fig. 4), although some cases may show minimal or no steatosis, especially those arising in hepatic vascular disorders [20,21]. The tumor cells demonstrate no significant nuclear atypia and they are usually arranged in thin trabeculae, although occasional pseudoglandular structures may be observed. Inflammatory cell infiltration is not a characteristic of H-HCA.

Immunohistochemically, the tumor cells demonstrate loss of liver fatty acid binding protein (LFABP) expression. H-HCAs demonstrate a low risk of HCC transformation compared to other types.

Unclassified HCA and sonic hedgehog-activated HCA

By definition, unclassified HCA (U-HCA) lacks the characteristics of other subtypes. The frequency of U-HCA (5%–10%) is decreasing, as HCAs belonging to this group are being increasingly characterized as specific subtypes. Sonic hedgehog-activated HCA (sh-HCA) is an emerging subtype of HCA with distinct clinicopathological features, including increased bleeding risk. sh-HCA has been demonstrated to account for ~4% of HCAs that were previously classified as U-HCA [10]. Molecular features of sh-HCA include *INBHE-GLI1* fusion and overexpression of *GLI1*, which is the key transcription factor of the sonic hedgehog pathway. Recently, potential surrogate immunohistochemical marker candidates have received attention, including

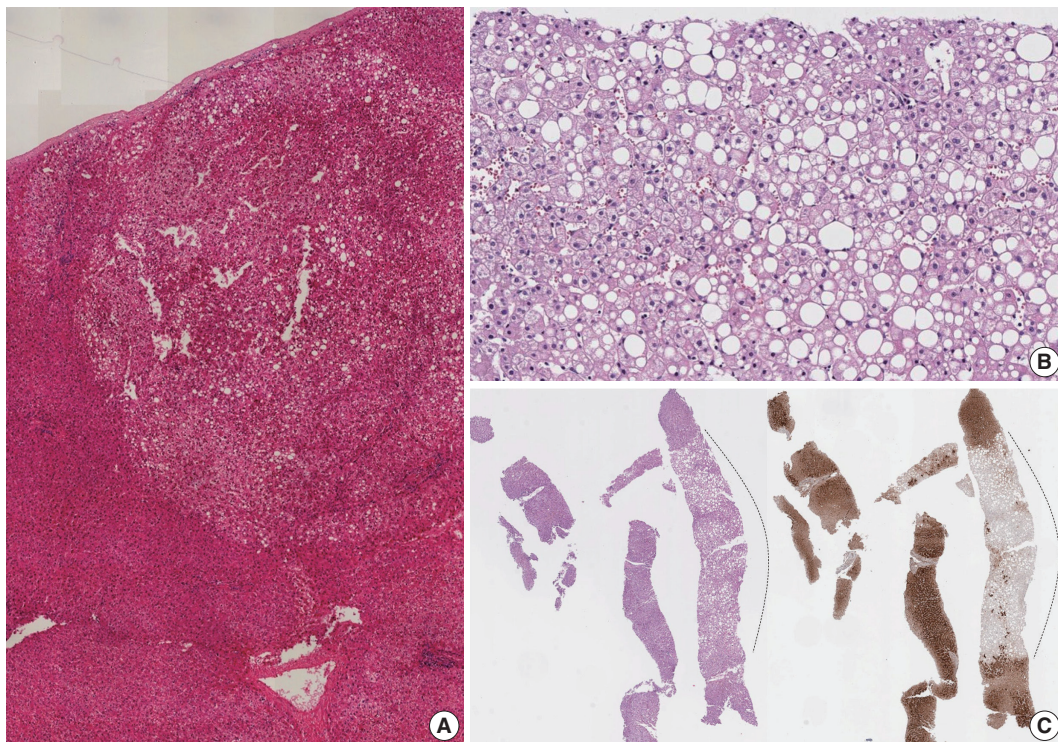


Fig. 4. HNF1A-inactivated hepatocellular adenoma. Diffuse steatosis is seen in the tumor, compared to the surrounding hepatic parenchyme (A–C). There is no significant cytological or architectural atypia on higher-power magnification (B). Immunohistochemically, the tumor displays loss of liver fatty acid-binding protein expression (C) (dotted line: tumor).

lipocalin-type prostaglandin D2 synthase and argininosuccinate synthase 1 [22–25].

COMMON PRACTICAL ISSUES FOR PATHOLOGISTS

Atypia in HCAs: HCCs or atypical hepatocellular neoplasms?

In practice, pathologists are often faced with having to distinguish between HCA and well-differentiated HCC, which is a difficult challenge especially on needle biopsies. Features that favor the possibility of HCC include cytological atypia which is more than minimal and patchy, thickened hepatocyte trabeculae, frequent pseudoglandular structures, cholestasis, small cell change and loss of reticulin staining (Fig. 5). Caution should be exercised when interpreting reticulin loss, as focal reticulin loss in an HCA is acceptable when there is marked steatosis [26]. Conversely, well differentiated HCCs show only a partial loss of reticulin [27]. Identification of stromal invasion or a nodule-in-nodule growth pattern adds more confidence to the diagnosis of HCC. In the latter case, the outer and inner nodules are usually composed of HCA and HCC, respectively. The 3-marker panel—glypican-3, heat shock protein 70 (HSP70) and GS—which is

commonly used in the differential diagnosis between dysplastic nodules and HCC may be also be helpful for the discrimination between HCA and HCC [27–29]. However, as the challenging question of “HCA versus HCC” usually arises in the context of B-HCAs with strong/moderate β -catenin activation that express diffuse GS, the additional expression of glypican-3 and/or HSP70 would be more helpful in practice [29]. Although HCC often demonstrates increased sinusoidal capillarization compared to HCA (highlighted by CD34), this is a relative increase without definite cut-off values, and therefore CD34 immunohistochemistry on its own has limited use in the differential diagnosis.

The terms “atypical hepatocellular neoplasm (AHN)” and “hepatocellular neoplasm of uncertain malignant potential (HUMP)” have been proposed for hepatocellular neoplasms that demonstrate features atypical for HCA but insufficient for a confident diagnosis of HCC [30–32]. These terms have been coined to emphasize the borderline characteristics of these tumors, including increased risk for HCC development, and to convey to the clinicians the necessity for surgical intervention or at least close follow-up. There are currently no widely accepted guidelines on when to use these terms, although the following features have been consistently described in AHN/HUMPs: (1) morpho-

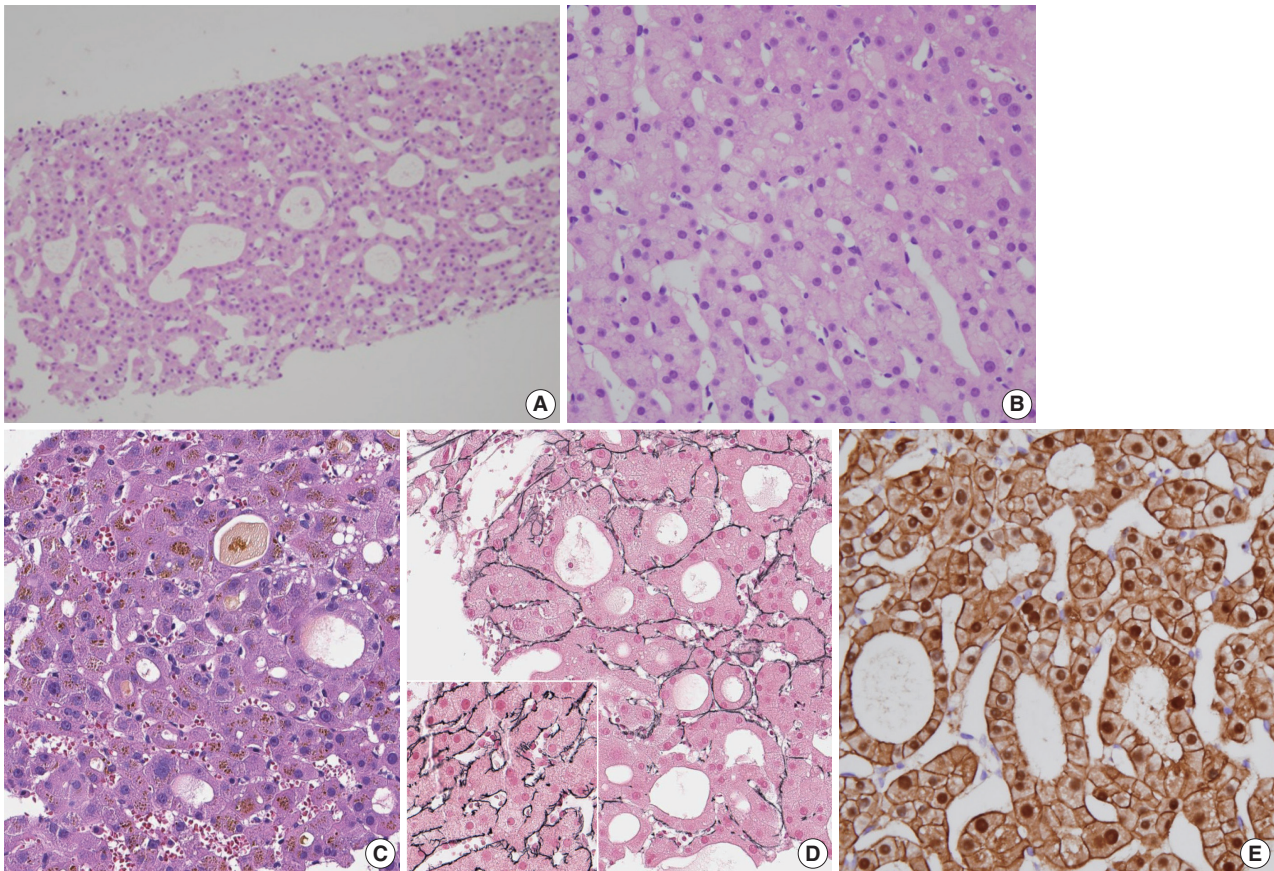


Fig. 5. Atypia in hepatocellular neoplasms. When features atypical for hepatocellular adenomas, such as frequent pseudoglandular structures (A, C–E), nuclear atypia (B, C) and focal reticulin loss (D; inset: preserved reticulin framework for comparison), are identified, the differential diagnosis should be between atypical hepatocellular neoplasm and well-differentiated hepatocellular carcinoma. When these features are only focally present (<5%), the terminology of atypical hepatocellular neoplasm may be used. Nuclear β -catenin expression is often identified in such cases (E).

logical atypia (nuclear atypia, small cell change, pseudoglandular structures, loss of reticulin fibers) that is only focal (<5% of the tumor), (2) presence of β -catenin activation or *CTNNB1* mutation, and (3) atypical demographic features (e.g., male, age > 50 years) [30–33]. Of note, Evason et al. [31] demonstrated similar cytogenetic alterations to HCC in their series of AHNs, and also documented recurrence and metastasis in AHNs with β -catenin activation, suggesting that these tumors may actually represent an extremely well-differentiated group of HCCs [31]. The presence of nuclear β -catenin expression, diffuse GS expression, or indeterminate diffuse GS expression in hepatocellular neoplasms (thus, suggestive of B^{ex3}-HCA) have been suggested as criteria for AHN, especially on biopsied specimens [30]. This would guide the clinician to surgically resect the nodule in question, rather than subjecting the patient to follow up, which is important as (1) an overt HCC may be present elsewhere in the nodule, and (2) B^{ex3}-HCA have been associated with increased

risk of HCC development. On resected specimens, the diagnosis of B-HCA may be made when the degree of cytoarchitectural atypia is insufficient for HCC, although some still prefer to use AHN in this setting [30].

IHCA vs. FNH vs. mass effect

The presence of ductular reaction, pseudoportal tracts and abnormal thick-walled vessels may result in the resemblance of IHCA to FNH. There is indeed a significant histological overlap between FNH and IHCA, and in fact, lesions previously described as telangiectatic FNH have now been reclassified as IHCA on the basis of molecular studies [34–36]. Discriminating between IHCA and FNH on a needle biopsy is a common difficult challenge for pathologists. FNH is a reactive polyclonal proliferation of hepatocytes in response to vascular abnormalities. Grossly, it is a well-demarcated multinodular mass with a central depressed stellate scar and radiating fibrous septa. Microscopically, central

fibrous scars and radiating fibrous septa with abnormal vasculature, including eccentrically thickened vascular walls, and marked ductular reaction are the typical findings. The hepatocytes demonstrate no significant atypia, and the hepatocyte plates are 1–3 cells thick. The nodularity, fibrous septa and ductular reaction may also be seen in IHCA; in these situations, immunohistochemistry for GS, SAA, and CRP may be helpful. FNH demonstrates a remarkable “map-like” GS expression pattern, characterized by broad bands of hepatocytes that strongly express GS, and these bands appear to anastomose together to produce a complex lace-like or map-like architecture (Figs. 3, 6) [37,38].

On biopsies, the GS expression appears as patchy broad bands of strong GS expression, which contrast with the punctate or linear perivenular GS pattern in the adjacent normal parenchyme (Fig. 6). Nuclear β -catenin staining is absent in FNH, and SAA and CRP are usually negative in FNH. Thus, SAA and/or CRP expression and absence of “map-like” GS expression pattern strongly supports a diagnosis of IHCA over FNH.

Mass effect may appear as sinusoidal dilatation and ductular reaction in the non-lesional hepatic parenchyme, which may lead to an erroneous diagnosis of IHCA [39]. The presence of portal tract edema and fibrosis with neutrophilic infiltration should alert

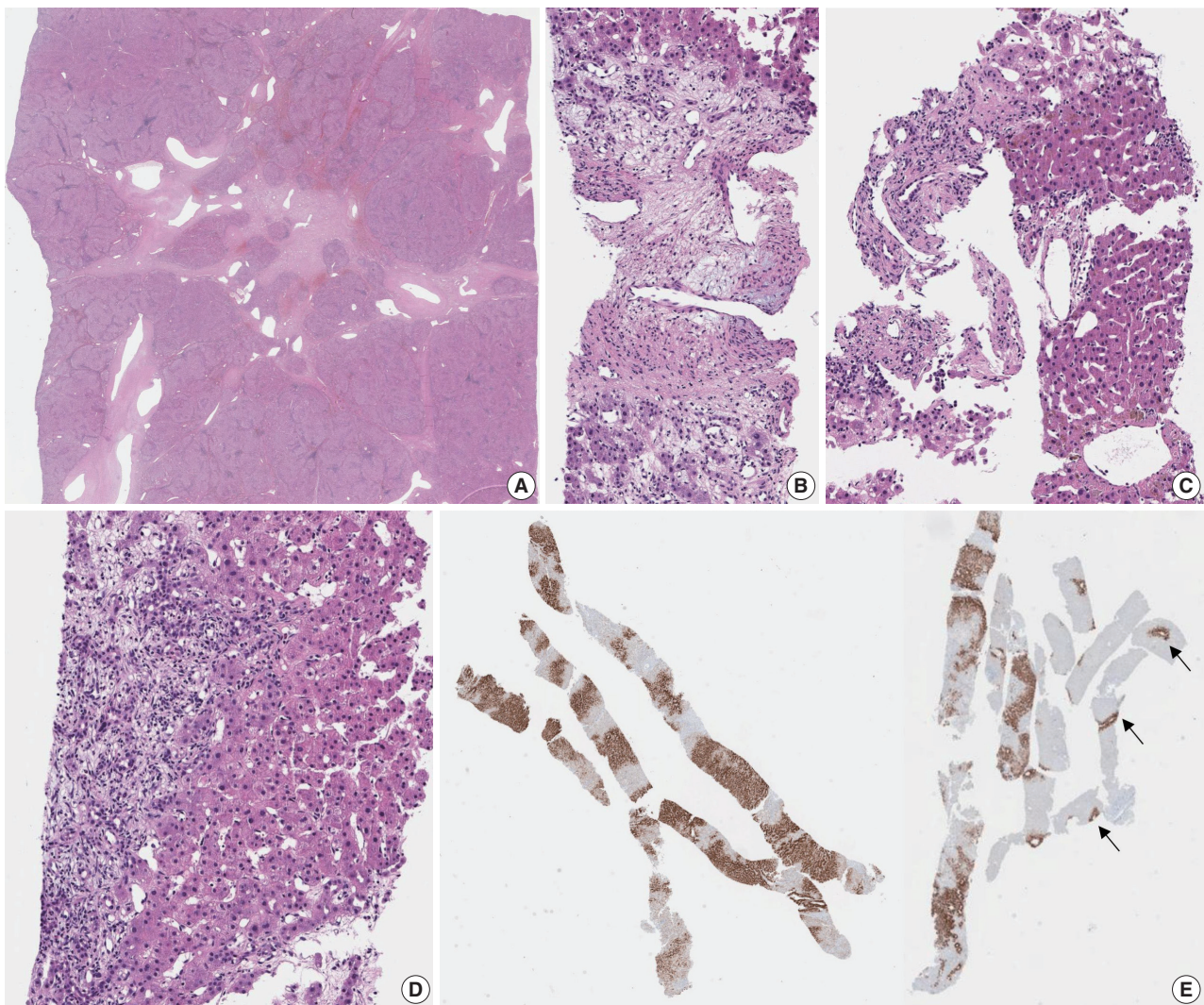


Fig. 6. Focal nodular hyperplasia. A typical low power view of a resected case (A). A central stellate scar with radiating fibrous septa is seen, containing multiple irregular-shaped vascular structures. When needle biopsy specimens are obtained from the central scar or fibrous septa (B, C), it is easy to identify the abnormal vascular channels with varying calibers, shape and irregular wall thickness. Sometimes biopsies include the peripheral portions without the obvious vascular anomalies; instead there is at least mild hepatocellular nodularity with ductular reaction (D). Glutamine synthetase immunohistochemistry demonstrates broad bands of GS-expressing hepatocytes (E), which corresponds to the map-like pattern in Fig. 3, in contrast to the normal perivenular pattern (arrows).

the pathologist to the possibility that the biopsy core was obtained from the perilesional parenchyme and clinicoradiological correlation is mandatory. Recognizing the presence of evenly spaced portal tracts and central veins, perhaps with the help of trichrome and GS stains, may also be helpful in suggesting the non-neoplastic nature of the biopsied tissue.

Diagnostic pitfalls in the interpretation of immunohistochemical stain results

GS, β -catenin, SAA, CRP, and LFABP are indeed helpful immunohistochemical tools for subtyping HCAs and/or discriminating between HCA and FNH. However, they should also be used with care and in the correct context. SAA and CRP expression have been reported in 17% and ~50% of HCCs, respectively, and loss of LFABP expression has been demonstrated in 16%–25% of HCCs [40–42]. In addition, as previously mentioned, the background liver may show focal expression of SAA or CRP, especially in the setting of inflammation or hemorrhage; therefore, positivity for these markers should be interpreted carefully, taking the histology into account. Moreover, some cirrhotic nodules may express SAA and/or CRP, such as in the SAA-positive nodules in alcoholic cirrhosis [43]. Therefore, these markers are not specific for HCA.

GS expression is a well-known component of the 3-marker panel (glypican-3, HSP70, and GS) for diagnosing HCCs [28,44]. Therefore, immunostains used for subtyping HCAs should only be used after an initial impression of HCA has been made, and not for distinguishing between HCA and HCC.

CONCLUSION

Although simply defined as a benign neoplasm of hepatocellular origin, HCA is a heterogeneous entity from both molecular and histomorphological aspects. The molecular classification of HCA has helped to increase our understanding of the biology of these tumors. More importantly for pathologists, the molecular classification has also helped to characterize the morphological and immunohistochemical features in HCAs in detail. The association between *CTNNB1* mutation status and the clinical behavior of HCA brings enormous translational impact, as the presence of strong β -catenin activation may influence management decisions in favor of surgical treatment. As for H-HCAs, the identification of individuals with liver adenomatosis composed of H-HCA should prompt molecular testing for germline *HN-1A* mutation status, in addition to familial screening for liver adenomatosis. It is also possible that additional subtypes of HCA will be identified in the future.

Ethics Statement

Not applicable.

Availability of Data and Material

Data sharing not applicable to this article as no datasets were generated or analyzed during the study.

Code Availability

Not applicable.

ORCID

Haeryoung Kim <https://orcid.org/0000-0002-4205-9081>

Young Nyun Park <https://orcid.org/0000-0003-0357-7967>

Author Contributions

Conceptualization: HK, YNP. Funding acquisition: HK, YNP. Study supervision: HK, YNP. Writing—original draft: HK. Writing—review & editing: HK, YNP. Approval of final manuscript: HK, YNP.

Conflicts of Interest

H.K., a contributing editor of the *Journal of Pathology and Translational Medicine*, was not involved in the editorial evaluation or decision to publish this article. Remaining author has declared no conflicts of interest.

Funding Statement

This work was supported by the National Research Foundation of Korea (NRF) grant funded by the Korea government (NRF-2019R1A2C2010056, NRF-2016R1D1A1A09919042 to HK; NRF-2020R1A2B5B01001646 to YNP) and by the Bio and Medical Technology Development Program of the NRF funded by the Ministry of Science and ICT (MSIT) (NRF-2016M3A9D5A01952416) (YNP).

References

1. Bioulac-Sage P, Kakar S, Nault JC. Hepatocellular adenoma. In: WHO classification of tumours: digestive system tumours. 5th ed. Lyon: International Agency for Research on Cancer; 2019; 224–8.
2. Lin H, van den Esschert J, Liu C, van Gulik TM. Systematic review of hepatocellular adenoma in China and other regions. *J Gastroenterol Hepatol* 2011; 26: 28–35.
3. Sasaki M, Yoneda N, Kitamura S, Sato Y, Nakanuma Y. Characterization of hepatocellular adenoma based on the phenotypic classification: the Kanazawa experience. *Hepatol Res* 2011; 41: 982–8.
4. Sasaki M, Nakanuma Y. Overview of hepatocellular adenoma in Japan. *Int J Hepatol* 2012; 2012: 648131.
5. Liu HP, Zhao Q, Jin GZ, et al. Unique genetic alterations and clinicopathological features of hepatocellular adenoma in Chinese population. *Pathol Res Pract* 2015; 211: 918–24.
6. Huang WC, Liao JY, Jeng YM, et al. Hepatocellular adenoma in Taiwan: distinct ensemble of male predominance, overweight/obesity, and inflammatory subtype. *J Gastroenterol Hepatol* 2020; 35: 680–8.
7. Zucman-Rossi J, Jeannot E, Nhieu JT, et al. Genotype-phenotype correlation in hepatocellular adenoma: new classification and relationship with HCC. *Hepatology* 2006; 43: 515–24.
8. Nault JC, Bioulac-Sage P, Zucman-Rossi J. Hepatocellular benign tumors—from molecular classification to personalized clinical care. *Gastroenterology* 2013; 144: 888–902.
9. Scazecz JY. Hepatocellular adenomas: one step beyond. *Gut* 2019;

- 68: 1140-2.
10. Nault JC, Couchy G, Balabaud C, et al. Molecular classification of hepatocellular adenoma associates with risk factors, bleeding, and malignant transformation. *Gastroenterology* 2017; 152: 880-94.
 11. Nault JC, Zucman Rossi J. Molecular classification of hepatocellular adenomas. *Int J Hepatol* 2013; 2013: 315947.
 12. Shin JH, Yu E, Kim EN, Kim CJ. C-reactive protein overexpression in the background liver of hepatitis B virus-associated hepatocellular carcinoma is a prognostic biomarker. *J Pathol Transl Med* 2018; 52: 267-74.
 13. Rebouissou S, Franconi A, Calderaro J, et al. Genotype-phenotype correlation of *CTNNB1* mutations reveals different β -catenin activity associated with liver tumor progression. *Hepatology* 2016; 64: 2047-61.
 14. Pilati C, Letouze E, Nault JC, et al. Genomic profiling of hepatocellular adenomas reveals recurrent FRK-activating mutations and the mechanisms of malignant transformation. *Cancer Cell* 2014; 25: 428-41.
 15. Mounajjed T, Yasir S, Aleff PA, Torbenson MS. Pigmented hepatocellular adenomas have a high risk of atypia and malignancy. *Mod Pathol* 2015; 28: 1265-74.
 16. Bioulac-Sage P, Sempoux C, Balabaud C. Hepatocellular adenoma: classification, variants and clinical relevance. *Semin Diagn Pathol* 2017; 34: 112-25.
 17. Cappellen D, Balabaud C, Bioulac-Sage P. A difficult case of beta-catenin-mutated hepatocellular adenoma: a lesson for diagnosis. *Histopathology* 2019; 74: 355-7.
 18. Ibarrola C, Castellano VM, Colina F. Focal hyperplastic hepatocellular nodules in hepatic venous outflow obstruction: a clinicopathological study of four patients and 24 nodules. *Histopathology* 2004; 44: 172-9.
 19. Paradis V, Bioulac-Sage P, Balabaud C. Congenital hepatic fibrosis with multiple HNF1alpha hepatocellular adenomas. *Clin Res Hepatol Gastroenterol* 2014; 38: e115-6.
 20. Lee Y, Park H, Lee K, Lee Y, Lee K, Kim H. Multiple hepatocyte nuclear factor 1A (HNF1A)-inactivated hepatocellular adenomas arising in a background of congenital hepatic fibrosis. *J Pathol Transl Med* 2021; 55: 154-8.
 21. Sempoux C, Balabaud C, Paradis V, Bioulac-Sage P. Hepatocellular nodules in vascular liver diseases. *Virchows Arch* 2018; 473: 33-44.
 22. Frulio N, Balabaud C, Laurent C, Trillaud H, Bioulac-Sage P. Unclassified hepatocellular adenoma expressing ASS1 associated with inflammatory hepatocellular adenomas. *Clin Res Hepatol Gastroenterol* 2019; 43: e63-7.
 23. Henriot E, Abou Hammoud A, Dupuy JW, et al. Argininosuccinate synthase 1 (ASS1): a marker of unclassified hepatocellular adenoma and high bleeding risk. *Hepatology* 2017; 66: 2016-28.
 24. Nault JC, Couchy G, Caruso S, et al. Argininosuccinate synthase 1 and periportal gene expression in sonic hedgehog hepatocellular adenomas. *Hepatology* 2018; 68: 964-76.
 25. Sala M, Gonzales D, Leste-Lasserre T, et al. ASS1 overexpression: a hallmark of sonic Hedgehog hepatocellular adenomas: recommendations for clinical practice. *Hepatol Commun* 2020; 4: 809-24.
 26. Singhi AD, Jain D, Kakar S, Wu TT, Yeh MM, Torbenson M. Reticulin loss in benign fatty liver: an important diagnostic pitfall when considering a diagnosis of hepatocellular carcinoma. *Am J Surg Pathol* 2012; 36: 710-5.
 27. Kim H, Park YN. Role of biopsy sampling for diagnosis of early and progressed hepatocellular carcinoma. *Best Pract Res Clin Gastroenterol* 2014; 28: 813-29.
 28. Di Tommaso L, Destro A, Seok JY, et al. The application of markers (HSP70 GPC3 and GS) in liver biopsies is useful for detection of hepatocellular carcinoma. *J Hepatol* 2009; 50: 746-54.
 29. Lagana SM, Salomao M, Bao F, Moreira RK, Lefkowitz JH, Remotti HE. Utility of an immunohistochemical panel consisting of glypican-3, heat-shock protein-70, and glutamine synthetase in the distinction of low-grade hepatocellular carcinoma from hepatocellular adenoma. *Appl Immunohistochem Mol Morphol* 2013; 21: 170-6.
 30. Choi WT, Kakar S. Atypical hepatocellular neoplasms: review of clinical, morphologic, immunohistochemical, molecular, and cytogenetic features. *Adv Anat Pathol* 2018; 25: 254-62.
 31. Evason KJ, Grenert JP, Ferrell LD, Kakar S. Atypical hepatocellular adenoma-like neoplasms with beta-catenin activation show cytogenetic alterations similar to well-differentiated hepatocellular carcinomas. *Hum Pathol* 2013; 44: 750-8.
 32. Kakar S, Evason KJ, Ferrell LD. Well-differentiated hepatocellular neoplasm of uncertain malignant potential: proposal for a new diagnostic category: reply. *Hum Pathol* 2014; 45: 660-1.
 33. Roncalli M, Sciarra A, Tommaso LD. Benign hepatocellular nodules of healthy liver: focal nodular hyperplasia and hepatocellular adenoma. *Clin Mol Hepatol* 2016; 22: 199-211.
 34. Laumonier H, Frulio N, Laurent C, Balabaud C, Zucman-Rossi J, Bioulac-Sage P. Focal nodular hyperplasia with major sinusoidal dilatation: a misleading entity. *BMJ Case Rep* 2010; 2010: bcr0920103311.
 35. Paradis V, Benzekri A, Dargere D, et al. Telangiectatic focal nodular hyperplasia: a variant of hepatocellular adenoma. *Gastroenterology* 2004; 126: 1323-9.
 36. Bioulac-Sage P, Rebouissou S, Sa Cunha A, et al. Clinical, morphologic, and molecular features defining so-called telangiectatic focal nodular hyperplasias of the liver. *Gastroenterology* 2005; 128: 1211-8.
 37. Bioulac-Sage P, Cubel G, Taouji S, et al. Immunohistochemical markers on needle biopsies are helpful for the diagnosis of focal nodular hyperplasia and hepatocellular adenoma subtypes. *Am J Surg Pathol* 2012; 36: 1691-9.
 38. Joseph NM, Ferrell LD, Jain D, et al. Diagnostic utility and limitations of glutamine synthetase and serum amyloid-associated protein immunohistochemistry in the distinction of focal nodular hyperplasia and inflammatory hepatocellular adenoma. *Mod Pathol* 2014; 27: 62-72.
 39. Agostini-Vulaj D, Sharma AK, Findeis-Hosey JJ, McMahon LA, Gonzalez RS. Distinction between inflammatory hepatocellular adenoma and mass effect on liver sampling. *Hum Pathol* 2017; 61: 105-10.
 40. Kim H, Lee H, Park YN. Loss of liver fatty acid binding protein expression in hepatocellular carcinomas is associated with a decreased recurrence-free survival. *J Liver Cancer* 2015; 15: 30-5.
 41. Liu L, Shah SS, Naini BV, et al. Immunostains used to subtype hepatic adenomas do not distinguish hepatic adenomas from hepatocellular carcinomas. *Am J Surg Pathol* 2016; 40: 1062-9.
 42. Torbenson M. Hepatic adenomas: classification, controversies, and consensus. *Surg Pathol Clin* 2018; 11: 351-66.
 43. Sasaki M, Yoneda N, Kitamura S, Sato Y, Nakanuma Y. A serum amyloid A-positive hepatocellular neoplasm arising in alcoholic cirrhosis: a previously unrecognized type of inflammatory hepatocellular tumor. *Mod Pathol* 2012; 25: 1584-93.
 44. Di Tommaso L, Franchi G, Park YN, et al. Diagnostic value of HSP70, glypican 3, and glutamine synthetase in hepatocellular nodules in cirrhosis. *Hepatology* 2007; 45: 725-34.

Molecular biomarker testing for non–small cell lung cancer: consensus statement of the Korean Cardiopulmonary Pathology Study Group

Sunhee Chang¹, Hyo Sup Shim², Tae Jung Kim³, Yoon-La Choi⁴, Wan Seop Kim⁵, Dong Hoon Shin⁶, Lucia Kim⁷, Heae Surng Park⁸, Geon Kook Lee⁹, Chang Hun Lee¹⁰, Korean Cardiopulmonary Pathology Study Group

¹Department of Pathology, Inje University Ilsan Paik Hospital, Goyang;

²Department of Pathology, Yonsei University College of Medicine, Seoul;

³Department of Hospital Pathology, College of Medicine, The Catholic University of Korea, Seoul;

⁴Department of Pathology, Samsung Medical Center, Sungkyunkwan University School of Medicine, Seoul;

⁵Department of Pathology, Konkuk University School of Medicine, Seoul;

⁶Department of Pathology, Pusan National University Yangsan Hospital, Yangsan;

⁷Department of Pathology, Inha University School of Medicine, Incheon;

⁸Department of Pathology, Ewha Womans University Seoul Hospital, Seoul;

⁹Department of Pathology, National Cancer Center, Goyang;

¹⁰Department of Pathology, Pusan National University Hospital, Pusan National University School of Medicine, Busan, Korea

Molecular biomarker testing is the standard of care for non–small cell lung cancer (NSCLC) patients. In 2017, the Korean Cardiopulmonary Pathology Study Group and the Korean Molecular Pathology Study Group co-published a molecular testing guideline which contained almost all known genetic changes that aid in treatment decisions or predict prognosis in patients with NSCLC. Since then there have been significant changes in targeted therapies as well as molecular testing including newly approved targeted drugs and liquid biopsy. In order to reflect these changes, the Korean Cardiopulmonary Pathology Study Group developed a consensus statement on molecular biomarker testing. This consensus statement was crafted to provide guidance on what genes should be tested, as well as methodology, samples, patient selection, reporting and quality control.

Key Words: Carcinoma, non-small-cell lung; Biomarker; Precision medicine; Consensus

Received: October 30, 2020 **Revised:** March 18, 2021 **Accepted:** March 23, 2021

Corresponding Author: Chang Hun Lee, MD, Department of Pathology, Pusan National University Hospital, Pusan National University School of Medicine, 179 Gudeok-ro, Seo-gu, Busan 49241, Korea

Tel: +82-51-240-7718, Fax: +82-51-242-7422, E-mail: cnlee@pusan.ac.kr

Since the IRESSA Pan-Asia Study demonstrated that epidermal growth factor receptor (*EGFR*) mutations are a predictive biomarker for response to *EGFR* tyrosine kinase inhibitor (TKI) therapy in non–small cell lung cancer (NSCLC) patients, biomarker testing has become the standard of care for NSCLC patients [1]. Currently, various targeted drugs and their predictive biomarkers have been approved by the Korea Ministry of Food and Drug Safety (MFDS) and U.S. Food and Drug Administration (FDA) (Table 1).

The Korean Cardiopulmonary Pathology Study Group (KCPSG) has developed molecular pathology guidelines to respond to these challenges [2-5]. In 2017, the KCPSG and the

Korean Molecular Pathology Study Group (KMPSG) jointly published a guideline for molecular testing, including almost all known genetic changes that aid in treatment decisions or predict prognosis in patients with NSCLC [4]. Since then, major changes have been made to targeted therapies and molecular tests, such as newly approved targeted drugs or liquid biopsies. In order to reflect recent changes, the KCPSG has crafted a consensus statement to address issues of which genes should be tested, methodology, samples, patient selection, reporting and quality control.

The purpose of this consensus statement is to provide standardized guidelines for molecular biomarker testing to help se-

Table 1. Consensus statement of the Korean Cardiopulmonary Pathology Study Group

1. Which genes should be tested in non-small cell lung cancer patients in Korea?
EGFR, *ALK*, *ROS1*, and *BRAF* tests must be performed. *NTRK*, *MET*, *RET*, *HER2*, and *KRAS* tests are recommended when the results of *EGFR*, *ALK*, *ROS1*, and *BRAF* tests are negative or as part of broad testing panels.
2. Which testing method should be used?
 Pathologists should use appropriate testing methods approved by Ministry of Food and Drug Safety for biomarker test.
3. Which samples can be used for molecular testing?
 Any adequate tissue and cytology samples are acceptable for molecular testing. Liquid biopsy can be used when tissue is insufficient or not available for *EGFR* mutation test. If plasma test is negative, tissue biopsy is recommended.
4. What samples are adequate for molecular testing?
 The minimum tumor cell content for proper analysis should be determined according to the analytic sensitivity of the testing method. Pathologist should pay attention to maximizing tumor cell content and the quality of nucleic acids for proper analysis.
5. Which patients should be tested?
 Molecular testing for targetable alterations should be performed in all patients with non-small cell lung cancer.
6. How should the results be reported?
 Reporting should follow the quality control guidance of the Korean Society of Pathologists and the Korean Institute of Genetic Testing Evaluations.
7. How should quality control be performed?
 Internal and external quality control programs should be regularly implemented in accordance with the regulations of the Korean Society of Pathologists and the Korean Institute of Genetic Testing Evaluations.

EGFR, epidermal growth factor receptor; *ALK*, anaplastic lymphoma kinase; *ROS1*, ros proto-oncogene 1 receptor tyrosine kinase; *BRAF*, serine/threonine-protein kinase B-raf; *NTRK*, neurotrophic tyrosine receptor kinase; *MET*, mesenchymal epithelial transition; *RET*, rearranged during transfection; *HER2*, human epidermal growth factor receptor 2; *KRAS*, Kirsten rat sarcoma virus.

lect NSCLC patients for targeted therapy in Korea. The KCPSG Molecular Testing Working Group reviewed and assessed existing guidelines developed by the KCPSG/KMPSG [4], the College of American Pathologists (CAP)/International Association for the Study of Lung Cancer (IASLC)/Association for Molecular Pathology (AMP) [6], the American Society of Clinical Oncology (ASCO) [7], and the National Comprehensive Cancer Network (NCCN) [8]. The workgroup endorsed most recommendations within the existing guidelines, but made minor modifications based on recent changes in targeted therapy as well as current Korean medical system (Table 1).

WHICH GENES SHOULD BE TESTED IN NON-SMALL CELL LUNG CANCER PATIENTS IN KOREA?

EGFR, *ALK*, *ROS1*, and *BRAF* tests must be performed; *NTRK*, *MET*, *RET*, *HER2*, and *KRAS* tests are recommended when the results of *EGFR*, *ALK*, *ROS1*, and *BRAF* tests are negative or as part of broad testing panels

The important oncogenic drivers in NSCLC are mutations of *EGFR*, anaplastic lymphoma kinase (*ALK*), ros proto-oncogene 1 receptor tyrosine kinase (*ROS1*), serine/threonine-protein kinase B-raf (*BRAF*), neurotrophic tyrosine receptor kinase (*NTRK*), mesenchymal epithelial transition (*MET*), rearranged during transfection (*RET*), human epidermal growth factor receptor 2 (*HER2*), and Kirsten rat sarcoma virus (*KRAS*) [9]. Of these, sensitizing *EGFR* mutations, *ALK* and *ROS1* fusions, *BRAF* V600E mutations, *NTRK* fusions, *MET* exon 14 skipping mu-

tations, and *RET* mutations or fusions, all have targeted drugs approved by the MFDS or FDA in NSCLC (Table 2). Targeted drugs for *HER2* mutations are currently being investigated in clinical trials [10].

Sensitizing *EGFR* mutations occur within the kinase domain in exons 18 to 21. In particular, exon 19 deletions and exon 21 substitutions such as L858R account for about 90% of *EGFR* sensitizing mutations [9]. *EGFR* mutations occur in 37% to 40% of adenocarcinoma [11-13] and 9% of squamous cell carcinoma in Korea [13]. *T790M* is the most common resistance mechanism to *EGFR* TKI and occurs in 43%–50% of patients with acquired resistance to gefitinib/erlotinib [14]. Third-generation *EGFR* TKIs such as osimertinib inhibit both *T790M* and *EGFR* sensitizing mutations. Afatinib, erlotinib, gefitinib, and osimertinib have received reimbursement-approval by MFDS and National Health Insurance Service (NHIS) for NSCLC patients with *EGFR* mutations.

ALK fusions occur in about 5% of NSCLC patients, primarily in young never-smokers with adenocarcinoma [3,9,15]. More than 20 different *ALK* fusion partners have been discovered, of which *EML4-ALK* is the most common fusion protein in NSCLC [3,9,15]. Alectinib, brigatinib, ceritinib, and crizotinib have received reimbursement-approval for NSCLC patients with *ALK* fusions.

ROS1 fusions are reported in 1%–2% of NSCLC patients, primarily in young never-smokers with adenocarcinoma [9]. *ROS1* is related to the *ALK* and insulin receptor superfamily. Because of high sequence homology to *ALK*, several *ALK* TKIs harbor dual inhibitory activity against *ALK* and *ROS1* [9]. Crizo-

Table 2. Targetable genetic alterations in non-small cell lung cancer patients

Gene	Alteration	Method	Approved drug
<i>EGFR</i>	Mutation (Ex21L858R, Ex19del, Ex18, Ex20)	RT-PCR, NGS (approved commercial test: PANAMutyper R <i>EGFR</i> ^a , Cobas <i>EGFR</i> Mutation Test v2 ^a , GenesWell dd <i>EGFR</i> Mutation Test, Oncomine Dx Target Test ^b)	Afatinib, erlotinib, gefitinib, osimertinib
<i>ALK</i>	Fusion	Immunohistochemistry, FISH, NGS (approved commercial test: Vysis <i>ALK</i> Break Apart FISH, <i>ALK</i> D5F3 CDx)	Alectinib, brigatinib, ceritinib, crizotinib
<i>ROS1</i>	Fusion	Immunohistochemistry ^c , FISH, RT-PCR, NGS (approved commercial test: AmoyDx <i>ROS1</i> Gene Fusions Detection Kit, <i>ROS1</i> SP384 Assay ^a , Oncomine Dx Target Test ^b)	Crizotinib
<i>BRAF</i>	V600E mutation	RT-PCR, NGS (approved commercial test: PNAclamp <i>BRAF</i> Mutation Detection kit ^b , Oncomine Dx Target Test ^b)	Dabrafenib+trametinib
<i>NTRK</i>	Fusion	Immunohistochemistry ^c , NGS (approved commercial test: pan-TRK EPR17341 Assay ^c)	Larotrectinib ^d , Entrectinib ^d
<i>MET</i>	Exon 14 skipping mutation	NGS	Crizotinib ^e , capmatinib ^f , tepotinib ^f
<i>RET</i>	Fusion, mutations	NGS	Selpercatinib ^f
<i>HER2</i>	Mutation (Ex20ins)	NGS	Trastuzumab ^e
TMB		NGS (approved commercial test: FoundationOne CDx)	Pembrolizumab ^f

EGFR, epidermal growth factor receptor; RT-PCR, real time polymerase chain reaction; NGS, next generation sequencing; *ALK*, anaplastic lymphoma kinase; FISH, fluorescent in situ hybridization; *ROS1*, ros proto-oncogene 1 receptor tyrosine kinase; *BRAF*, serine/threonine-protein kinase B-raf; *NTRK*, neurotrophic tyrosine receptor kinase; *MET*, mesenchymal epithelial transition; *RET*, rearranged during transfection; *HER2*, human epidermal growth factor receptor 2.

^aApproved for tissue and plasma; ^bApproved as new health technology; ^cFor screening; ^dNon-reimbursement approval; ^eApproval of non-reimbursement use of drugs exceeding the scope of product approval; ^fNot approved in Korea (as of March 17, 2021).

tinib has received reimbursement-approval for NSCLC patients with *ROS1* fusions.

BRAF is a serine/threonine kinase downstream of *KRAS* in the mitogen-activated protein kinase (MAPK) signaling pathway. *BRAF* mutations occur in 1%–2% of NSCLC patients and are mostly represented by V600E [9]. Specific clinical or pathological features associated with *BRAF* mutations have not defined. Compared to *BRAF* inhibitor monotherapy, treatment with combination *BRAF* and *MEK* inhibitors improved response rates and progression free survival due to delays in MAPK-driven acquired resistance as well as reduced toxicities from paradoxical MAPK pathway activation [8,9]. The combination therapy with *BRAF* and *MEK* inhibitors has received reimbursement-approval for NSCLC patients with *BRAF* V600E mutations.

NTRK encodes for three transmembrane proteins, *TRKA*, *TRKB*, and *TRKC*, which play an important role in central nervous system development and maturation [8,9]. *NTRK* fusions have been identified in several types of solid tumors and occur in less than 1% of NSCLC patients [8,9,16]. Larotrectinib received non-reimbursement-approved for the *NTRK*-positive solid tumors including NSCLC.

Genetic alterations in *MET* such as exon 14 skipping mutations, amplification, and protein overexpression, are functionally important in cell proliferation, migration, and invasion [8,9]. *MET* exon 14 skipping mutations occur in 3%–4% of adenocarcinoma and 1%–2% of other NSCLC histologies [8,9]. TKIs targeting *MET* are subdivided into multikinase such as crizo-

tinib and selective *MET* inhibitors such as tepotinib and capmatinib. Crizotinib, tepotinib, and capmatinib were granted breakthrough therapy status in 2018, 2019, and 2020, respectively, for the treatment of NSCLC patients with *MET* exon 14 skipping mutations by FDA. In Korea, crizotinib received approval for non-reimbursement use of drugs exceeding the scope of product approval.

RET fusions occur in 1%–2% of NSCLC and are more frequent in young never-smokers with adenocarcinomas [8,9]. Selpercatinib was granted breakthrough therapy status for the treatment of NSCLC patients with *RET* fusions by FDA in 2020. In Korea, ceritinib received approval for non-reimbursement use of drugs exceeding the scope of product approval.

HER2 amplification and mutations are found in up to 4% and 35%, respectively, of NSCLC [9]. Most *HER2* mutations occur in exon 20 and lead to uncontrolled signaling activation through the same pathways activated by *EGFR* [9]. To date, no specific *HER2* inhibitors have been approved and trials targeting *HER2* exon 20 mutations or gene amplification have been investigated [8,9]. In Korea, trastuzumab received approval for non-reimbursement use of drugs exceeding the scope of product approval.

KRAS mutations occur in about 25% of NSCLC [8,9]. *KRAS* mutations are mutually exclusive to other oncogenic driver mutations and allow the identification of patients who are unlikely to have targetable alterations [8,9]. Studies aimed at exploring effective targeted therapies for *KRAS* mutations have been performed, with a recent clinical trial for *KRAS* G12C inhibitors

showed promising results in preclinical and clinical settings [17]. The predictive role of *KRAS* mutations for response to chemotherapy, targeted therapy, anti-vascular therapy, or immunotherapy is currently controversial [17]. It is impractical to perform multiple single gene tests for all oncogenic drivers due to limited samples and as well as the financial burden on both patients and healthcare insurance. The 2018 CAP/IASLC/AMP guideline recommended that tests for *EGFR*, *ALK*, and *ROS1* must be offered by all laboratories as an absolute minimum [6]. *BRAF*, *MET*, *RET*, *HER2*, and *KRAS* should be included in any expanded panel if adequate material is available. All other genes can be considered for clinical trials at the time of publication. The 2018 ASCO guideline endorsed the CAP/IASLC/AMP guideline but added *BRAF* in the absolute minimum category [7]. This is because dabrafenib/trametinib combination therapy for NSCLC with *BRAF* v600E mutations was approved in 2017 by FDA [6], just after the 2018 CAP/IASLC/AMP guideline panel completed its literature review [7,18]. The 2020 NCCN guideline also recommended tests for *EGFR* (category 1), *ALK* (category 1), *ROS1* (category 2A), and *BRAF* (category 2A) [8]. The 2020 NCCN guideline added tests for *MET* (category 2A) and *RET* (category 2A) based on recent data showing the efficacy and FDA approval of corresponding TKIs [8]. For *HER2*, *KRAS*, and *NTRK*, NCCN guideline strongly advised broad molecular profiling (category 2A) [8].

The extent of what constitutes the absolute minimum of predictive biomarkers should be decided by the approval and reimbursement status of the corresponding targeted therapies in each country. In Korea, targeted drugs for NSCLC patients with *EGFR* mutations, *ALK* fusions, *ROS1* fusions, or *BRAF* V600E mutations received reimbursement-approval as of October 15, 2020 (Table 1). Thus, we recommend *EGFR*, *ALK*, *ROS1*, and *BRAF* tests must be performed for treatment decision in NSCLC patients. Targeting drug for *MET* exon 14 skipping mutations, *RET* fusions, and *HER2* mutations can be used only as non-reimbursement use of drugs exceeding the scope of product approval in NSCLC patients. *NTRK* TKI is approved as non-reimbursement. Therefore *MET*, *RET*, *HER2*, *KRAS*, and *NTRK* tests are recommended when the results of *EGFR*, *ALK*, *ROS1*, and *BRAF* tests are negative or as part of broad panels. Molecular testing for other genetic alterations can be performed for clinical trials.

Although not an oncogenic driver, tumor mutational burden (TMB) is an emerging biomarker for selection of patients with NSCLC for immunotherapy. TMB is defined as the number of mutations per megabase (Mb) of DNA [6,8,19]. In NSCLC,

smoking exposure and the associated genomic profile contribute significantly to high TMB [20]. Mutant proteins derived from somatic mutations produce neoantigens. Tumors with more neoantigens could elicit a stronger CD8 T-cell response in the presence of immunotherapy agents [20]. Therefore, TMB is considered a surrogate marker of neoantigen burden and therefore a predictive biomarker for immunotherapy. Several clinical trials have investigated tissue or blood based TMB as a predictive biomarker for immunotherapy [19]. The KEYNOTE-158 trials showed a higher response rate for patients with high TMB, which was defined as ≥ 10 mutations/Mb on a FoundationOne CDx assay (Foundation Medicine, Cambridge, MA, USA) to pembrolizumab [19,21].

WHICH TESTING METHOD SHOULD BE USED?

Pathologists should use appropriate testing methods approved by MFDS for biomarker test

It is important to consider the clinical utility, status of approval, and reimbursement in determining testing methods (Table 1). For *EGFR* testing, the CAP/ASCO/IASLC guideline recommended that testing methods must be able to detect molecular alterations in specimens with as little as 20% cancer cells. Furthermore, assays capable of detecting abnormality in as little as 5% tumor cells should be used for *EGFR* T790M mutation [6]. Recently developed polymerase chain reaction (PCR)-based methods such as real time PCR (RT-PCR) and digital PCR (dPCR) are more sensitive than Sanger sequencing and can reliably detect low frequency mutations in samples with as little as 5%–10% cancer cells. In Korea, peptide nucleic acid clamping RT-PCR (Panagene, Daejeon, Korea), Cobas *EGFR* Mutation test (Roche, Indianapolis, IN, USA), pyrosequencing, and next generation sequencing (NGS) are commonly used for *EGFR* mutation test. Recently, droplet digital PCR (dd*EGFR* mutation test, Gencurix Inc., Seoul, Korea) and targeted NGS panel (Thermo Fisher Scientific, Waltham, MA, USA) have been approved as new health technologies. Mutation specific immunohistochemistry (IHC) is not encouraged for detection of *EGFR* mutations because it has low sensitivity and recent advances in molecular technology enable the detection of mutations in limited amounts of sample [6,8]. *EGFR* gene amplification or total protein expression should not be used to select patients for *EGFR* TKIs [6].

For *ALK* fusions, fluorescent in situ hybridization (FISH) and IHC with *ALK* D5F3 CDx assay (Ventana Medical Systems Inc., Tucson, AZ, USA) are recommended [6,8,22]. Only Vysis *ALK* Break Apart FISH (Abbott Molecular Inc., Abbott Park,

IL, USA) received approval for selection of NSCLC patients for treatment with brigatinib. The ALK D5F3 CDx assay has an overall sensitivity of 81%–100% and specificity of 91%–100%. The ALK CDx is an equivalent alternative to ALK FISH [6,8,22]. The ALK CDx assay is widely used due to low cost, shorter turnaround time, and ease of use. It is important to understand several potential pitfalls of ALK CDx interpretation [22]. False positive staining, often weaker than true positive expression, may be seen in alveolar macrophages, airway epithelial cells, extracellular mucin, and necrotic debris. Tumor cells with neuroendocrine differentiation may show false positive staining although their expressions are typically heterogeneous or in a checkerboard pattern [22]. Therefore, samples with focal or equivocal expression are recommended to be retested with ALK FISH.

For *ROS1* fusions, AmoyDx *ROS1* gene fusions detection kit (Amoy Diagnostics Co., Xiamen, China) received approval for selection of NSCLC patients for crizotinib. FISH and NGS are available for detection of *ROS1* fusion but cannot be used for treatment decisions in Korea. *ROS1* IHC may be used as a screening test [8]. For *BRAF* V600E mutations, NGS and PNAClamp *BRAF* mutation detection kit (Panagene) can be used for treatment decision.

For other genetic alterations, the CAP/ASCI/IASLC guideline and NCCN guideline recommends that broad panels are preferred over multiple single gene tests to identify other treatment options [6,8]. We agree with this, and recommend NGS for *NTRK*, *MET*, *RET*, *HER2*, and *KRAS*. When NGS is not available, IHC may be used as a screening test for *NTRK* fusions and positive results should be confirmed by NGS [23]. NGS allows the assessment of many targetable genetic alterations from small samples at once [8,24]. Targeted NGS using amplicon resequencing enables the detection of point mutations with much higher sensitivity compared to single gene targeted tests [8,24]. NGS can detect gene fusions, in particular using an RNA-based approach [25]. Despite these advantages, NGS has not yet become a standard practice in Korea. NGS receives reimbursement only when performed by an approved medical institution. NGS is still more expensive than the sum of single gene tests for *EGFR*, *ALK*, *ROS1*, and *BRAF* as of 2020 in Korea. In addition, NGS is not approved for treatment decisions for NSCLC patients with *ROS1* or *ALK* fusions. A detailed laboratory guideline for NGS is beyond the scope of this paper (see Kim et al. [26] for guidelines and requirements for clinical NGS tests).

WHICH SAMPLES CAN BE USED FOR MOLECULAR TESTING?

Any adequate tissue and cytology samples are acceptable for molecular testing; Liquid biopsy can be used when tissue is insufficient or not available for *EGFR* mutation test; If plasma test is negative, tissue biopsy is recommended

The CAP, ASCO, and NCCN guidelines recommended that any tissue and cytology samples with adequate cellularity and preservation are suitable for molecular testing [6-8]. We agree this recommendation and encourage active utilization of cytology samples for molecular testing because patients with advanced lung cancer often cannot undergo tissue biopsy or, may have biopsies with insufficient tumor tissue.

Various cytology preparations including cell blocks, direct smears, cytopsin preparations, and liquid-based cytology are acceptable and reliable for biomarker testing [6-8]. Molecular testing results using cytology samples are highly concordant with those of the corresponding tissue samples, in particular with more sensitive methods [27-32]. A study comparing concurrently acquired fine needle aspiration and core needle biopsy samples showed better cellularity, higher tumor fraction, and higher mutation allelic frequencies in aspiration smears than biopsy samples [30]. It is important to understand the advantages and disadvantages of cytology samples for appropriate triaging of biomarker tests.

Formalin-fixed, paraffin-embedded (FFPE) cell blocks are widely used for molecular testing. The main advantage of cell blocks is to allow serial sections for multiple tests. Because most biomarker assays have been validated on FFPE samples, cell blocks do not require additional validation [33-38]. Compared to alcohol-fixed cytology samples, the limitations of cell blocks are due to formalin artifacts in DNA and nuclear truncation [33-36]. Formalin leads to cross-linking and chemical modification of nucleic acids which may affect DNA quality. In FISH, the presence of truncated nuclei in cellblock sections may result in artifactual loss of probe signal, as seen in conventional FFPE block [3]. Cell blocks often exhibit depletion of tumor cells on deeper sections.

Air dried or alcohol-fixed cytology samples such as smears and cytopsin may offer higher quality nucleic acids than cell blocks [33-38]. Smears, cytopsin, and liquid-based cytology allow an evaluation of the adequacy and cellularity of tumor cells on site and the opportunity to scrape tumor cells by macro/microdissection [33-38]. They enable the presentation of whole tumor nuclei for FISH [3]. The main limitation of smears is the sacri-

fic of archival stained slides. Whole slide imaging may be used for archiving cytology slides. The use of non-FFPE cytology samples may require further validation of molecular testing. ALK CDx has not been approved for non-FFPE cytology samples.

Tissue-based molecular testing is often not available in NSCLC patients due to the invasiveness and high risk of complications of biopsy procedures or due to insufficient tumor tissue obtained [5,39]. In addition, failure rate for re-biopsy was reported to be about 20% in NSCLC patients with progression or metastasis [40]. The liquid biopsy is a non-invasive way to detect genetic alterations. Tumor biopsies are often not able to encompass comprehensive genomic profiles due to tumor heterogeneity. However liquid biopsy is more likely representative of whole tumor clones because tumor DNA is constantly released into the bloodstream from all tumor sites [39,41]. Studies using various analytes such as circulating tumor cells, circulating tumor DNA (ctDNA), tumor educated platelets and tumor-derived exosomes obtained from blood or other body fluids have shown promising results for detection of genetic alterations in NSCLC patients. But, plasma ctDNA assay is only approved by MFDS and FDA. Plasma ctDNA testing for detection of *EGFR* mutations to select patients for EGFR TKIs has been covered in Korea since 2018.

The limitation of liquid biopsy is that ctDNA level is often extremely low and requires highly sensitive techniques. Moreover, germline cell free DNA (cfDNA) contamination from white cells could dilute ctDNA levels. In meta-analysis studies, the sensitivity of plasma ctDNA assay was about 67% [6,42]. The sensitivity can be increased up to 72% and 87% by use of more sensitive methods such as dPCR and NGS, respectively [42]. The specificity of plasma ctDNA assay was 96% for overall mutations and 80% for T790M [6,42]. The relatively low specificity could be in part, due to the high tumor heterogeneity, which can lead to false negative results in tissue tests [42]. This is supported by results of clinical trials showing that plasma T790M-positive patients had similar outcomes to tissue T790M-positive patients for osimertinib treatment [43,44]. Therefore, plasma testing should be performed in patients whose tissue material is unavailable or insufficient. And if plasma test is negative, repeat biopsy should be done for *EGFR* testing and other genetic alterations.

WHAT SAMPLES ARE ADEQUATE FOR MOLECULAR TESTING?

The minimum tumor cell content for proper analysis should be determined according to the analytic sensitivity of the testing method. Pathologist should pay attention to maximizing tumor cell content and the quality of nucleic acids for proper analysis

Sample adequacy is determined by the quantity and quality of tumor cells. The minimum tumor cell content for mutational testing is largely dependent on the analytic sensitivity of the testing method. Recently developed RT-PCR and dPCR techniques require samples with a minimum of 10% tumor cell content. However, in an unpublished survey of KCPSG, half of respondents said they performed *EGFR* tests even when tumor cell content was less than 10% or there were less than 200 tumor cells. Various approaches for tumor saving and enrichment enable the detection of genetic alterations even in samples with a tumor content less than the platform threshold [45].

The most commonly used strategy for tumor enrichment is manual macro/microdissection [45]. Pathologists review hematoxylin and eosin (H&E) stained slides and mark tumor areas directly on the slide. Subsequently, the corresponding areas are manually scraped off from the slides or procured directly from the block using the marked H&E slide as a guide. The EURTAC trial showed similar analytic accuracy in samples with less than or equal to 10% tumor content with microdissection, compared to samples with more than 10% without microdissection for *EGFR* test [46]. Samples with more than or equal to 30% tumor content in the dissected area showed good success rates of 95.6%, regardless of the size of the dissected area [31].

In small samples such as needle biopsy or cell block, tumor cell content is often limited and disappears on deeper sections. Thus, tumor saving is important for biomarker testing. The most effective tumor saving strategy is the pathologist ordered reflex test, in which the pathologist orders a predefined set of biomarker tests at the time of pathologic diagnosis [45,47]. In reflex testing, predefined tests are performed all at once using pre-cut unstained slides. This avoids tissue waste due to trimming or refacing and increases the quality of molecular testing [45,47-49]. In addition, this standardized and comprehensive approach by the pathologist led to reductions in turnaround time and an increase in the number of patients with biomarker testing results available at the time of treatment decision [48,49]. The limitation of reflex testing is that early-stage NSCLCs would be included. Several trials for adjuvant and neoadjuvant target therapy in early-stage NSCLC

patients are ongoing with promising preliminary results [50,51]. The aura 3 trial showed longer disease-free survival among those who received osimertinib than among those who received placebo in patients with stage II to IIIA *EGFR* mutation–positive NSCLC [51].

The second strategy for tissue saving is to make one block for one core for needle biopsy specimen. The one core-one block strategy also avoids unnecessary trimming and allows representative cross-sections of all tissue cores embedded in a single block [45]. Multiple blocks are distributed to appropriate tests according to the tumor cell content of individual blocks, allowing efficient use of the tissue [45]. Finally, IHC to distinguish between adenocarcinoma and squamous cell carcinoma should be minimized in small samples. Large IHC panels may not provide an advantage over a limited immunohistochemical workup using thyroid transcription factor 1 (or Napsin A) and p40 (or p63) [8,52].

ALK or ROS1 FISH requires a minimum of 50 to 100 viable tumor cells based on the interpretation guideline and if the result is equivocal, an additional 50 nuclei should be evaluated by the second reader [4]. It is recommended to avoid areas of necrosis and areas where the nuclear borders overlap or are indistinguishable from the adjacent stromal cells. If the tumor is very focal within the sample, the area to be examined on the slide can be marked for easy identification with a dark field fluorescence microscope. The ALK D5F3 CDx can be performed on FFPE samples with any tumor cells.

The important preanalytical factors affecting nucleic acid and protein quality are cold ischemia time, total fixation time, fixatives, and decalcification [53,54]. One hour or less of cold ischemia time (time between specimen removal from the body and its stabilization in formalin) is recommended [53,54]. Cold ischemia time of less than 1 hour for FISH, less than 2 hours for protein and RNA, and 24 hours or less for DNA have been reported to be acceptable [53]. The recommended fixative is 10% neutral, phosphate-buffered formalin. The 10% neutral buffered formalin is the most commonly used fixative for routine histology, providing excellent morphological preservation. Most IHC and molecular tests are validated for FFPE samples. Total fixation time of 6 to 24 hours is recommended. Fixation time of 6 to 24 hours for protein, 8 to 48 hours for RNA, and less than 72 hours for DNA is acceptable [53,54]. Strict quality control for concentration and pH of formalin and total fixation time is required to minimize formalin artifacts that can affect nuclei acid [54]. Of liquid based cytology preservative, CytoRich Red containing small amounts of formaldehyde may affect DNA yield [55]. Ethylenediaminetetraacetic acid (EDTA) is recom-

mended for decalcification, in particular for needle biopsy and small samples [56,57]. EDTA preserves morphology and nucleic acid but slowly decalcifies. Decalcifying agents containing strong acids do not yield adequate DNA for molecular testing but rapidly decalcify. Use of hydrochloric acid should be limited to large resection specimens such as rib and the ability to be cut with a blade should be monitored every day.

The ctDNA is rapidly degraded by nucleases and contaminated by non-tumor DNA from white cells in whole blood [5]. Therefore, plasma should be separated as quickly as possible after the blood draw. Specialized cfDNA stabilizing tubes can be used for longer storage times. For future analysis, plasma should be frozen in single use fractions until DNA extraction [54].

WHICH PATIENTS SHOULD BE TESTED?

Molecular testing for targetable alterations should be performed in all patients with non-small cell lung cancer

It is uncontroversial that molecular testing for targetable alterations should be performed in all patients with adenocarcinoma or an adenocarcinoma component [6-8]. For tumors with other histologies, the CAP guideline recommends that biomarker testing may be performed when clinical features, such as young age and never-smoker, indicate a higher probability of targetable alterations [6]. The ASCO guideline recommends biomarker testing for patients with nonsquamous NSCLC or with squamous cell carcinoma who are light or never-smokers or younger than 50 years of age [7]. The NCCN guideline recommends biomarker testing for patients with large cell carcinoma or NSCLC not otherwise specified (category 1) [8]. For squamous cell carcinoma, tests for *EGFR* and *ALK* should be considered in never-smokers or small biopsy specimens, or those with mixed histology (category 2A) and tests for *ROS1*, *BRAF*, *MET*, and *RET* should be considered in small biopsies or mixed histologies (category 2A) [8].

In squamous cell carcinoma, the frequency of *EGFR* mutations is about 7%–8% and *ALK* fusion occurs in less than 1% [13,58,59]. The detection of *EGFR* mutations in small samples diagnosed as squamous cell carcinoma may be a result of incomplete sampling of adenosquamous cell carcinoma [59-62]. Because of histologic heterogeneity, small biopsies and cytology samples may not be representative of the total tumor and an adenocarcinoma component cannot be completely excluded. Undersampling of adenosquamous cell carcinoma is possible even in resection specimens of which only representative sections are submitted for pathologic examination. Several studies have

shown that the adenocarcinoma component and squamous cell carcinoma component of most adenosquamous cell carcinomas shared genetic alterations including *EGFR* mutations [60,63]. Restriction to adenocarcinoma histology may exclude some patients with squamous cell carcinoma from the potential benefits of targeted therapy. Therefore, molecular testing for targetable alterations should be performed in all NSCLC to select patients for targeted therapy.

HOW SHOULD THE RESULTS BE REPORTED?

Reporting should follow the quality control guidance of the Korean Society of Pathologists and the Korean Institute of Genetic Testing Evaluations

Reporting on molecular tests should follow the quality control guidance of the Korean Society of Pathologists (KSP) and the Korean Institute of Genetic Testing Evaluations (KIGTE). Reporting should provide information the clinician needs for arriving at treatment decisions. When reporting *EGFR* mutations, the clinical significance of the results should be included (e.g., response to EGFR TKI, resistance to EGFR TKI, or limited data on response). The sample adequacy and any limitations of the testing methods should be included for correct interpretation of the result by the clinician.

HOW SHOULD QUALITY CONTROL BE PERFORMED?

Internal and external quality control programs should be regularly implemented in accordance with the regulations of the Korean Society of Pathologists and the Korean Institute of Genetic Testing Evaluations

Regular quality control is necessary to maintain a high degree of reliability in molecular testing. The KSP and KIGTE provide guidance on internal quality control. Laboratories should also be enrolled in an external quality control and quality improvement program of the KSP and the KIGTE.

FUTURE PERSPECTIVES

With advances in precision medicine, NGS will become a routine practice. Tumor samples are often too limited to enable the detection of all targetable alterations with multiple single genetic tests. And biomarkers such as TMB can only be tested with NGS. Targeted NGS can rapidly and comprehensively detect multiple genetic alterations and save tumor tissue. The cost of

NGS is dropping rapidly. However, issues of reimbursement and approval with regard to NGS will need to be resolved for lung cancer patients to benefit from this technology. In USA, FoundationOne CDx, Oncomine Dx Target Test (Thermo Fisher Scientific, Carlsbad, CA, USA), FoundationOne Liquid CDx (Foundation Medicine), and Guardant360 CDx (Guardant Health, Inc., Redwood City, CA, USA) are currently FDA approved NGS panels as companion diagnostics for NSCLC patients. FoundationOne CDx detects genetic alterations in 324 genes and provides information on microsatellite instability and TMB using DNA isolated from FFPE tissue. Oncomine Dx Target Test detects genetic alterations in 23 genes using DNA and fusions in *ROS1* using RNA from FFPE tissue. FoundationOne Liquid CDx and Guardant360 CDx detects on genetic alterations in 311 genes and 55 genes, respectively, using ctDNA from plasma. And these two panels have been utilized for evaluation of blood TMB in clinical trials [19].

TMB may be used as a biomarker for immunotherapy in the foreseeable future. Although the FDA has approved high TMB as a biomarker for pembrolizumab treatment of solid tumors, TMB is still considered an emerging biomarker for NSCLC patients in the NCCN guideline [8]. Different assays, platforms and cutoffs to assess TMB have been used in many clinical trials and retrospective analyses [64]. Therefore, standardization of TMB assessment is key to its use in clinical practice. The ctDNA analysis could be used as a monitoring tool for treatment responses as recent clinical trials have demonstrated a correlation between changes in, or clearance of plasma EGFR mutational burden with EGFR TKI response [19,65]. However, consensus on how to appropriately measure treatment response has not yet been established.

CONCLUSION

In the era of targeted therapies and personalized medicine, the role of the pathologists is important in the management of NSCLC patients. At a minimum, tests for *EGFR*, *ALK*, *ROS1*, and *BRAF* should be performed for treatment decisions in all NSCLC patients. In the near future, *NTRK*, *MET*, *RET*, *HER2*, and *KRAS* tests will also be mandatory tests. Although advances in technology allow the detection of molecular alterations not only in tissue and cytology samples but also in ctDNA, tumor sample limitations are still a major challenge for molecular testing. Pathologists should pay attention to tumor saving strategies and enrichment through standardized and comprehensive approaches. Pathologists must also utilize a regular quality control program for

reliable analyses. New targeted therapies, predictive biomarkers, and technologies are continually emerging. KCPSPG will keep pace with these advances through regular updates of these molecular guidelines for lung cancer patients.

Ethics Statement

Not applicable.

Availability of Data and Material

Data sharing not applicable to this article as no datasets were generated or analyzed during the study.

Code Availability

Not applicable.

ORCID

Sunhee Chang	https://orcid.org/0000-0002-7775-4711
Hyo Sup Shim	https://orcid.org/0000-0002-5718-3624
Tae Jung Kim	https://orcid.org/0000-0003-3140-3681
Yoon-La Choi	https://orcid.org/0000-0002-5788-5140
Wan Seop Kim	https://orcid.org/0000-0001-7704-5942
Dong Hoon Shin	https://orcid.org/0000-0002-4980-9295
Lucia Kim	https://orcid.org/0000-0002-4100-6607
Heae Surng Park	https://orcid.org/0000-0003-1849-5120
Geon Kook Lee	https://orcid.org/0000-0003-3138-3908
Chang Hun Lee	https://orcid.org/0000-0003-4216-2836

Author Contributions

Conceptualization: GKL, YLC, SC. Data curation: SC. Formal analysis: SC. Investigation: SC, HSS, TJK, YLC, WSK, DHS, LK, HSP. Methodology: SC, HSS, TJK. Project administration: SC. Supervision: CHL, YLC. Writing—original draft preparation: SC. Writing—review & editing: HSS, WSK, CHL. Approval of final manuscript: all authors.

Conflicts of Interest

The authors declare that they have no potential conflicts of interest.

Funding Statement

This research was supported by a 2-year research grant from Pusan National University.

References

1. Fukuoka M, Wu YL, Thongprasert S, et al. Biomarker analyses and final overall survival results from a phase III, randomized, open-label, first-line study of gefitinib versus carboplatin/paclitaxel in clinically selected patients with advanced non-small-cell lung cancer in Asia (IPASS). *J Clin Oncol* 2011; 29: 2866-74.
2. Shim HS, Chung JH, Kim L, et al. Guideline recommendations for EGFR mutation testing in lung cancer: proposal of the Korean Cardiopulmonary Pathology Study Group. *Korean J Pathol* 2013; 47: 100-6.
3. Kim H, Shim HS, Kim L, et al. Guideline recommendations for testing of *ALK* gene rearrangement in lung cancer: a proposal of the Korean Cardiopulmonary Pathology Study Group. *Korean J Pathol* 2014; 48: 1-9.
4. Shim HS, Choi YL, Kim L, et al. Molecular testing of lung cancers. *J Pathol Transl Med* 2017; 51: 242-54.
5. Shin DH, Shim HS, Kim TJ, et al. Provisional guideline recommendation for *EGFR* gene mutation testing in liquid samples of lung cancer patients: a proposal by the Korean Cardiopulmonary Pathology Study Group. *J Pathol Transl Med* 2019; 53: 153-8.
6. Lindeman NI, Cagle PT, Aisner DL, et al. Updated molecular testing guideline for the selection of lung cancer patients for treatment with targeted tyrosine kinase inhibitors: guideline from the College of American Pathologists, the International Association for the Study of Lung Cancer, and the Association for Molecular Pathology. *Arch Pathol Lab Med* 2018; 142: 321-46.
7. Kalemkerian GP, Narula N, Kennedy EB, et al. Molecular testing guideline for the selection of patients with lung cancer for treatment with targeted tyrosine kinase inhibitors: American Society of Clinical Oncology Endorsement of the College of American Pathologists/International Association for the Study of Lung Cancer/Association for Molecular Pathology clinical practice guideline update. *J Clin Oncol* 2018; 36: 911-9.
8. Ettinger DS, Wood DE, Aisner DL, et al. NCCN Clinical practice guidelines in oncology (NCCN Guidelines) for non-small cell lung cancer, version 8.2020 [Internet]. Plymouth Meeting: National Comprehensive Cancer Network, 2020 [cited 2020 Oct 15]. Available from: https://www.nccn.org/professionals/physician_gls/pdf/nscl.pdf.
9. Genova C, Rossi G, Tagliamento M, et al. Targeted therapy of oncogenic-driven advanced non-small cell lung cancer: recent advances and new perspectives. *Expert Rev Respir Med* 2020; 14: 367-83.
10. Del Re M, Cucchiara F, Petrini I, et al. *erbB* in NSCLC as a molecular target: current evidences and future directions. *ESMO Open* 2020; 5: e000724.
11. Yoon HY, Ryu JS, Sim YS, et al. Clinical significance of EGFR mutation types in lung adenocarcinoma: a multi-centre Korean study. *PLoS One* 2020; 15: e0228925.
12. Choi CM, Kim HC, Jung CY, et al. Report of the Korean Association of Lung Cancer Registry (KALC-R), 2014. *Cancer Res Treat* 2019; 51: 1400-10.
13. Lee SH, Kim WS, Choi YD, et al. Analysis of mutations in epidermal growth factor receptor gene in Korean patients with non-small cell lung cancer: summary of a nationwide survey. *J Pathol Transl Med* 2015; 49: 481-8.
14. Janne PA. Challenges of detecting *EGFR* T790M in gefitinib/erlotinib-resistant tumours. *Lung Cancer* 2008; 60 Suppl 2: S3-9.
15. Kwak EL, Bang YJ, Camidge DR, et al. Anaplastic lymphoma kinase inhibition in non-small-cell lung cancer. *N Engl J Med* 2010; 363: 1693-703.
16. Farago AE, Taylor MS, Doebele RC, et al. Clinicopathologic features of non-small-cell lung cancer harboring an *NTRK* gene fusion. *JCO Precis Oncol* 2018;2018:PO.18.00037.
17. Ghimessy A, Radeckzy P, Laszlo V, et al. Current therapy of *KRAS*-mutant lung cancer. *Cancer Metastasis Rev* 2020; 39: 1159-77.
18. Pennell NA, Arcila ME, Gandara DR, West H. Biomarker testing for patients with advanced non-small cell lung cancer: real-world issues and tough choices. *Am Soc Clin Oncol Educ Book* 2019; 39: 531-42.
19. Rolfo C, Cardona AF, Cristofanilli M, et al. Challenges and opportunities of cfDNA analysis implementation in clinical practice: perspective of the International Society of Liquid Biopsy (ISLB). *Crit Rev Oncol Hematol* 2020; 151: 102978.
20. Tafe LJ. Non-small cell lung cancer as a precision oncology para-

- digm: emerging targets and tumor mutational burden (TMB). *Adv Anat Pathol* 2020; 27: 3-10.
21. Marabelle A, Fakih M, Lopez J, et al. Association of tumour mutational burden with outcomes in patients with advanced solid tumours treated with pembrolizumab: prospective biomarker analysis of the multicohort, open-label, phase 2 KEYNOTE-158 study. *Lancet Oncol* 2020; 21: 1353-65.
 22. Uruga H, Mino-Kenudson M. ALK (D5F3) CDx: an immunohistochemistry assay to identify ALK-positive NSCLC patients. *Pharmacogenomics Pers Med* 2018; 11: 147-55.
 23. Marchio C, Scaltriti M, Ladanyi M, et al. ESMO recommendations on the standard methods to detect NTRK fusions in daily practice and clinical research. *Ann Oncol* 2019; 30: 1417-27.
 24. Ku BM, Heo MH, Kim JH, et al. Molecular screening of small biopsy samples using next-generation sequencing in Korean patients with advanced non-small cell lung cancer: Korean Lung Cancer Consortium (KLCC-13-01). *J Pathol Transl Med* 2018; 52: 148-56.
 25. Bruno R, Fontanini G. Next generation sequencing for gene fusion analysis in lung cancer: a literature review. *Diagnostics (Basel)* 2020; 10: 521.
 26. Kim J, Park WY, Kim NK, et al. Good laboratory standards for clinical next-generation sequencing cancer panel tests. *J Pathol Transl Med* 2017; 51: 191-204.
 27. Lee SE, Lee SY, Park HK, et al. Detection of *EGFR* and *KRAS* mutation by pyrosequencing analysis in cytologic samples of non-small cell lung cancer. *J Korean Med Sci* 2016; 31: 1224-30.
 28. Sun PL, Jin Y, Kim H, Lee CT, Jheon S, Chung JH. High concordance of *EGFR* mutation status between histologic and corresponding cytologic specimens of lung adenocarcinomas. *Cancer Cytopathol* 2013; 121: 311-9.
 29. Asaka S, Yoshizawa A, Nakata R, et al. Utility of bronchial lavage fluids for epithelial growth factor receptor mutation assay in lung cancer patients: comparison between cell pellets, cell blocks and matching tissue specimens. *Oncol Lett* 2018; 15: 1469-74.
 30. Roy-Chowdhuri S, Chen H, Singh RR, et al. Concurrent fine needle aspirations and core needle biopsies: a comparative study of substrates for next-generation sequencing in solid organ malignancies. *Mod Pathol* 2017; 30: 499-508.
 31. Shiau CJ, Babwah JP, da Cunha Santos G, et al. Sample features associated with success rates in population-based *EGFR* mutation testing. *J Thorac Oncol* 2014; 9: 947-56.
 32. da Cunha Santos G, Wyeth T, Reid A, et al. A proposal for cellularity assessment for *EGFR* mutational analysis with a correlation with DNA yield and evaluation of the number of sections obtained from cell blocks for immunohistochemistry in non-small cell lung carcinoma. *J Clin Pathol* 2016; 69: 607-11.
 33. Roy-Chowdhuri S, Aisner DL, Allen TC, et al. Biomarker testing in lung carcinoma cytology specimens: a perspective from members of the Pulmonary Pathology Society. *Arch Pathol Lab Med* 2016; 140: 1267-72.
 34. Lozano MD, Echeveste JI, Abengozar M, et al. Cytology smears in the era of molecular biomarkers in non-small cell lung cancer: doing more with less. *Arch Pathol Lab Med* 2018; 142: 291-8.
 35. Jain D, Roy-Chowdhuri S. Molecular pathology of lung cancer cytology specimens: a concise review. *Arch Pathol Lab Med* 2018; 142: 1127-33.
 36. da Cunha Santos G, Saieg MA, Troncone G, Zeppa P. Cytological preparations for molecular analysis: a review of technical procedures, advantages and limitations for referring samples for testing. *Cytopathology* 2018; 29: 125-32.
 37. Auger M, Brimo F, Kanber Y, Fiset PO, Camilleri-Broet S. A practical guide for ancillary studies in pulmonary cytologic specimens. *Cancer Cytopathol* 2018; 126 Suppl 8: 599-614.
 38. Aisner DL. The revised College of American Pathologists/International Association for the Study of Lung Cancer/Association for Molecular Pathology guideline: a step forward for molecular cytopathology. *Arch Pathol Lab Med* 2018; 142: 684-5.
 39. Chang S, Hur JY, Choi YL, Lee CH, Kim WS. Current status and future perspectives of liquid biopsy in non-small cell lung cancer. *J Pathol Transl Med* 2020; 54: 204-12.
 40. Nosaki K, Satouchi M, Kurata T, et al. Re-biopsy status among non-small cell lung cancer patients in Japan: a retrospective study. *Lung Cancer* 2016; 101: 1-8.
 41. Siravegna G, Marsoni S, Siena S, Bardelli A. Integrating liquid biopsies into the management of cancer. *Nat Rev Clin Oncol* 2017; 14: 531-48.
 42. Passiglia F, Rizzo S, Di Maio M, et al. The diagnostic accuracy of circulating tumor DNA for the detection of *EGFR*-T790M mutation in NSCLC: a systematic review and meta-analysis. *Sci Rep* 2018; 8: 13379.
 43. Oxnard GR, Thress KS, Alden RS, et al. Association between plasma genotyping and outcomes of treatment with osimertinib (AZD9291) in advanced non-small-cell lung cancer. *J Clin Oncol* 2016; 34: 3375-82.
 44. Remon J, Caramella C, Jovelet C, et al. Osimertinib benefit in *EGFR*-mutant NSCLC patients with T790M-mutation detected by circulating tumour DNA. *Ann Oncol* 2017; 28: 784-90.
 45. Aisner DL, Rumery MD, Merrick DT, et al. Do more with less: tips and techniques for maximizing small biopsy and cytology specimens for molecular and ancillary testing: the University of Colorado Experience. *Arch Pathol Lab Med* 2016; 140: 1206-20.
 46. Cobas *EGFR* mutation test v2 [Internet]. Silver Spring: U.S. Food and Drug Administration, 2020 [cited 2020 Oct 15]. Available from: https://www.accessdata.fda.gov/cdrh_docs/pdf12/P120019S007c.pdf.
 47. Lim C, Sekhon HS, Cutz JC, et al. Improving molecular testing and personalized medicine in non-small-cell lung cancer in Ontario. *Curr Oncol* 2017; 24: 103-10.
 48. Anand K, Phung TL, Bernicker EH, Cagle PT, Olsen RJ, Thomas JS. Clinical utility of reflex ordered testing for molecular biomarkers in lung adenocarcinoma. *Clin Lung Cancer* 2020; 21: 437-42.
 49. Cheema PK, Menjak IB, Winterton-Perks Z, et al. Impact of reflex *EGFR*/ *ALK* testing on time to treatment of patients with advanced nonsquamous non-small-cell lung cancer. *J Oncol Pract* 2017; 13: e130-8.
 50. Indini A, Rijavec E, Bareggi C, Grossi F. Novel treatment strategies for early-stage lung cancer: the oncologist's perspective. *J Thorac Dis* 2020; 12: 3390-8.
 51. Wu YL, Tsuboi M, He J, et al. Osimertinib in resected *EGFR*-mutated non-small-cell lung cancer. *N Engl J Med* 2020; 383: 1711-23.
 52. Pelosi G, Fabbri A, Bianchi F, et al. DeltaNp63 (p40) and thyroid transcription factor-1 immunoreactivity on small biopsies or cell-blocks for typing non-small cell lung cancer: a novel two-hit, sparing-material approach. *J Thorac Oncol* 2012; 7: 281-90.
 53. Bass BP, Engel KB, Greytak SR, Moore HM. A review of preanalytical factors affecting molecular, protein, and morphological analysis

- of formalin-fixed, paraffin-embedded (FFPE) tissue: how well do you know your FFPE specimen? *Arch Pathol Lab Med* 2014; 138: 1520-30.
54. Compton CC, Robb JA, Anderson MW, et al. Preanalytics and precision pathology: pathology practices to ensure molecular integrity of cancer patient biospecimens for precision medicine. *Arch Pathol Lab Med* 2019; 143: 1346-63.
 55. Dejmek A, Zendehrokh N, Tomaszewska M, Edsjo A. Preparation of DNA from cytological material: effects of fixation, staining, and mounting medium on DNA yield and quality. *Cancer Cytopathol* 2013; 121: 344-53.
 56. Miquelestorena-Standley E, Jourdan ML, Collin C, et al. Effect of decalcification protocols on immunohistochemistry and molecular analyses of bone samples. *Mod Pathol* 2020; 33: 1505-17.
 57. Choi SE, Hong SW, Yoon SO. Proposal of an appropriate decalcification method of bone marrow biopsy specimens in the era of expanding genetic molecular study. *J Pathol Transl Med* 2015; 49: 236-42.
 58. COSMIC (catalogue of somatic mutations in cancer) [Internet]. COSMIC, 2020 [cited 2020 Oct 15]. Available from: <https://cancer.sanger.ac.uk/cosmic>.
 59. Wang H, Sun L, Sang Y, et al. A study of ALK-positive pulmonary squamous-cell carcinoma: From diagnostic methodologies to clinical efficacy. *Lung Cancer* 2019; 130: 135-42.
 60. Paik PK, Varghese AM, Sima CS, et al. Response to erlotinib in patients with EGFR mutant advanced non-small cell lung cancers with a squamous or squamous-like component. *Mol Cancer Ther* 2012; 11: 2535-40.
 61. Dragnev KH, Gehr G, Memoli VA, Tafe LJ. *ALK*-rearranged adenosquamous lung cancer presenting as squamous cell carcinoma: a potential challenge to histologic type triaging of NSCLC biopsies for molecular studies. *Clin Lung Cancer* 2014; 15: e37-40.
 62. Mamesaya N, Nakashima K, Naito T, Nakajima T, Endo M, Takahashi T. *ALK*-rearranged lung squamous cell carcinoma responding to alectinib: a case report and review of the literature. *BMC Cancer* 2017; 17: 471.
 63. Lin G, Li C, Li PS, et al. Genomic origin and EGFR-TKI treatments of pulmonary adenosquamous carcinoma. *Ann Oncol* 2020; 31: 517-24.
 64. Sholl LM, Hirsch FR, Hwang D, et al. The promises and challenges of tumor mutation burden as an immunotherapy biomarker: a perspective from the International Association for the Study of Lung Cancer Pathology Committee. *J Thorac Oncol* 2020; 15: 1409-24.
 65. Sakai K, Takahama T, Shimokawa M, et al. Predicting osimertinib-treatment outcomes through *EGFR* mutant-fraction monitoring in the circulating tumor DNA of *EGFR* T790M-positive patients with non-small cell lung cancer (WJOG8815L). *Mol Oncol* 2021; 15: 126-37.

Identification of PI3K-AKT signaling as the dominant altered pathway in intestinal type ampullary cancers through whole-exome sequencing

Niraj Kumari^{1,4}, Rajneesh K. Singh², Shravan K. Mishra¹, Narendra Krishnani¹, Samir Mohindra³, Raghvendra L.¹

Departments of ¹Pathology, ²Surgical Gastroenterology, and ³Gastroenterology, Sanjay Gandhi Postgraduate Institute of Medical Sciences, Lucknow; ⁴Department of Pathology & Lab Medicine, All India Institute of Medical Sciences, Raebareilly, India

Background: The genetic landscape of intestinal (INT) and pancreatobiliary (PB) type ampullary cancer (AC) has been evolving with distinct as well as overlapping molecular profiles. **Methods:** We performed whole-exome sequencing in 37 cases of AC to identify the targetable molecular profiles of INT and PB tumors. Paired tumor-normal sequencing was performed on the HiSeq 2500 Illumina platform. **Results:** There were 22 INT, 13 PB, and two cases of mixed differentiation of AC that exhibited a total of 1,263 somatic variants in 112 genes (2–257 variants/case) with 183 somatic deleterious variants. INT showed variations in 78 genes (1–31/case), while PB showed variations in 51 genes (1–29/case). Targetable mutations involving one or more major pathways were found in 86.5% of all ACs. Mutations in *APC*, *CTNNB1*, *SMAD4*, *KMT2*, *EPHA*, *ERBB*, and Notch genes were more frequent in INT tumors, while chromatin remodeling complex mutations were frequent in PB tumors. In the major signaling pathways, the phosphoinositide 3-kinase (PI3)/AKT and RAS/mitogen-activated protein kinase (MAPK) pathways were significantly mutated in 70% of cases (82% INT, 46% PB, $p = .023$), with PI3/AKT mutation being more frequent in INT and RAS/MAPK in PB tumors. Tumor mutation burden was low in both differentiation types, with 1.6/Mb in INT and 0.8/Mb in PB types ($p = .217$). **Conclusions:** The exome data suggest that INT types are genetically more unstable than PB and involve mutations in tumor suppressors, oncogenes, transcription factors, and chromatin remodeling genes. The spectra of the genetic profiles of INT and PB types suggested primary targeting of PI3/AKT in INT and RAS/RAF and PI3/AKT pathways in PB carcinomas.

Key Words: Ampullary; Exome; Intestinal; Pancreatobiliary

Received: October 7, 2020 **Revised:** January 11, 2021 **Accepted:** January 23, 2021

Corresponding Author: Niraj Kumari, MD, Department of Pathology & Lab Medicine, All India Institute of Medical Sciences, Raebareilly-229405, UP, India
 Tel: +91-5222495236, Fax: +91-5222268017, E-mail: nirajpath@gmail.com

Cancers arising from the ampulla of Vater, though designated as one entity of ampullary cancer (AC), are heterogeneous at morphological and molecular levels as well as in clinical behavior. The ampulla is a common channel formed by joining of the common bile duct and pancreatic duct that opens onto the intestinal (INT) surface, involving cancers arising from biliary, pancreatic ductal, or INT epithelium. These cancers exhibit complex morphological and molecular characteristics and can be located within the ampulla, be exophytic on the INT surface as a papillary lesion, or present as an infiltrative/stricturous lesion involving the ampullary bulb [1]. AC is a rare cancer and accounts for less than 1% of all gastrointestinal malignancies [2,3]. INT and pancreatobiliary (PB) differentiation exhibit distinct relationships with prognosis, where PB behaves aggressively compared to the INT phenotype [4]. The two differentiation types respond differently

to chemotherapy [5-7]. The genomic biology and behavior of AC from India has not been well-studied. The genetic landscape of AC is evolving and has not been fully elucidated. In this study, we present the molecular profile of AC and the spectrum of genetic alterations in INT and PB differentiation.

MATERIALS AND METHODS

Fresh tumor tissues from 38 consecutive cases of AC and paired blood samples as normal controls were included for whole-exome sequencing (WES). Fresh specimens of pancreatoduodenectomy were received in the pathology department, where the tumor content was estimated on frozen sections, and 3–5 mm tumor tissue in its greatest dimension was stored at -80°C before processing for WES. Following this, the speci-

men was fixed in 10% buffered formalin and processed for routine histopathology.

Histopathology

All the cases were histologically evaluated for tumor grade, depth of infiltration (pT category, American Joint Committee on Cancer 8th edition), lymphovascular invasion, perineural invasion (PNI), lymph node metastasis, and distant metastasis. The differentiation of tumors was categorized as INT, PB, or mixed according to the criteria of Kimura et al. [8] and later modified by Albores-Saveedra et al. [9]. The INT differentiation was similar to that of colorectal cancers with glands lined by tall columnar epithelial cells having elongated basally located nuclei frequently displaying pseudo-stratification and occasional apical mucin. The PB differentiation resembled pancreatic cancer with simple small glands and cuboidal to low columnar epithelium, markedly pleomorphic nuclei with or without nuclear pseudo-stratification, and intense desmoplastic reactions. Cases with > 30% of both subtypes were classified as mixed differentiation. Immunohistochemistry (IHC) for differentiation (INT: CDX2, cytokeratin [CK] 20, MUC2; PB: CK7, CK17, MUC1) was used in cases with mixed histological differentiation, which then were re-categorized into INT and PB subtypes. Those with equivocal IHC results were retained as mixed differentiation which histologically required any one of the differentiation types to be > 30%, but < 70% of the overall tumor area [10].

Whole-exome sequencing

DNA was extracted from fresh tissue and blood using a Qia-gen GeneRead FFPE kit (Qiagen, Hilden, Germany), and the quality was assessed on QIAXPERT and Cubit. The Agilent Sure Select XT Kit (V5 + UTR) (Agilent Technologies, Santa Clara, CA, USA) was used for library preparation, and sequencing was

performed on the HiSeq 2500 Illumina platform (Illumina, San Diego, CA, USA) with a mean coverage of 100× for blood DNA and 200× for tumor tissue DNA.

Variant analysis

The bioinformatics tools used for alignment were BWA, GATK, SAM, and PICARD. For variant calling and annotation, Strelka, VariMAT, and OncoMD were used. Variant effect prediction was analyzed using Polyphen2, SIFT, Mutation Assessor, CONDEL, PhyloP, FATHMM, and SiPhy.

Functional, structural, and pathway analysis

Functional, structural, and pathway analyses of the mutated genes were studied with Gene Ontology software using the PANTHER (Protein Analysis Through Evolutionary Relationships) classification system and Reactome ver. 72.

Validation of the five most frequent mutations was performed by real-time polymerase chain reaction (PCR) and deep targeted sequencing.

RESULTS

Thirty-eight cases of AC were analyzed by WES. One case was excluded from the study because the blood DNA failed quality control before library preparation. The rest of the 37 cases that were successfully sequenced and analyzed for WES were composed of 26 males and 11 females with an age range of 24–76 years (mean, 53.4 years; median, 54 years).

Histological differentiation was categorized as INT (Fig. 1A, B) in 21 cases and PB (Fig. 2A, B) in 12 cases, along with mixed differentiation in four cases according to the morphological criteria. IHC exhibited expression of INT markers (CDX2, CK20, and MUC2) (Fig. 3) in one case and PB markers (CK7, CK17,

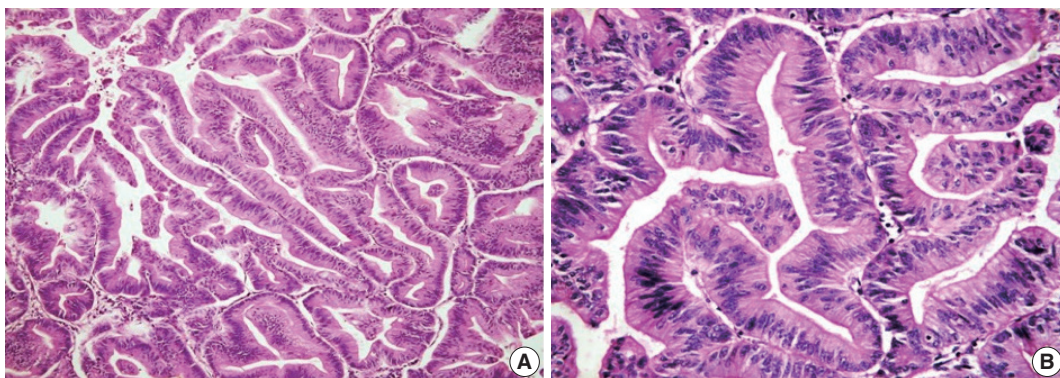


Fig. 1. Microphotograph of intestinal differentiation. Low-power (A) and high-power (B) views showing tall columnar cells with elongated to oblong basal nuclei and nuclear stratification.

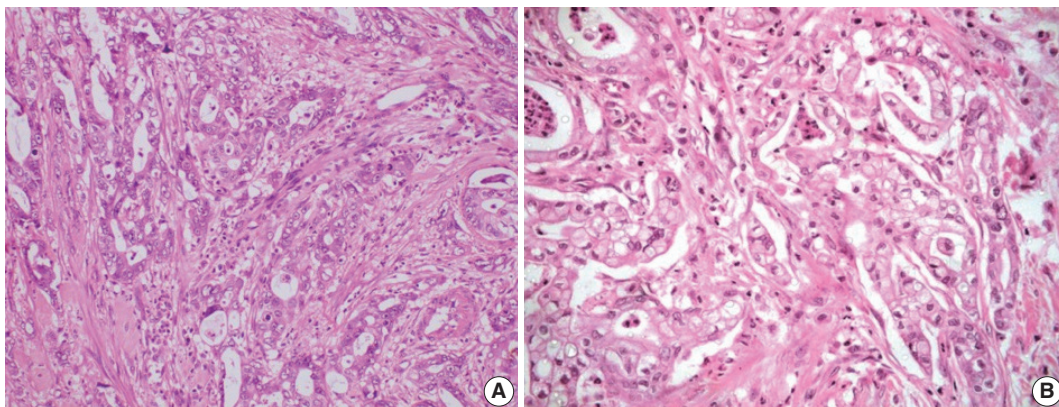


Fig. 2. Microphotograph of pancreatobiliary differentiation. Low-power (A) and high-power (B) views showing cuboidal to low columnar cells with rounded centrally placed nuclei with no nuclear stratification. Desmoplastic stroma can be observed between the tumor glands.

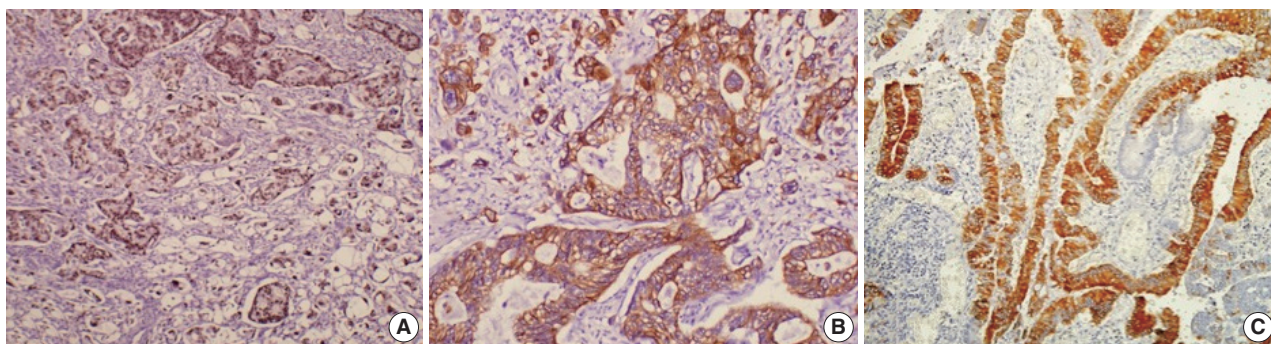


Fig. 3. Immunohistochemical stains (A, CDX2; B, cytokeratin 20; C, MUC2) expressed in the intestinal type of ampullary cancer.

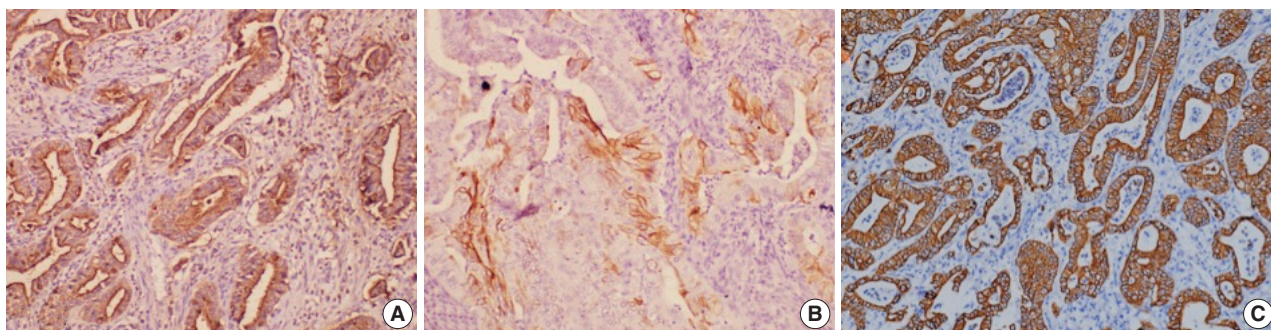


Fig. 4. Immunohistochemical stains (A, MUC1; B, cytokeratin [CK] 17; C, CK7) expressed in the pancreatobiliary type of ampullary cancer.

and MUC1) (Fig. 4) in another case. Two cases of mixed differentiation with overlapping expression of IHC markers were kept in the mixed category. Therefore, with the combined morphology and IHC panel, 22 cases were classified as INT, 13 cases as PB, and two cases as mixed differentiation. The correlations of different histological parameters with INT and PB differentiation are shown in Table 1. Lower tumor pathological (T-) category was significantly associated with INT differentiation, and high PNI was associated with PB differentiation.

Whole-exome analysis

The overall read alignment was approximately 99.97%, and the average passed alignment (percentage of reads aligning to hg19) was 97% for all samples. The average on-target coverage was approximately 85.67%. Read depth for each variant ranged between 10–560 (mean coverage 100×) in blood DNA and between 1–378 (mean coverage 200×) for tumor DNA. The variants present in blood were subtracted from the tumor tissue variants to exclude the germline variants present in these 37 pa-

tients. Variants present only in the coding regions were included in further analysis (Fig. 5).

The number of total somatic variants in tumor DNA ranged

Table 1. Histological characteristics of ampullary carcinoma according to histological differentiation

Feature	Intestinal (n=22)	Pancreatobiliary (n=13)	p-value
Sex			0.142
Male	14 (63.6)	11 (84.6)	
Female	8 (36.4)	2 (15.4)	
Tumor grade			0.128
Well	18 (81.8)	7 (53.8)	
Moderate	3 (13.6)	3 (23.1)	
Poor	1 (4.6)	3 (23.1)	
Tumor grade grouping			0.091
Well + moderate	21 (95.5)	10 (77.0)	
Poor	1 (4.5)	3 (23.0)	
T category			0.006
T1	7 (31.8)	1 (7.7)	
T2	8 (36.4)	0	
T3	7 (31.8)	12 (92.3)	
T category grouping			0.152
T1	7	1	
T2 + T3	15	12	
PNI	3 (13.6)	9 (69.2)	0.001
LVI	4 (18.2)	3 (22.7)	0.643
Nodal metastasis	5 (22.7)	4 (30.8)	0.371
TNM stage			0.062
Stage I	10 (45.5)	1 (7.7)	
Stage II	7 (31.8)	8 (61.5)	
Stage III	5 (22.7)	4 (30.8)	

Values are presented as number (%). PNI, perineural invasion; LVI, lymphovascular invasion.

from 14 to 30,153. Somatic variants having fewer than 50 reads and a mutant allele frequency <5% were excluded from the analysis, after which 1,263 somatic variants were observed, with 2 to 257 variants per patient. Furthermore, after excluding non-deleterious variants, there were 183 variants across 112 genes, with 78 exhibiting variations in INT and 51 in PB differentiation (Supplementary Table S1). Five cases (four cases with PB and one case with INT differentiation) did not show any deleterious somatic variant. In the 32 remaining patients, deleterious

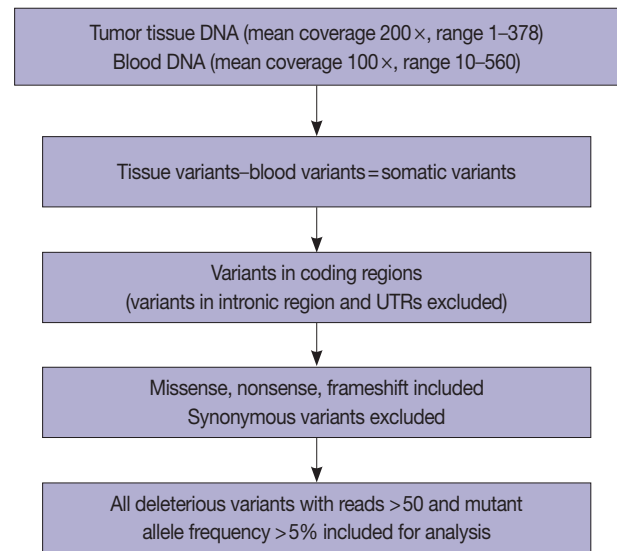


Fig. 5. Schema representing the workflow for whole-exome sequencing and data analysis. UTR, untranslated region.

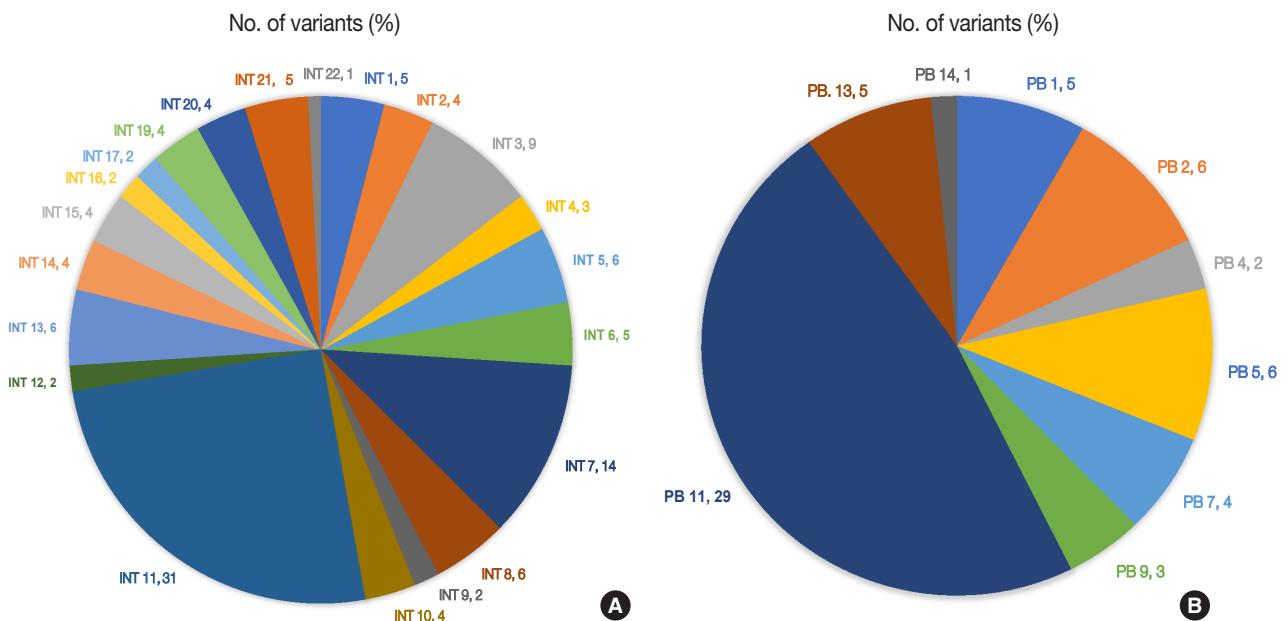


Fig. 6. (A) Deleterious somatic variants in intestinal (INT) ampullary cancers. (B) Deleterious somatic variants in pancreatobiliary (PB) ampullary cancers.

variants ranged from 1 to 31 per patient in patients with INT differentiation and 1 to 29 per patient in patients with PB differentiation (Fig. 6A, B). In the two cases that had mixed differentiation, both showed mutations in *KRAS*, while mutations in *SMAD4*, *KEAP1*, *STK11*, and *CSFR1* were found in either of the two cases (Supplementary Table S2). Five of the genes that showed mutations in at least 10% or more of patients (*APC*, 20.5%; *CTNNB1*, 10.2%; *KRAS*, 25.6%; *SMAD4*, 20.5%; *TP53*, 33.3%) were validated by real-time PCR and/or targeted next-generation sequencing. The WES revealed targetable mutations in genes involved in one or more major pathways in cancer in 86.5% of all patients with AC of both INT and PB subtypes. KMT2 complex, *APC*, *SMAD4*, *EPHA* complex, *ERBB* complex, and Notch complex of genes were mutated at a higher frequency in INT types of AC compared to PB types, in that decreasing order, even though the difference was not statistically significant (Table 2). *TP53* and *KRAS* were mutated nearly equally in INT and PB differentiation.

Functional, structural, and pathway analyses of variants in INT and PB subtypes

Functional, structural, and pathway analyses of the mutated genes were compared between INT and PB subtypes of AC. The number of genes responsible for different cellular components such as organelles and protein-containing complexes were mutated more frequently in INT than PB subtype, whereas it was similar for both subtypes for genes coding membrane and cell junctions (Fig. 7A).

In the group of genes coding for different classes of proteins, mutations were frequent in the INT subtype compared to the PB subtype, whereas the genes responsible for transcription factors,

receptors, and hydrolases were mutated more frequently in the PB subtype (Fig. 7B). The gene coding proteins involved in defense and immunity were mutated in the PB subtype. In relation to different biological functions and processes, mutations in genes coding cellular and metabolic processes and biological regulation were slightly higher in the INT subtype than the PB subtype. Mutations in genes responsible for transcription regulation were significantly more frequent in the PB subtype, while those for binding and catalytic activity were marginally higher in the INT subtype (Fig. 7C).

Analysis of the signaling pathways revealed 31 signaling cascades that were significantly mutated ($p > .002$) in AC (Fig. 8). We divided the signaling pathways into six major groups of TP53, RAS-RAF-mitogen-activated protein kinase (MAPK), PI3-AKT, WNT, transforming growth factor β (TGF- β), and chromatin remodeling pathways, similar to Yachida et al. [11] and Gingras et al. [12]. The combined RAS-RAF-MAPK/PI3-AKT pathway was most frequently altered, in 70% of AC with ~82% in INT differentiation and 46% in PB differentiation ($p = .021$). This was followed by TP53 (~38%), WNT signaling (~32%), TGF- β (24%), and the chromatin remodeling complex pathway (16%). The PI3-AKT pathway was mutated predominantly in the INT type (63.6%), while the RAS-RAF-MAPK pathway was most frequently mutated in PB differentiation (59.1%). The next most common pathways to be mutated in the INT type were RAS-RAF-MAPK in 59.1%, WNT in 45.4%, TP53 in 41.0%, TGF- β in 22.7%, and the chromatin remodeling complex pathway in 13.6% of cases. On the other hand, PB differentiation harbored mutations predominantly in the RAS-RAF-MAPK pathway (46.2%), followed by TP53 (38.4%), PI3-AKT (30.7%), TGF- β (22.7%), chromatin remodeling complex

Table 2. Most commonly mutated targetable genes in patients with intestinal or pancreatobiliary differentiation

Gene	Total mutation frequency (n=37)	Intestinal differentiation (n=22)	Pancreatobiliary differentiation (n=13)	p-value
<i>TP53</i>	12 (32.4)	8 (36.4)	4 (30.7)	0.724
<i>KRAS</i>	10 (27.0)	5 (22.7)	3 (23.1)	0.903
<i>ERBB</i> family	6 (16.2)	4 (18.2)	2 (15.4)	0.840
<i>SMAD4</i>	8 (21.6)	5 (22.7)	2 (15.4)	0.604
<i>APC</i>	7 (18.9)	6 (27.3)	1 (7.8)	0.185
<i>CTNNB1</i>	4 (10.8)	3 (13.6)	1 (7.8)	0.541
KMT2 (family)	9 (24.3)	7 (31.8)	2 (15.4)	0.256
Notch family	5 (13.5)	4 (18.2)	1 (7.8)	0.383
<i>EPHA</i> family	5 (13.5)	5 (22.7)	0	0.063
<i>ARID2</i>	3 (8.1)	2 (9.1)	1 (7.8)	0.827
<i>PIK3CA</i>	2 (5.4)	2 (9.1)	0	0.222
<i>TAP1</i>	3 (8.1)	1 (4.5)	2 (15.4)	0.217
<i>ROS1</i>	3 (8.1)	1 (4.5)	2 (15.4)	0.264

Values are presented as number (%).

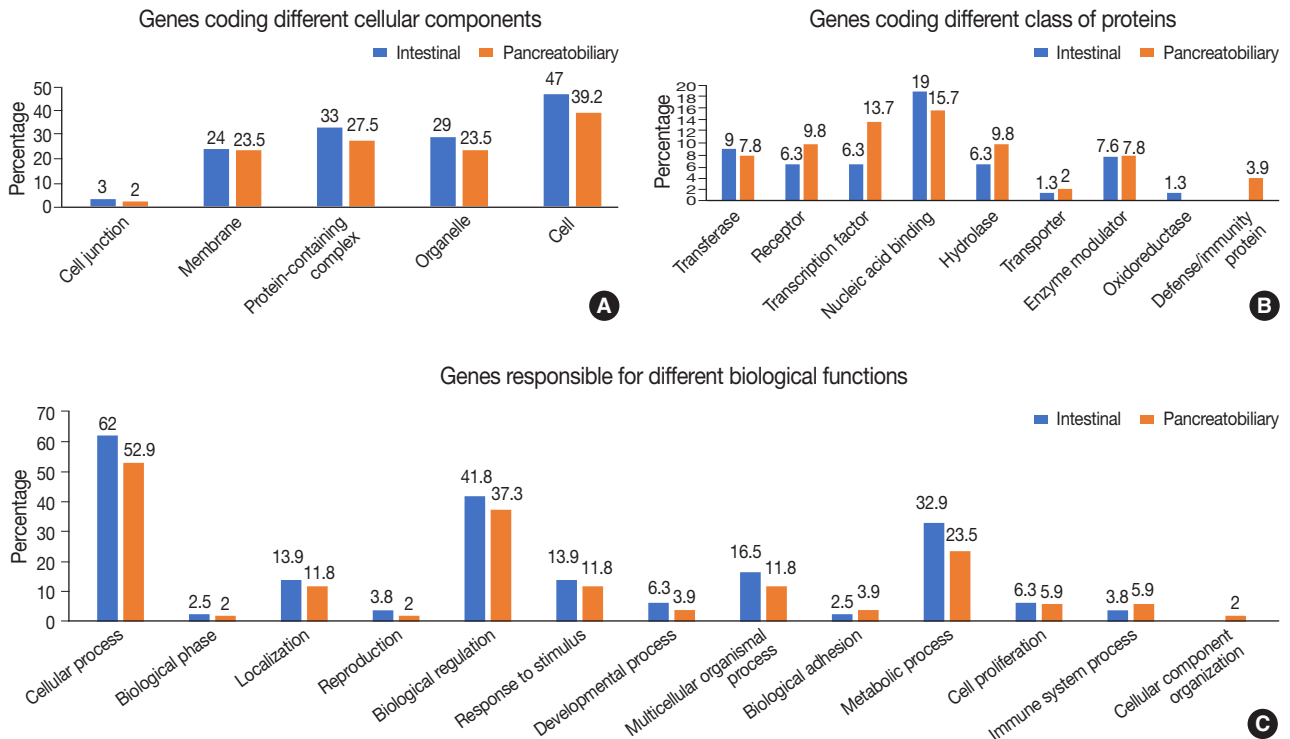


Fig. 7. (A) Genes forming part of the cellular component in intestinal and pancreatobiliary types of ampullary carcinoma. (B) Genes responsible for different classes of proteins in intestinal and pancreatobiliary types of ampullary carcinoma. (C) Genes involved in different biological functions and processes in intestinal and pancreatobiliary types of ampullary carcinoma.

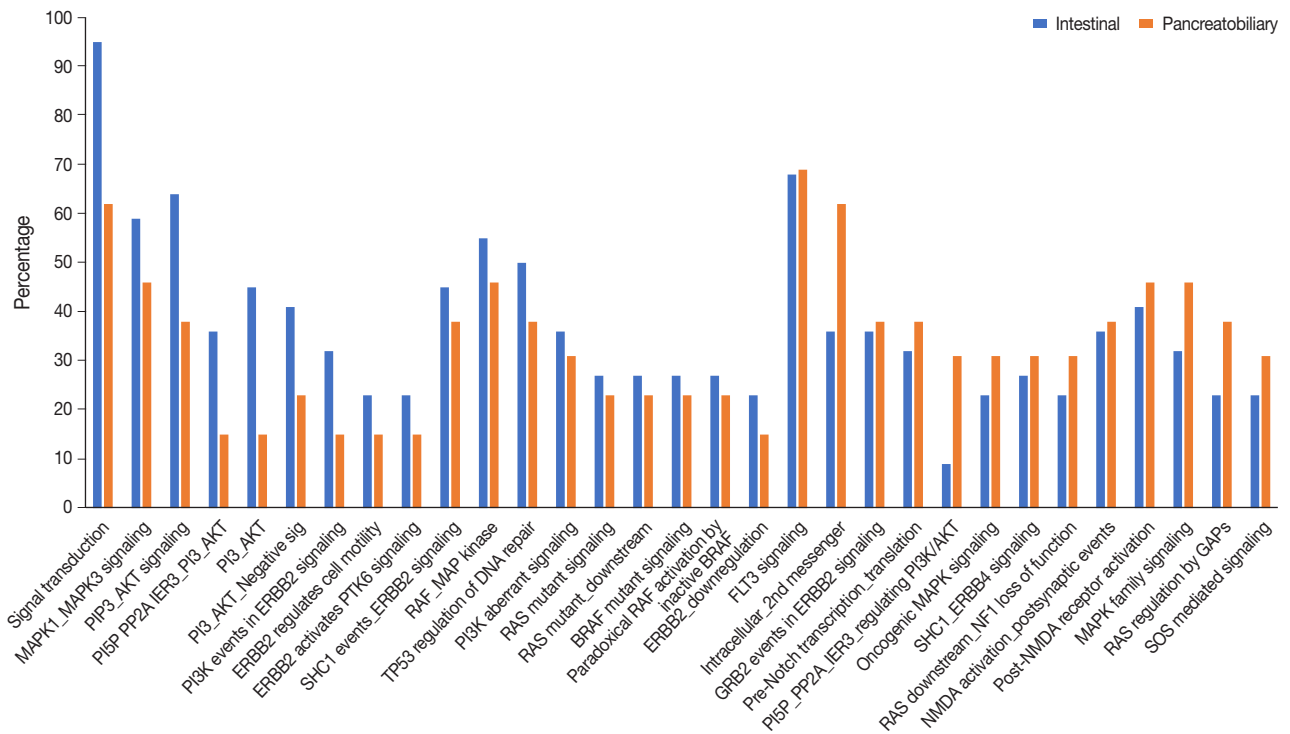


Fig. 8. Pathways involving the significantly most frequently mutated genes in intestinal and pancreatobiliary subtypes of ampullary carcinoma ($p < .002$).

Table 3. Major signaling pathways mutated in intestinal and pancreatobiliary differentiation of ampullary cancer

Pathway	Intestinal (n=22)	Pancreatobiliary (n=13)	Mixed (n=2)	p-value
TP53 pathway (n=14, 38%)	9 (41.0)	5 (38.4)	0	0.826
PI3/AKT/MAPK pathways combined (n=26, 70%)	18 (81.8)	6 (46.2)	2 (100)	0.024
RAS/MAPK (n=21, 57%)	13 (59.1)	6 (46.2)	2 (100)	0.437
PI3/AKT (n=18, 49%)	14 (63.6)	4 (30.7)	0	0.601
WNT pathway (n=12, 32%)	10 (45.4)	2 (15.4)	0	0.075
TGF- β pathway (n=9, 24%)	5 (22.7)	3 (23.1)	1 (50.0)	0.902
Chromatin remodeling complex (n=6, 16%)	3 (13.6)	3 (23.1)	0	0.419

Values are presented as number (%).

(23.1%), and the WNT pathway (15.4%). The results suggest that PI3-AKT, RAS-RAF-MAPK, and WNT cascades were more frequently mutated in INT type, while the chromatin remodeling complex was more frequently mutated in the PB type. TP53 and TGF- β pathway alterations were similar in the differentiation types (Table 3).

Tumor mutation burden (TMB) compared between the two differentiation types showed that INT type had 1.6 mutations/Mb, while PB type had 0.8 mutations/Mb, with both of them falling into the low TMB group ($p = .294$).

DISCUSSION

The morphology of AC has emerged as an important prognostic factor in recent years and its subtyping as INT and PB types based on differentiation has shown INT type to have a better prognosis than PB type ($p = .01$) [10]. High-throughput sequencing techniques have revolutionized the genetic landscape of cancers. We studied the genetic map of AC and evaluated the pattern of mutational status according to morphologic subtype through WES. Major somatic mutations were found in nine genes in >10% of cases, similar to Lundgren et al. [13], who found *TP53* and *KRAS* to be the most commonly mutated genes in their cohort. Genes harboring somatic mutations in >10% patients of AC in the present study were *TP53* (32.4%), *KRAS* (27.0%), *KMT2* complex (24.3%), *SMAD4* (21.6%), *APC* (18.9%), *ErbB* complex (16.2%), *EphA* complex (13.5%), *Notch* complex (13.5%), *CTNNB1* (10.8%), and *FAT1* (10.8%) genes. Other potentially targetable genes of *ROS1*, *ARID2*, and *TAP1* were observed but at a lower frequency. The mutation profile of AC in the present study exhibited a similar spectrum to that reported in the two WES studies by Yachida et al. [11] and Gingras et al. [12], as well as studies with targeted panels of genes by Lundgren et al. [13] and Perkins et al. [14] with minor variations. Unlike Perkins et al. [14] who found mutations in *CDKN2A* and *FBXW7* in 4% of cases and Lundgren

et al. [13] who discovered *CDKN2A* mutations, we found *FBXW7* in 2% of cases and *CDKN2A* mutations in none of the cases. *CDKN2A* mutations also were reported by Yachida et al. [11] and Gingras et al. [12], although at a lower frequency (4%), which was not reflected in our study population. One of the major findings reported by both these authors was mutation of the *ELF3* driver gene (12%–13.3%), which was not detected in our study. In another study, Overman et al. [15] studied gene expression with a 92-gene classifier and found *IRX3*, *PYCR1*, and *TMPRSS3* to be significantly associated with overall survival and relapse-free survival. However, pathogenic mutations in these genes were not found in the present study. Although there is a significant overlap between the genetic profiles of the present study and those of previous studies, there are certain differences as well, which could be attributed to the type of cancers studied (ampullary vs. periampullary), number of cases included (37 to 175), type of profiling methodology (whole exome vs. targeted panel comprising of a variable number of genes for somatic mutation vs. gene expression), and the ethnic diversity of the population studied.

Even though INT differentiation carries a better prognosis, it represents a genetically more unstable phenotype than PB differentiation (78 vs. 51 mutated genes), with a higher mutation frequency in *APC*, *SMAD4*, *CTNNB1*, *TP53*, *EphA*, *KMT2*, and *Notch* complex of genes, while *ROS1* and *TAP1* mutations were more frequent in PB differentiation. The *KRAS* and *ErbB* complex of genes harbored mutations in nearly equal frequency in both INT and PB differentiation. Lundgren et al. reported *APC* and *ERBB3* mutations exclusively in the INT type of AC, which was reflected in our study with two cases of *ERBB3* mutations exclusively found in INT differentiation. However, *APC* mutations were observed in both but were more frequent (27.3% vs. 7.8%) in the INT type of AC [13]. The genetic profiles of AC in different studies are presented in Table 4.

The major signaling pathways were grouped into six broad categories similar to those of Yachida et al. [11] and Gingras et

Table 4. Comparison of genetic profile studies in ampullary cancer

Characteristic	Yachida et al. [11]	Gingras et al. [12]	Perkins et al. [14]	Lundgren et al. [13]	Present study
No. of cases studied	172 (ampullary Ca)	160 (ampullary 98, distal CBD 44, duodenal 18)	91 (ampullary Ca)	175 (ampullary 70, distal CBD 45, HOP 46, duodenal 14)	37 (ampullary Ca)
Methodology	WES in 60 cases with mean coverage 188×, targeted 92-gene panel sequencing in 113 cases	WES with mean cover- age 120×	Targeted 50-gene panel	Targeted 70-gene panel	WES with mean coverage 200×
No. of genes significantly mutated in > 10% patients	24	19	18	9	18
Gene (%)					
<i>TP53</i>	55.8	58	38	50	32.4
<i>KRAS</i>	47.6	55	46	46.1	27
KMT2 family	-	-	-	-	24.3
<i>SMAD4</i>	16.3	20	9	14	21.6
<i>APC</i>	33.7	27	15	10	18.9
ErbB family	22	6	2	13	16.2
EphA family	18.6	-	-	-	13.5
Notch family	-	-	-	-	13.5
<i>CTNNB1</i>	23.2	13	-	-	10.8
<i>ARID2</i>	15.7	12	-	-	8.1
<i>PIK3CA</i>	5.8	18	14	-	5.4
<i>CDKN2A</i>	4	4	4	11.5	0
<i>FBXW7</i>	5.8	6	4	-	2
<i>ELF3</i>	13.3	12	-	-	0
Major signaling pathway (%)					
TP53	58	68	-	-	38
RAS-MAPK	65.7	70	-	-	57
PI3K-AKT	11.6	-	-	-	49
WNT	55.8	49	-	-	32
TGF-β	28.5	40	-	-	24
Chromatin remodeling	25.6	44	-	-	16

Ca, carcinoma; CBD, common bile duct; HOP, head of pancreas; WES, whole-exome sequencing.

al. [12]. The combined RAS-RAF-MAPK/PI3-AKT pathway was the major signaling pathway (70%) altered in AC, followed by TP53 (~38%), WNT signaling (~32%), TGF-β (24%), and the chromatin remodeling complex pathways (16%). The INT differentiation harbored mutations predominantly in the combined RAS-RAF-MAPK/PI3-AKT pathway in ~82% of cases, with PI3-AKT mutations more common (63.6%) than RAS-RAF-MAPK mutations (59.1%). The next most common pathways to be mutated in INT type were WNT (45.4%), TP53 (41.0%), TGF-β (22.7%), and the chromatin remodeling complex pathways (13.6%). The PB differentiation also harbored mutations predominantly in RAS-RAF-MAPK/PI3-AKT (46.2%) but at a significantly lower frequency ($p = .02$), and RAS-RAF-MAPK mutations were more frequent (46.2%) than PI3-AKT mutations (30.7%). The mutation frequencies of the TP53 pathway (38.4%) and the TGF-β pathway (22.7%) were similar in PB differentiation to that of INT type, while the WNT

pathway (15.4%) had a much lower frequency, with the chromatin remodeling complex pathway (23.1%) having a higher mutation frequency in PB differentiation.

Yachida et al. [11] (WNT, TGF-β, PI3K, RTK-RAS, and p53-Rb signaling) and Gingras et al. [12] (TP53/cell division, RAS/PI3K, WNT, TGF-β, and chromatin remodeling pathways) in their WES studies observed a similar spectrum of mutated pathways to the present study. The WNT signaling pathway was reported as most frequently mutated in INT differentiation (67% in Gingras et al. [12], 76% in Yachida et al. [11]). However, it was the third most common pathway to be mutated in the INT type in the present study, after PI3-AKT and RAS-RAF-MAPK signaling. The oncogene panel (CHPv2 – Ampliseq, ABI) of Perkins et al. [14] found WNT to be the most commonly altered pathway in INT type, with mutations of KRAS and TP53 signaling to be more frequent in the PB type, similar to Yachida et al. [11,14]. TP53 mutations in our study had similar mutation

frequency in the two types of differentiation, in contrast to those in the literature, where it has been reported to be more frequent in PB differentiation [11-14]. The Cancer Genome Atlas (TCGA) database states similarities between the molecular profile of INT differentiation and colorectal cancer harboring frequent *APC* mutations and WNT pathway alterations and that of PB differentiation and pancreatic adenocarcinoma harboring frequent *TP53* and *KRAS* mutations [16,17].

The genetic profile of AC and those reported in the literature using WES or an oncogene panel through high-throughput sequencing suggests distinct molecular trends of histological INT and PB subtypes, although with significant overlap. These molecular trends might be important for guiding the therapeutic decision-making process. A better understanding of the molecular profile and the emergence of newer targeted agents could lead to better treatment outcomes in AC, as seen in other cancers. Future studies on the relationship of the genetic profile and response to adjuvant therapeutic regimens will serve to improve and devise more precise therapeutic regimens for AC patients, which are currently extrapolated from the established treatment protocols for pancreatic, biliary, and intestinal cancers.

To summarize, we present the first WES data in AC from India providing a genetic map of INT and PB subtypes. Approximately 86% of AC patients harbor one or more targetable mutations. The WES data suggest that INT type cancers are more unstable genetically than PB types, and that both involve mutations in tumor suppressor, transcription factor, and chromatin remodeling complex genes. The most frequent targetable mutations were found in *KRAS*, *CTNNB1*, *TP53*, *APC*, and *SMAD4* genes. Our data suggest the PI3/AKT and RAS/MAPK kinase pathways to be predominantly mutated in AC, suggesting support of primary targeting of the PI3/AKT pathway in INT and the RAS/MAPK kinase pathway in PB type AC. Mutational profiling would enable better patient stratification and help to identify potential responders to targeted or personalized therapies in these cancers.

Supplementary Information

The Data Supplement is available with this article at <https://doi.org/10.4132/jptm.2021.01.23>.

Ethics Statement

The study was approved by the institutional ethics committee (IEC Code: 2016-21-EMP-EXP). The study was approved from institutional ethics committee and a waiver of consent was granted.

Availability of Data and Material

The datasets generated or analyzed during the study are available from the corresponding author and have been included in this published article as

supplementary information files.

Code Availability

Not applicable.

ORCID

Niraj Kumari <https://orcid.org/0000-0002-9674-448X>
 Shравan K. Mishra <https://orcid.org/0000-0001-7180-4952>
 Raghvendra L. <https://orcid.org/0000-0002-7883-0982>

Author Contributions

Conceptualization: NK. Data curation: SKM. Formal analysis: SM. Funding acquisition: NK. Investigation: RL. Methodology: RKS. Supervision: NK. Validation: NK. Writing—original draft: SKM. Writing—review & editing: RL. Approval of final manuscript: all authors.

Conflicts of Interest

The authors declare that they have no potential conflicts of interest.

Funding Statement

The work was funded by SERB, Department of Science and Technology, Ministry of Health and Family Welfare (EMR/2015/000041).

References

1. Adsay V, Ohike N, Tajiri T, et al. Ampullary region carcinomas: definition and site specific classification with delineation of four clinicopathologically and prognostically distinct subsets in an analysis of 249 cases. *Am J Surg Pathol* 2012; 36: 1592-608.
2. Benhamiche AM, Jouve JL, Manfredi S, Prost P, Isambert N, Faivre J. Cancer of the ampulla of Vater: results of a 20-year population-based study. *Eur J Gastroenterol Hepatol* 2000; 12: 75-9.
3. Demeure MJ, Craig DW, Sinari S, et al. Cancer of the ampulla of Vater: analysis of the whole genome sequence exposes a potential therapeutic vulnerability. *Genome Med* 2012; 4: 56.
4. Kim WS, Choi DW, Choi SH, Heo JS, You DD, Lee HG. Clinical significance of pathologic subtype in curatively resected ampulla of vater cancer. *J Surg Oncol* 2012; 105: 266-72.
5. Colussi O, Voron T, Pozet A, et al. Prognostic score for recurrence after Whipple's pancreaticoduodenectomy for ampullary carcinoma; results of an AGEO retrospective multicenter cohort. *Eur J Surg Oncol* 2015; 41: 520-6.
6. Neoptolemos JP, Moore MJ, Cox TF, et al. Effect of adjuvant chemotherapy with fluorouracil plus folinic acid or gemcitabine vs observation on survival in patients with resected periampullary adenocarcinoma: the ESPAC-3 periampullary cancer randomized trial. *JAMA* 2012; 308: 147-56.
7. Shoji H, Morizane C, Hiraoka N, et al. Twenty-six cases of advanced ampullary adenocarcinoma treated with systemic chemotherapy. *Jpn J Clin Oncol* 2014; 44: 324-30.
8. Kimura W, Futakawa N, Yamagata S, et al. Different clinicopathologic findings in two histologic types of carcinoma of papilla of Vater. *Jpn J Cancer Res* 1994; 85: 161-6.
9. Albores-Saveedra J, Henson DE, Klimstra DS. Tumors of the gallbladder, extrahepatic bile ducts, and ampulla of Vater. *Atlas of tumor pathology. 3rd series. Vol. 27.* Washington, DC: Armed Forces Institute of Pathology, 2000; 259-316.
10. Kumari N, Prabha K, Singh RK, Baitha DK, Krishnani N. Intestinal and pancreatobiliary differentiation in periampullary carcinoma: the role of immunohistochemistry. *Hum Pathol* 2013; 44: 2213-9.

11. Yachida S, Wood LD, Suzuki M, et al. Genomic sequencing identifies ELF3 as a driver of ampullary carcinoma. *Cancer Cell* 2016; 29: 229-40.
12. Gingras MC, Covington KR, Chang DK, et al. Ampullary cancers harbor ELF3 tumor suppressor gene mutations and exhibit frequent WNT dysregulation. *Cell Rep* 2016; 14: 907-19.
13. Lundgren S, Hau SO, Elebro J, et al. Mutational landscape in resected periampullary adenocarcinoma: relationship with morphology and clinical outcome. *JCO Precis Oncol* 2019; 3: PO.18.00323.
14. Perkins G, Svrcek M, Bouchet-Doumenq C, et al. Can we classify ampullary tumours better? Clinical, pathological and molecular features: results of an AGEO study. *Br J Cancer* 2019; 120: 697-702.
15. Overman MJ, Soifer HS, Schueneman AJ, et al. Performance and prognostic utility of the 92-gene assay in the molecular subclassification of ampullary adenocarcinoma. *BMC Cancer* 2016; 16: 668.
16. The Cancer Genome Atlas Network. Comprehensive molecular characterization of human colon and rectal cancer. *Nature* 2012; 487: 330-7.
17. Cancer Genome Atlas Research Network. Integrated genomic characterization of pancreatic ductal adenocarcinoma. *Cancer Cell* 2017; 32: 185-203.

Mismatch repair deficiency and clinicopathological characteristics in endometrial carcinoma: a systematic review and meta-analysis

Alaa Salah Jumaah¹, Hawraa Sahib Al-Haddad², Mais Muhammed Salem¹, Katherine Ann McAllister³, Akeel Abed Yasseen¹

¹Department of Pathology and Forensic Medicine, Faculty of Medicine, University of Kufa, Kufa;

²Al-Furat Al-Awsat Hospital, Kufa, Iraq;

³School of Biomedical Sciences, Ulster University, Northern Ireland, UK

Background: Loss of mismatch repair (MMR) occurs frequently in endometrial carcinoma (EC) and is an important prognostic marker. However, the frequency of MMR deficiency (D-MMR) in EC remains inconclusive. This systematic review and meta-analysis addressed this inconsistency and evaluated related clinicopathology. **Methods:** Electronic databases were searched for articles: PubMed, Science Direct, Web of Science, EMBASE, and the Wiley Online Library. Data were extracted from 25 EC studies of D-MMR to generate a clinical dataset of 7,459 patients. A random-effects model produced pooled estimates of D-MMR EC frequency with 95% confidence interval (CI) for meta-analysis. **Results:** The overall pooled proportion of D-MMR was 24.477% (95% CI, 21.022 to 28.106) in EC. The Lynch syndrome subgroup had 22.907% pooled D-MMR (95% CI, 14.852 to 32.116). D-MMR was highest in type I EC (25.810) (95% CI, 22.503 to 29.261) compared to type II (13.736) (95% CI, 8.392 to 20.144). Pooled D-MMR was highest at EC stage and grades I-II (79.430% and 65.718%, respectively) and lowest in stages III-IV and grade III (20.168% and 21.529%). The pooled odd ratios comparing D-MMR to proficient MMR favored low-stage EC disease (1.565; 0.894 to 2.740), lymphovascular invasion (1.765; 1.293 to 2.409), and myometrial invasion >50% (1.271; 0.871 to 1.853). **Conclusions:** Almost one-quarter of EC patients present with D-MMR tumors. The majority has less aggressive endometrioid histology. D-MMR presents at lower tumor stages compared to MMR-proficient cases in EC. However other metastatic parameters are comparatively higher in the D-MMR disease setting.

Key Words: Microsatellite instability; MMR-D; Endometrial carcinoma

Received: May 13, 2020 **Revised:** January 20, 2021 **Accepted:** February 19, 2021

Corresponding Author: Akeel Abed Yasseen, PhD, Department of Pathology and Forensic Medicine, Faculty of Medicine, University of Kufa, Kufa, P.O. Box 21, Najaf Governorate, Iraq
 Tel: +9647811131586, E-mail: akeelyasseen@uokufa.edu.iq

Endometrial carcinoma (EC) is the most common cancer of the female genital tract [1]. The majority of endometrial cancers is sporadic (90%), while up to 5% are inherited cases such as Lynch syndrome. In the United States, there are approximately 60,000 new cases and 10,470 deaths per year [1]. The reason for the increasing worldwide trend of EC incidence is ill-defined. However, one possibility is an increase in aggressive uterine cancer subtypes. In 2013, the Cancer Genome Atlas Research Network (TCGA) classified EC into four molecular subgroups that correlated with survival [2,3]. The subgroups were ranked from best to worse prognosis as (1) ultra-mutated (*POLE*-mutated), (2) hypermutator phenotype caused by mismatch repair deficiency (D-MMR) that also features microsatellite instability (MSI), and (3) either a copy number low, or (4) high phenotype. Tumors with D-MMR can have a more favorable prognosis [2], despite the advantages

offered by a proficient MMR system.

Indeed, MMR plays a critical role during DNA replication by recognizing and fixing incorrectly paired nucleotides. This safeguarding of DNA integrity prevents mutagenesis and cancer development. Most sporadic EC cases are caused by genetic alterations that cause loss of MMR proteins (D-MMR) [4]. Tumors with D-MMR also feature the concordant molecular fingerprint of MSI. There are now up to seven identified human genes that function as a multi-subunit complex to facilitate MMR: *bMLH1*, *bMLH3*, *bMSH2*, *bMSH3*, *bMSH6*, *bPMS1*, and *bPMS2*. In sporadic endometrial cancers, deficient MMR typically arises from hypermethylation of the *bMLH1* gene promoter region, as reviewed by Nojadedh et al. [5]. Furthermore, inherited Lynch syndrome cases are caused by a germline heterozygous mutation in one of the four MMR genes—*bMLH1*, *bMSH2*, *bMSH6*, and

bPMS2 [4].

Disruption of MMR pathway genes in EC causes loss of key proteins (D-MMR) that is measurable using immunohistochemistry (IHC) and/or molecular approaches. However, there is a wide disparity in D-MMR frequency reported using IHC and molecular studies of EC—ranging from 6.612% to 43.351% [6-30]. This meta-analysis aimed to consolidate the conflicting estimates to report overall frequency of D-MMR in EC. In principle, the final estimate of D-MMR proportion in EC might be affected by inclusion of germline mutation cases. This possibility was investigated by subgroup analysis of Lynch syndrome cases. Furthermore, EC has been historically classified into estrogen-dependent (type I) cancer with a more favorable prognosis or as independent (type II) cancers that are typically less common and more aggressive [31]. Both D-MMR frequencies in type I and type II endometrial tumors were estimated by meta-analysis. Finally, the clinicopathologic characteristics were pooled to determine the prognostic value of the D-MMR subtype.

MATERIALS AND METHODS

Systematic review

The systematic review was conducted according to the guidelines of the Preferred Reporting Items for Systematic Reviews and Meta-Analyses (PRISMA) [32]. The PRISMA flow chart for search strategy leading to meta-analysis is illustrated in Fig. 1. The following databases were searched independently by two reviewers (ASJ and HSAH): PubMed, Science Direct, Web of Science, EMBASE, and the Wiley Online Library from inception to March 1, 2020. The search terms included the following: “Endometrial cancer” OR “endometrial carcinoma” OR “uterine cancer” “Mismatch repair gene” OR “*bMLH1*” OR “*bMSH2*” OR “*bMSH3*” OR “*bMSH6*” OR “*bPMSH1*” OR “*bPMSH2*” OR MMR. The references within the included studies were screened to identify suitable publications. The search was not limited by date or language. Two reviewers (ASJ and HSAH) assessed the title and abstracts of the studies, and full texts were retrieved to determine eligible studies. The eligibility criterion was applied independently by the other two authors (AAY and MMS). Any disagreements in selection of studies were resolved by consensus under guidance of the senior author.

Study inclusion criteria

The inclusion criteria used were (1) diagnosed with EC, (2) expression of MMR-related genes was measured using IHC and/or molecular methods such as polymerase chain reaction (PCR) in

the EC, (3) the proportion of MMR in EC was investigated, and (4) publication as a full paper. There were no limits applied for language, and any foreign papers were translated. When the same team reported several studies from the same patients, the most recent was included. Case reports, review articles, and studies published in abstract format only were excluded.

The exclusion criteria were as follows: (1) did not sufficiently meet all of the abovementioned inclusion criteria, (2) duplicate publication or data, and (3) single case reports, commentaries, review articles, editorials, and unrelated articles or letters to the editor.

Data collection

Two authors extracted eligible study data of (1) first author name and year of publication, (2) study participant data (total number of cases, number of D-MMR mutant ECs, histological type (endometrioid vs. non-endometrioid), stage and grade of disease, and extent of myometrial and lymphovascular invasion [LVI]), and (3) MMR characteristic data (gene subtype test method and study country of origin). Articles that did not display the relevant data were recorded as ‘not reported.’ Any disagreements regarding collection and refinement of data were discussed between the two authors under direction of the senior author.

Study quality assessment

The Quality Assessment Tool for Diagnostic Accuracy Studies-2 (QUADAS-2) [33] was used to assess study quality. The tool comprises four domains of “patient selection,” “index test,” “reference standard,” and “flow and timing.” Each domain was considered in terms of risk of bias, and the first three domains were used to examine study applicability. Risk of bias and applicability were assessed with signaling questions as “yes,” “no,” or “unclear.” The final result categorizing risk of bias was “high,” “low,” or “unclear.”

Meta-analysis and statistical methods

Mismatch repair alterations were analyzed in both EC types. Type I included endometrioid and mucinous types, while type II included any other variants [34]. The meta-analysis was conducted using MedCalc statistical software [35] according to PRISMA [32]. The pooled proportion of D-MMR was calculated using the random effect model [36] for meta-analysis. The heterogeneity test used the inconsistency index (I^2) [36,37] and Q statistic, for which a p-value less than .1 was considered to represent significant heterogeneity. The I^2 represents the proportion of total variation contributed by between-study varia-

tions. The level of heterogeneity was considered low ($I^2 = 25\%$), medium ($I^2 = 50\%$), or high ($I^2 = 75\%$). The types and histological variants were pooled, and results were reported with 95% confidence interval. Publication bias was assessed using a visual method by funnel plot tests [38]. A subgroup analysis was performed according to detection method of (1) IHC alone or (2) molecular technique. A further subgroup analysis was performed according to the study country of origin—whether based in Western or Asian countries. In addition, subgroup analysis was performed for studies that included cases diagnosed with Lynch syndrome. Sensitivity analysis was performed by removing each result in turn and re-estimating the pooled proportion to assess the influence of the data removed on final calculations and the robustness of observations.

RESULTS

Study characteristics and quality assessment

A total of 2565 EC studies were identified to clarify D-MMR, as shown in the PRISMA flow diagram (Fig. 1). Of the 2471 excluded, 1261 were duplicates, 452 were irrelevant based on title or abstract; 321 reviews, 256 case reports or editorials, and

181 commentaries were unsuitable. The remaining 94 articles were evaluated by reading the full-text, and further 69 were excluded (39 were irrelevant, 28 lacked data, and 2 had duplicate study populations). A final 25 eligible studies [6–30] were included for quantitative meta-analysis (Fig. 1). The studies comprised a total of 7,459 EC patients, of which D-MMR presented in 1783. The study characteristics, including individual D-MMR proportion (%) and clinicopathological features, are presented in Table 1. Quality assessment of studies was performed using QUADAS-2. Most studies showed low risk of bias and applicability concerns (Supplementary Figs. S1, S2).

Meta-analysis of pooled D-MMR in EC

The pooled prevalence of D-MMR tumors in EC in 25 studies comprising the 7467 patients was calculated as 24.477% (95% confidence interval [CI], 21.022 to 28.106) (Table 2, Fig. 2). There was significant heterogeneity between all the studies ($I^2 = 91.890\%$; 95% CI, 89.250 to 93.880) (Fig. 2). To minimize heterogeneity, a conservative approach to the present meta-analysis was selected using the random effect model. Publication bias was investigated using the funnel plot [38] as depicted in Supplementary Fig. S3.

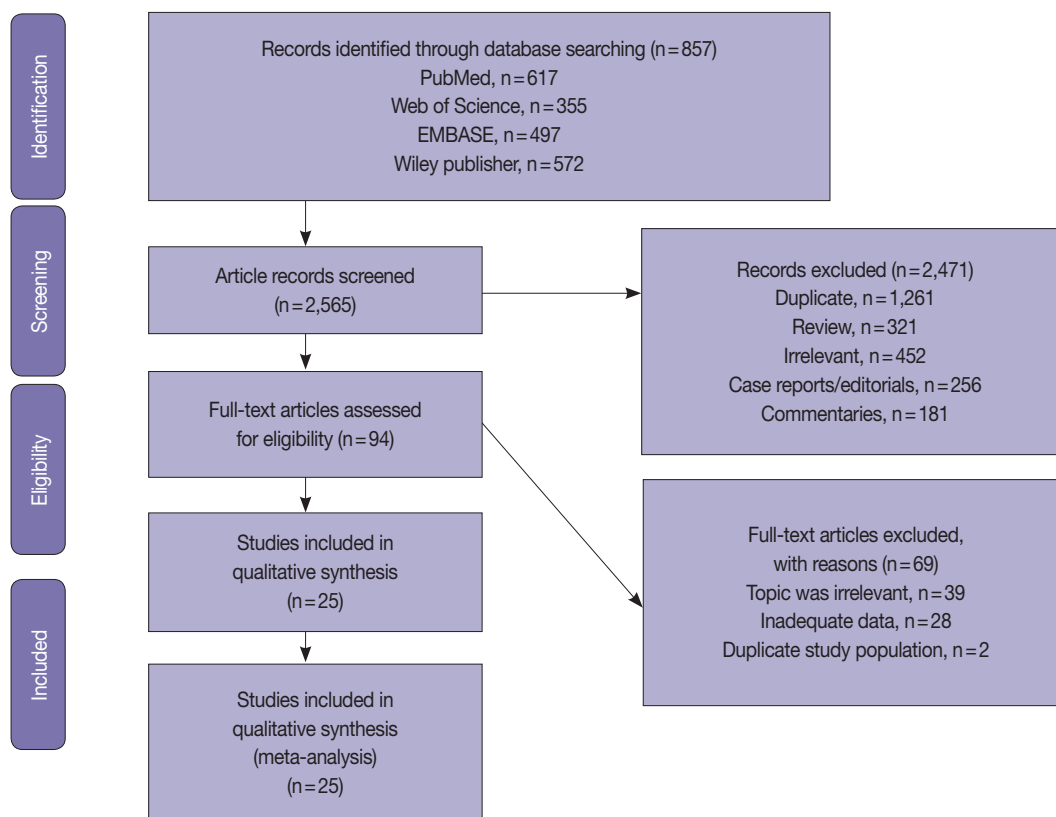


Fig. 1. PRISMA flow chart for search strategy, leading to selection of 25 studies for meta-analysis.

Table 1. The characteristics and clinicopathology of the included 25 studies for meta-analysis

Study	Sample size	D-MMR EC (%)	Study site	Detection method and D-MMR marker	Clinicopathologic characteristics					
					D-MMR subjects Grade I-II EC	D-MMR Stage I-II/EC	D-MMR Stage III-IV/EC	D-MMR subjects with MI <50% ^a	D-MMR subjects with MI >50% ^b	D-MMR EC with positive LVI
Buchanan et al. (2014) [6]	702	24.501	Australia	IHC markers: MLH1, MSH2, MSH6, PMS2 (protein loss or presence)	NR	NR	NR	NR	NR	NR
Stelboer et al. (2016) [7]	884	26.259	Netherlands	IHC markers: MLH1, MSH2, MSH6, PMS2 proteins	NR	NR	NR	148	71	19
An et al. (2007) [8]	93	18.280	South Korea	PCR	12	NR	NR	7	10	7
Arabi et al. (2009) [9]	91	27.473	USA	IHC markers: MLH1, MSH2, MSH6 proteins	NR	NR	13	15	10	14
Auguste et al. (2018) [10]	102	20.588	USA, Canada	IHC markers: MLH1, MLH2, MSH6, PMS2	NR	NR	NR	NR	NR	NR
Basil et al. (2000) [11]	229	30.568	USA	PCR markers: BAT26, BAT25, D5S346, D2S123, D17S250	NR	NR	61	9	NR	NR
Bosse et al. (2018) [12]	376	43.351	USA, Canada, UK	IHC markers: MLH1, MSH2, MSH6, PMSU proteins	NR	NR	NR	NR	NR	NR
Broadbent et al. (2006) [13]	138	18.841	USA	IHC markers: MLH1 and MSH2 (n=50) sequencing of MLH1 and MSH2 genes	NR	NR	16	10	NR	14
Cohn et al. (2001) [14]	210	24.286	USA	PCR markers: BAT-25, BAT-26, D5S346, D2S123, D17S250	NR	NR	NR	NR	NR	NR
de Jong et al. (2012) [15]	463	33.477	Netherlands	IHC markers: MLH1, MSH2, MSH6 proteins	NR	NR	NR	NR	NR	98
Hirai et al. (2008) [16]	120	15.000	Japan	Sequencing of MLH1, MLH2, MSH6 genes	NR	NR	NR	NR	NR	NR
Huang et al. (2015) [17]	42	28.571	Taiwan	IHC (MLH1, PMS2, MSH6, and MSH2), PCR (BAT-25, BAT-26, NR-21, NR-24, and MONO-27)	NR	NR	NR	NR	NR	NR
Black et al. (2006) [18]	473	19.662	USA	PCR markers: BAT25, BAT26, D2S123M, D5S346, D17S250	72	21	77	16	67	30
Nagle et al. (2018) [19]	698	19.198	Australia	IHC (MLH1, MSH2, MSH6, PMS2), MLH1 methylation testing was conducted for all cases with MLH1/PMS2 loss	NR	NR	125	17	NR	47
Kommos et al. (2018) [20]	452	28.097	USA, Canada, Germany	IHC to detect MMR protein loss in markers PMS2 and MSH6	102	25	NR	NR	44	25
Mackay et al. (2010) [21]	163	19.632	Canada	PCR testing of MSI, markers are BAT25/26	21	11	NR	NR	NR	NR
Maruyama et al. (2001) [22]	146	36.301	Japan	IHC marker MSH2, MLH1	NR	NR	NR	NR	NR	NR
Mills et al. (2014) [23]	605	6.612	USA	IHC of MLH1, MSHU, MSH6, PMS2 proteins, PCR confirmation of MLH1/PMS2 DNA methylation	26	9	NR	NR	NR	NR
Djordjevic et al. (2013) [24]	186	24.731	USA	IHC detection of MLH1, MSH2, MSH6, PMS2 proteins, PCR confirmation of MLH1 methylation to confirm loss of MLH1 protein	28	8	NR	NR	NR	NR
Okoye et al. (2016) [25]	411	27.981	USA	IHC to detect loss of MLH1, MSH2, MSH6, PMS2, PCR confirmation of MLH1 methylation	NR	NR	NR	NR	NR	NR
Ruiz et al. (2014) [26]	212	30.189	Spain	IHC of MLH1, MSH2, MSH6, PMS2 markers	58	16	50	10	50	6
Shikama et al. (2016) [27]	221	28.054	Japan	IHC of MMR proteins MLH1, MSH2, MSH6, PMS2 PCR confirmation of MLH1 methylation	NR	NR	39	18	NR	27
Stelboer et al. (2015) [28]	116	16.379	Europe	IHC of MLH1, MSH2, MSH6, PMS2, PCR MLH1 methylation confirmation	NR	NR	NR	NR	NR	NR
Talhok et al. (2016) [29]	57	31.579	Canada, USA	Promega (ver. 1.2) PCR testing of MSI markers	10	6	9	3	6	5
Talhok et al. (2017) [30]	319	9.718	Canada	IHC of MMR proteins MLH1, MSH2, MSH6, PMS2 IHC for presence or absence MMR proteins MLH1, MSH2, MSH6, PMS2	NR	NR	NR	NR	NR	28

D-MMR, MMR deficiency; EC, endometrial carcinoma; MI, myometrial invasion; IHC, immunohistochemistry; NR, not reported; PCR, polymerase chain reaction; MMR, mismatch repair; MSI, microsatellite instability.

^aMI <50%; MI is less than 50% of the total myometrial thickness; ^bMI >50%; MI is greater than 50% of the total myometrial thickness.

Table 2. The association between D-MMR EC and clinicopathological characteristics

Clinicopathological characteristics in EC	Pooled % portion (95% CI)	No. of studies	I ² (95% CI, %)	p-value	Model
Overall D-MMR mutation	24.477 (21.022–28.106)	25	91.890 (89.250–93.880)	<.001	Random effect
D-MMR mutation in type I	25.810 (22.503–29.261)	14	80.440 (68.080–88.020)	<.001	Random effect
D-MMR mutation in type II	13.736 (8.392–20.144)	10	77.320 (58.360–87.650)	<.001	Random effect
Stage I-II	79.430 (71.500–86.357)	6	68.640 (25.980–86.710)	.007	Random effect
Stage III-IV	20.168 (13.746–27.469)	6	61.850 (7.020–84.350)	.022	Random effect
Grade I-II	65.718 (52.602–77.714)	10	91.700 (86.860–94.760)	<.001	Random effect
Grade III	21.529 (15.930–27.718)	10	94.050 (90.97–96.08)	<.001	Random effect
Lymphovascular invasion	32.105 (21.371–43.896)	10	91.380 (86.270–94.590)	<.001	Random effect
MI less than 50%	51.807 (38.514–64.971)	8	89.860 (82.410–94.150)	<.001	Random effect
MI more than 50%	42.346 (28.576–56.750)	8	91.360 (85.380–94.890)	<.001	Random effect

D-MMR, mismatch repair deficiency; EC, endometrial carcinoma; CI, confidence interval; MI, myometrial invasion.

Study	Sample size	Proportion (%)	95% CI
Buschman et al. 2014	702	24.501	21.361–27.857
Stelloo et al. 2016	834	26.259	23.301–29.386
An et al. 2007	100	17.000	10.226–25.818
Arabi et al. 2009	91	27.473	18.633–37.830
Auguste et al. 2018	102	20.588	13.219–29.733
Basil et al. 2000	229	30.568	24.669–36.977
Bosse et al. 2018	376	43.351	38.279–48.529
Broaddus RR et al. 2006	138	18.841	12.692–26.374
Cohn et al. 2001	210	24.286	18.649–30.664
de Jong et al. 2012	463	33.477	29.188–37.979
Hirai et al. 2008	120	15.000	9.139–22.667
Huang et al. 2015	42	28.571	15.719–44.584
Black et al. 2006	473	19.662	16.173–23.534
Nagle et al. 2018	698	23.352	20.260–26.672
Kommos et al. 2018	452	28.097	23.998–32.486
Mackay et al. 2010	163	19.632	13.833–26.569
Maruyama et al. 2001	146	36.301	28.511–44.660
Mills et al. 2014	605	6.612	4.765–8.895
Djordjevic et al. 2013	187	24.599	18.607–31.414
Okoye et al. 2016	411	27.981	23.691–32.590
Ruiz et al. 2014	212	30.189	24.090–36.851
Shikama et al. 2016	221	28.054	22.236–34.472
Stelloo et al. 2015	116	16.379	10.159–24.391
Talhok et al. 2016	57	28.070	16.973–41.543
Talhok et al. 2017	319	20.063	15.807–24.884
Total (fixed effects)	7467	24.219	23.253–25.206
Total (random effects)	7467	24.477	21.022–28.106
Q		295.967	
DF		24	
Significance level		P < .001	
I ² (inconsistency)		91.890%	
95% CI for I ²		89.250–93.880	

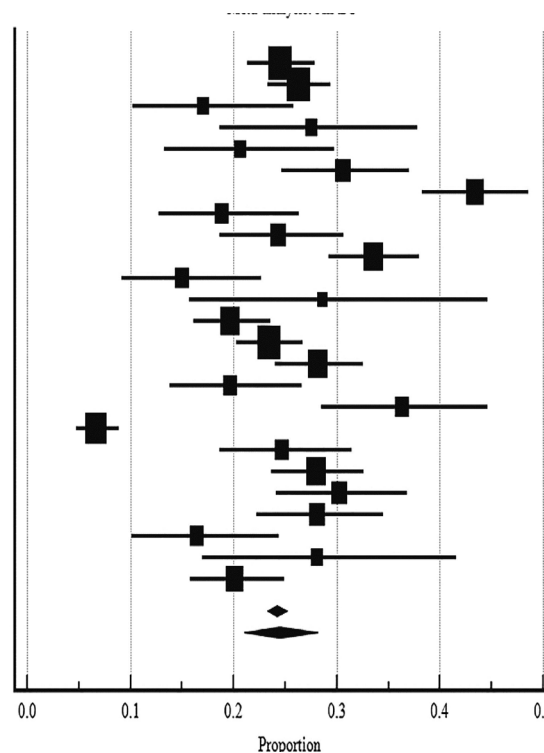


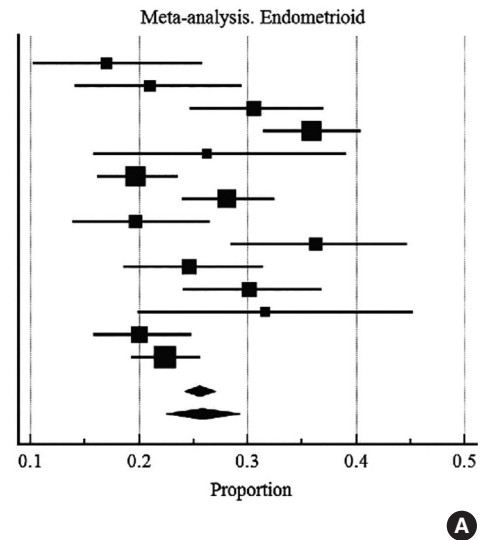
Fig. 2. The D-MMR gene proportions in each study are shown by forest plot [6-30]. D-MMR, mismatch repair deficiency; CI, confidence interval; EC, endometrial carcinoma.

Analysis of EC type I and type II variants

There were 14 studies investigated for D-MMR alterations in type I EC, with a total of 3679 patients (Fig. 3A). The pooled proportion of D-MMR using the random effect model was 25.810% (95% CI, 22.503 to 29.261) (Table 2). The heterogeneity between the studies was significant (I² = 80.440%; 95% CI, 68.080 to 88.020). There were 10 studies investigated for D-MMR alterations in type II EC, with a total of 648 patients (Fig. 3B). The meta-analysis determined a lower pooled D-MMR proportion of 13.736% (95% CI, 8.392 to 20.144) in type II EC

(Table 2). The heterogeneity test was significant (I² = 77.320%; 95% CI, 58.360 to 87.650). The pooled odds ratio of type I EC endometrioid histology in D-MMR versus MMR-proficient tumors was 1.389 (95% CI, 0.519 to 3.720) (Table 3). In contrast, the pooled odds ratio for the more aggressive type II non-endometrioid histology was 0.450 (0.349 to 0.579) (Table 3). These findings indicate that D-MMR EC tumors tend to present with less aggressive endometrioid histology compared to MMR-proficient tumors.

Study	Sample size	Proportion (%)	95% CI	
An et al. 2017	100	17.000	10.226–25.818	An et al. 2017
Arabi et al. 2009	119	21.008	14.081–29.431	Arabi et al. 2009
Basil et al. 2000	229	30.568	24.669–36.977	Basil et al. 2000
de Jong et al. 2012	463	35.853	31.479–40.409	de Jong et al. 2012
Huang et al. 2015	61	26.230	15.796–39.071	Huang et al. 2015
Black et al. 2006	473	19.662	16.173–23.534	Black et al. 2006
Kommoss et al. 2018	452	28.097	23.998–32.486	Kommoss et al. 2018
Mackay et al. 2010	163	19.632	13.833–26.569	Mackay et al. 2010
Maruyama et al. 2001	146	36.301	28.511–44.660	Maruyama et al. 2001
Djordjevic et al. 2013	187	24.599	18.607–31.414	Djordjevic et al. 2013
Ruiz et al. 2014	212	30.189	24.090–36.851	Ruiz et al. 2014
Talhok et al. 2016	57	31.579	19.905–45.243	Talhok et al. 2016
Talhok et al. 2017	319	20.063	15.807–24.884	Talhok et al. 2017
Nagle et al. 2018	698	22.350	19.310–25.625	Nagle et al. 2018
Total (fixed effects)	3679	25.621	24.220–27.062	Total (fixed effects)
Total (random effects)	3679	25.810	22.503–29.261	Total (random effects)
Q		66.474		
DF		13		
Significance level		P < .001		
I ² (inconsistency)		80.440%		
95% CI for I ²		68.080–88.020		



Study	Sample size	Proportion (%)	95% CI	
An et al. 2007	17	0.000	0.000–19.506	An et al. 2007
Arabi et al. 2009	25	44.000	24.402–65.072	Arabi et al. 2009
Basil et al. 2000	70	14.286	7.069–24.707	Basil et al. 2000
Black et al. 2006	93	6.452	2.404–13.515	Black et al. 2006
Nagle et al. 2018	156	14.744	9.582–21.297	Nagle et al. 2018
Kommoss et al. 2018	127	7.087	3.291–13.026	Kommoss et al. 2018
Mackay et al. 2010	32	3.125	0.0791–16.217	Mackay et al. 2010
Djordjevic et al. 2013	46	21.739	10.948–36.362	Djordjevic et al. 2013
Talhok et al. 2016	18	11.111	1.375–34.712	Talhok et al. 2016
alhok et al. 2017	64	25.000	15.016–37.399	Talhok et al. 2017
Total (fixed effects)	648	13.051	10.571–15.867	Total (fixed effects)
Total (random effects)	648	13.736	8.392–20.144	Total (random effects)
Q		39.681		
DF		9		
Significance level		P < .001		
I ² (inconsistency)		77.320%		
95% CI for I ²		58.360–87.650		

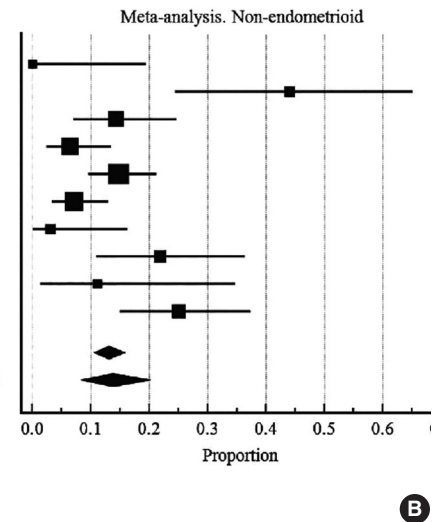


Fig. 3. D-MMR EC: type I EC (A) and type II EC (B) [8,9,11–15,17–22,24,26,29,30]. D-MMR, mismatch repair deficiency; CI, confidence interval; EC, endometrial carcinoma.

Subgroup analysis according to methodology, country, and Lynch syndrome

High heterogeneity was noted in the subgroup analysis ($I^2 > 75\%$) (Supplementary Figs. S4, S5). The IHC method alone (Supplementary Fig. S4B) had the highest pooled proportion of D-MMR at 27.918% (95% CI, 22.608 to 33.558), whereas studies involving molecular approaches had less frequent D-MMR (20.875%; 95% CI, 16.514 to 25.602) (Supplementary Fig. S4A). Studies from Asian countries had a slightly higher D-MMR proportion of 25.112% (95% CI, 17.675 to 33.370) in comparison to Western countries (at 23.666%; 95% CI, 19.519 to 28.080) (Supplementary Fig. S5A, B). Some studies included both sporadic EC and germline mutation (Lynch syn-

drome-associated) cases. Since the presence of germline mutation can affect the final estimate of D-MMR proportion in EC, a subgroup analysis was performed. All cases of D-MMR EC involving Lynch syndrome were grouped together and resulted in a proportion of 22.907% (95% CI, 14.852 to 32.116). Although subgroup heterogeneity was high, with I^2 (inconsistency) of 95.970% (95% CI, 93.680 to 97.440) (Supplementary Fig. S6), inclusion of Lynch cases did not significantly affect overall D-MMR estimates.

D-MMR and clinicopathological characteristics

The EC clinicopathological characteristics are shown in Supplementary Fig. S7–S14, and Tables 2 and 3 for D-MMR tumors.

Table 3. Pooled odds ratio of clinicopathologic variables in D-MMR EC vs. wild type

Clinicopathology D-MMR EC vs. wild type	Pooled odds ratio (95% CI)	No. of studies	I ² (95% CI, %)	p-value for I ²	Model
Stage I-II EC	1.565 (0.894–2.740)	6	70.100 (30.040–87.220)	.005	Random effect
Stage III-V EC	0.936 (0.593–1.478)	6	51.210 (0.000–80.580)	.068	Random effect
Grade I-II EC	0.706 (0.257–1.940)	9	94.400 (91.360–96.370)	<.001	Random effect
Grade III EC	1.384 (0.806–2.375)	7	69.430 (32.800–86.100)	.003	Random effect
LVI	1.765 (1.293–2.409)	10	51.590 (0.530–76.440)	.028	Random effect
MI less than 50%	1.230 (0.849–1.782)	8	65.900 (27.620–83.930)	.004	Random effect
MI more than 50%	1.271 (0.871–1.853)	8	65.750 (27.250–83.870)	.004	Random effect
Type I endometrioid histology	1.389 (0.519–3.720)	10	92.130 (87.630–95.000)	<.001	Random effect
Type II non-endometrioid histology	0.450 (0.349–0.579)	10	31.500 (0.000–67.300)	.156	Fixed effect

D-MMR, mismatch repair deficiency; EC, endometrial carcinoma; CI, confidence interval; LVI, lymphovascular invasion; MI, myometrial invasion.

There was substantial heterogeneity in the majority of clinicopathologic findings.

EC tumor stage and grade

The pooled proportion of D-MMR presented at higher levels in earlier stages of EC (Table 2 and Supplementary Fig. S7A, B). Stage I–II EC cases had high D-MMR level of 79.430% (95% CI, 71.500 to 86.357) that decreased to 20.168% (95% CI, 13.746 to 27.469) by stages III–IV. The pooled odds ratio of stage I–II D-MMR EC versus wild type was 1.565 (95% CI, 0.894 to 2.740), while that for stages III–IV was 0.936 (95% CI, 0.593 to 1.478) (Table 3 and Supplementary Fig. S8A, B). As shown in Table 2 and Supplementary Fig. S9A and B, the pooled proportion of D-MMR in grade I–II tumors was high at 65.718% (95% CI, 52.602 to 77.714) and decreased to 21.529% in more aggressive grade III tumors (95% CI, 15.930 to 27.718). However, the pooled odds ratio of grade I–II in D-MMR EC versus wild type tumors was 0.706 (95% CI, 0.257 to 1.940) (Table 3 and Supplementary Fig. S10A, B), with high heterogeneity (I² = 94.400%; 95% CI, 91.360 to 96.370). These findings indicate that D-MMR EC tumors present with higher grades at lower tumor stages compared to MMR-proficient tumors.

Lymphovascular and myometrial invasion in D-MMR tumors

The pooled proportion of LVI in D-MMR EC was 32.105% (95% CI, 21.371 to 43.896), as shown in Table 2 and Supplementary Fig. S11. The pooled odds ratio of LVI in D-MMR EC versus proficient one MMR was 1.765 (95% CI, 1.293 to 2.409) (Table 3 and Supplementary Fig. S12). This implies that MMR-proficient EC tumors have reduced the likelihood of LVI compared to D-MMR cases. The myometrial invasion (MI) data are shown in Table 2 and Supplementary Fig. S13. The pooled proportion of MI detected at less than 50% of the myometrium was 51.807% (95% CI, 38.514 to 64.971), and while that in > 50%

of myometrium was 42.346% (95% CI, 28.576 to 56.750). The pooled odds ratio of MI < 50% in D-MMR EC versus proficient MMR EC was 1.230 (95% CI, 0.849 to 1.782), while that for MI > 50% in D-MMR EC versus proficient MMR EC was 1.271 (95% CI, 0.871 to 1.853) (Table 3 and Supplementary Fig. S14).

Sensitivity analysis

Selected data removal did not affect the final estimation of D-MMR level by meta-analysis, indicating robustness of the final results. The meta-analysis was repeated after omitting studies with small sample size (< 100 and < 200). For sample sizes < 100, the pooled D-MMR level was 23.765% (95% CI, 19.604 to 28.194), and that for sample sizes < 200 was 24.454% (95% CI, 19.308 to 29.997) (Supplementary Fig. S15). Further sensitivity analysis was performed after omitting studies dealing with Lynch syndrome. The pooled proportion of D-MMR EC after exclusion of Lynch cases was 25.272 (22.089 to 28.594) (Supplementary Fig. S16). There was no significant difference from the estimated pooled proportion of D-MMR EC of any studies included in this meta-analysis (24.477%, 95% CI, 21.022 to 28.106) (Table 2 and Fig. 2).

DISCUSSION

The integrity of the genome is maintained by the MMR system that recognizes and repairs base mismatches and insertion/deletion errors generated during DNA replication and recombination. A defective MMR system results in genome-wide instability and progressive accumulation of mutations. This mainly occurs at regions of simple repetitive DNA sequences known as microsatellites, causing MSI [39,40]. The risk of carcinogenesis is greatly increased when mutations occur in tumor suppressor genes [41], as evidenced by the incidence of EC worldwide [42]. The majority of sporadic cases is caused by defective MMR and the resul-

tant MSI that leads to mutagenesis and carcinogenesis [43]. However, in the era of personalized medicine, knowledge of the MMR-related phenotype can provide invaluable prognostic information to protect patient health. The TCGA has classified endometrial cancers into four molecular subtypes that impact on prognosis—including an MSI hyper-mutated (D-MMR) genomic group [2]. Talhouk et al. [29] later showed that MMR assessment by IHC can accurately detect the related (TCGA) MSI molecular subtype. The IHC approach showed that defective MMR is confirmed by absence of MMR proteins (MLH1, MSH2, MSH6, and PMS2) after sequential immunostaining of the tumor specimen. MMR deficiency is typically evaluated using IHC to determine MMR protein expression levels and is confirmed by PCR assessment of *MLH1* promoter methylation and MSI markers. This present meta-analysis pooled many studies [6-30] with D-MMR frequency variations (6.610% to 43.351%) to determine the overall frequency of D-MMR. Our meta-analysis consolidated the proportions of D-MMR in relation to clinicopathological markers of prognostic value for EC patients.

The meta-analysis concludes that 24.477% EC patients harbor tumors with D-MMR. The defective MMR pathway was most prevalent in EC type I (25.810%) compared to type II (13.736%). The D-MMR EC tumors tend to present with less aggressive endometrioid histology compared to MMR-proficient tumors (odds ratio, 1.389).

The clinicopathologic characteristics that present in EC tumors with D-MMR are variable and have implications for treatment. For instance, D-MMR EC tumors presented at lower tumor stages compared to MMR-proficient cases (odds ratio, 1.565) and grades I–II tumors at higher stages (65.718%). However, the pooled odds ratio of low grades (I–II) in D-MMR compared to wild type favors the intact MMR system (odds ratio, 0.706). The clinical parameter of LVI is a marker of metastatic potential in cancer patients and was noted in 32.105% of endometrial cancers with D-MMR. The pooled odds ratio of LVI in D-MMR EC versus proficient was 1.765, suggesting that metastasis is more likely in D-MMR tumors. Furthermore, 42.346% of D-MMR EC had deep myometrial involvement that was defined as invasion > 50%. The pooled odds ratio of MI > 50% in D-MMR EC versus that in proficient MMR EC was 1.271. This suggests that the opportunity for extrauterine disease is greater in EC tumors with mismatch repair deficiency. The literature reports that MSI tumors can progress quickly to the metastatic stage and respond poorly to chemotherapies [44,45]. Yet, D-MMR cancers can have a more favorable prognosis compared with MMR-proficient counterparts [46]. MSI EC tumors do have a protective immune

phenotype and positively correlate with high immune infiltration. In theory, this protective immune phenotype can counteract the poor clinicopathological parameters that co-exist in D-MMR tumors.

Overall, the value of the MMR-related phenotype in EC provides an impetus for developing treatment approaches that target its tumor-specific molecular characteristics. Further investigations to clarify the involvement of MMR in EC etiology are vital for improved clinical decision making and selecting optimal patient treatment options. In colorectal cancer [47], some chemotherapeutic regimens have demonstrated improved treatment efficacy and amelioration of drug toxicity in D-MMR tumors. These findings highlight the importance of this molecular subset of tumors harboring D-MMR and MSI and the potential translation into improved clinical management of EC.

There are several study limitations to discuss. First, the detection methods for D-MMR were different between studies—some used IHC alone and others used a molecular approach. The definition of aberrant MMR in studies was inconsistent with that in IHC testing. There are studies that consider MMR expression negative when there is aberrant MMR, while others regard MMR expression as absent with negative expression of hMLH1 or hMLH2. MSI testing (IHC and methylation) for endometrial cancer is used mostly for sporadic cases. However, studies in this meta-analysis used sequencing methods mainly for Lynch syndrome. This could be a source of potential bias or limitation. The studies including cases with Lynch syndrome might affect the final pooled proportion of D-MMR EC. To address this, a Lynch subgroup analysis was carried out, along with a sensitivity analysis by omitting cases with Lynch syndrome.

Second, there was significant heterogeneity across the meta-analysis that was unresolved by subgroup analysis.

The documented variation in D-MMR can be attributed to differences in ethnicity and geographical distribution. Again, our analysis showed significant heterogeneity between the selected studies for our analysis. This finding is expected and noted in other meta-analysis studies of different cancer types [45]. The heterogeneity is probably caused by differences in population characteristics, number of cases (sample size), and differences in the number of markers used to evaluate MMR. Our study also tried to evaluate the role of population characteristics cited in each scientific paper (e.g., racial and ethnic background) in regard to D-MMR. However, this objective was not possible because the parameters were not documented clearly for consideration in our study. To solve the problem of heterogeneity, a conservative approach using a random effect model was chosen. The

sensitivity analysis omitted studies with small sample size (less than 100 and 200, respectively), and the re-estimated pooled proportions did not differ from the original calculations.

Furthermore, one of the pitfalls of any meta-analysis is publication bias or missed relevant articles during searches. To avoid this, we used strict criteria to limit missed papers. Any source of publication bias or non-significant findings were clarified using funnel plots. The scatter was located at the very top of the funnel, indicating absence of significant bias.

Our meta-analysis of D-MMR frequency consolidates wide published variations and is reflective of the MSI status in EC. The D-MMR pathway is very important for development of MSI and the pathogenesis of EC; most significantly for type I tumors. Although D-MMR causes a mix of clinicopathological features, this molecular subtype is linked to improved survival prospects in women with endometrial disease. These findings have clinical relevance for guiding treatment of EC patients with D-MMR tumors. Lastly, further efforts are required to evaluate and characterize the hormonal and environmental factors in women diagnosed with D-MMR EC. Such studies are imperative to provide researchers insight into possible interactions between genetic and environmental factors that contribute to development of this devastating disease of the female reproductive system.

Supplementary Information

The Data Supplement is available with this article at <https://doi.org/10.4132/jptm.2021.02.19>.

Ethics Statement

All procedures performed in the current study were approved by the Research Ethics Committee of the University of Kufa (IRB No.2019-01- 500) in accordance with the 1964 Helsinki declaration and its later amendments and revision in 2013. Formal written informed consent was not required after a waiver by the University of Kufa Research Ethics Committee.

Availability of Data and Material

All data generated or analyzed during the study are included in this published article (and its supplementary information files).

Code Availability

Not applicable.

ORCID

Alaa Salah Jumaah	https://orcid.org/0000-0001-9709-1460
Hawraa Sahib Al-Haddad	https://orcid.org/0000-0002-8564-3202
Mais Muhammed Salim	https://orcid.org/0000-0001-8014-1863
Katherine Ann McAllister	https://orcid.org/0000-0002-2893-7706
Akeel Abed Yasseen	https://orcid.org/0000-0001-5050-4408

Author Contributions

CCConceptualization: ASJ, MMS. Data curation: ASJ. Formal analysis: ASJ, MMS. Methodology: ASJ, HSAH, MMS. Project administration: HSAH,

MMS. Resources: HSAH. Software: ASJ, MMS. Supervision: ASJ, AAY. Validation: MMS, HSAH. Visualization: HSAH, MMS. Writing—original draft: ASJ, AAY, KAM. Writing—review & editing: AAY, ASJ, KAM, HSAH. Approval of final manuscript: all authors.

Conflicts of Interest

The authors declare that they have no potential conflicts of interest.

Funding Statement

No funding to declare.

References

1. Siegel RL, Miller KD, Jemal A. Cancer Statistics, 2017. *CA Cancer J Clin* 2017; 67: 7-30.
2. Cancer Genome Atlas Research Network; Kandoth C, Schultz N, et al. Integrated genomic characterization of endometrial carcinoma. *Nature* 2013; 497: 67-73.
3. Church DN, Stelloo E, Nout RA, et al. Prognostic significance of *POLE* proofreading mutations in endometrial cancer. *J Natl Cancer Inst* 2015; 107: 402.
4. Bell DW, Ellenson LH. Molecular genetics of endometrial carcinoma. *Annu Rev Pathol* 2019; 14: 339-67.
5. Nojadeh JN, Behrouz Sharif S, Sakhinia E. Microsatellite instability in colorectal cancer. *EXCLI J* 2018; 17: 159-68.
6. Buchanan DD, Tan YY, Walsh MD, et al. Tumor mismatch repair immunohistochemistry and DNA MLH1 methylation testing of patients with endometrial cancer diagnosed at age younger than 60 years optimizes triage for population-level germline mismatch repair gene mutation testing. *J Clin Oncol* 2014; 32: 90-100.
7. Stelloo E, Nout RA, Osse EM, et al. Improved risk assessment by integrating molecular and clinicopathological factors in early-stage endometrial cancer-combined analysis of the PORTEC cohorts. *Clin Cancer Res* 2016; 22: 4215-24.
8. An HJ, Kim KI, Kim JY, et al. Microsatellite instability in endometrioid type endometrial adenocarcinoma is associated with poor prognostic indicators. *Am J Surg Pathol* 2007; 31: 846-53.
9. Arabi H, Guan H, Kumar S, et al. Impact of microsatellite instability (MSI) on survival in high grade endometrial carcinoma. *Gynecol Oncol* 2009; 113: 153-8.
10. Auguste A, Genestie C, De Bruyn M, et al. Refinement of high-risk endometrial cancer classification using DNA damage response biomarkers: a TransPORTEC initiative. *Mod Pathol* 2018; 31: 1851-61.
11. Basil JB, Goodfellow PJ, Rader JS, Mutch DG, Herzog TJ. Clinical significance of microsatellite instability in endometrial carcinoma. *Cancer* 2000; 89: 1758-64.
12. Bosse T, Nout RA, McAlpine JN, et al. Molecular classification of grade 3 endometrioid endometrial cancers identifies distinct prognostic subgroups. *Am J Surg Pathol* 2018; 42: 561-8.
13. Broaddus RR, Lynch HT, Chen LM, et al. Pathologic features of endometrial carcinoma associated with HNPCC: a comparison with sporadic endometrial carcinoma. *Cancer* 2006; 106: 87-94.
14. Cohn DE, Mutch DG, Herzog TJ, et al. Genotypic and phenotypic progression in endometrial tumorigenesis: determining when defects in DNA mismatch repair and *KRAS2* occur. *Genes Chromosomes Cancer* 2001; 32: 295-301.
15. de Jong RA, Boerma A, Boezen HM, Mourits MJ, Hollema H, Nijman HW. Loss of HLA class I and mismatch repair protein expression in sporadic endometrioid endometrial carcinomas. *Int J Can-*

- cer 2012; 131: 1828-36.
16. Hirai Y, Banno K, Suzuki M, et al. Molecular epidemiological and mutational analysis of DNA mismatch repair (MMR) genes in endometrial cancer patients with HNPCC-associated familial predisposition to cancer. *Cancer Sci* 2008; 99: 1715-9.
 17. Huang HN, Lin MC, Tseng LH, et al. Ovarian and endometrial endometrioid adenocarcinomas have distinct profiles of microsatellite instability, PTEN expression, and ARID1A expression. *Histopathology* 2015; 66: 517-28.
 18. Black D, Soslow RA, Levine DA, et al. Clinicopathologic significance of defective DNA mismatch repair in endometrial carcinoma. *J Clin Oncol* 2006; 24: 1745-53.
 19. Nagle CM, O'Mara TA, Tan Y, et al. Endometrial cancer risk and survival by tumor MMR status. *J Gynecol Oncol* 2018; 29: e39.
 20. Kommos S, McConechy MK, Kommos F, et al. Final validation of the ProMisE molecular classifier for endometrial carcinoma in a large population-based case series. *Ann Oncol* 2018; 29: 1180-8.
 21. Mackay HJ, Gallinger S, Tsao MS, et al. Prognostic value of microsatellite instability (MSI) and PTEN expression in women with endometrial cancer: results from studies of the NCIC Clinical Trials Group (NCIC CTG). *Eur J Cancer* 2010; 46: 1365-73.
 22. Maruyama A, Miyamoto S, Saito T, Kondo H, Baba H, Tsukamoto N. Clinicopathologic and familial characteristics of endometrial carcinoma with multiple primary carcinomas in relation to the loss of protein expression of MSH2 and MLH1. *Cancer* 2001; 91: 2056-64.
 23. Mills AM, Liou S, Ford JM, Berek JS, Pai RK, Longacre TA. Lynch syndrome screening should be considered for all patients with newly diagnosed endometrial cancer. *Am J Surg Pathol* 2014; 38: 1501-9.
 24. Djordjevic B, Barkoh BA, Luthra R, Broaddus RR. Relationship between PTEN, DNA mismatch repair, and tumor histotype in endometrial carcinoma: retained positive expression of PTEN preferentially identifies sporadic non-endometrioid carcinomas. *Mod Pathol* 2013; 26: 1401-12.
 25. Okoye EI, Bruegl AS, Fellman B, Luthra R, Broaddus RR. Defective DNA mismatch repair influences expression of endometrial carcinoma biomarkers. *Int J Gynecol Pathol* 2016; 35: 8-15.
 26. Ruiz I, Martin-Arruti M, Lopez-Lopez E, Garcia-Orad A. Lack of association between deficient mismatch repair expression and outcome in endometrial carcinomas of the endometrioid type. *Gynecol Oncol* 2014; 134: 20-3.
 27. Shikama A, Minaguchi T, Matsumoto K, et al. Clinicopathologic implications of DNA mismatch repair status in endometrial carcinomas. *Gynecol Oncol* 2016; 140: 226-33.
 28. Stelloo E, Bosse T, Nout RA, et al. Refining prognosis and identifying targetable pathways for high-risk endometrial cancer: a TransPORTEC initiative. *Mod Pathol* 2015; 28: 836-44.
 29. Talhouk A, Hoang LN, McConechy MK, et al. Molecular classification of endometrial carcinoma on diagnostic specimens is highly concordant with final hysterectomy: earlier prognostic information to guide treatment. *Gynecol Oncol* 2016; 143: 46-53.
 30. Talhouk A, McConechy MK, Leung S, et al. Confirmation of ProMisE: a simple, genomics-based clinical classifier for endometrial cancer. *Cancer* 2017; 123: 802-13.
 31. Jumaah AS, Salim MM, Al-Haddad HS, McAllister KA, Yasseen AA. The frequency of *POLE*-mutation in endometrial carcinoma and prognostic implications: a systemic review and meta-analysis. *J Pathol Transl Med* 2020; 54: 471-9.
 32. Moher D, Shamseer L, Clarke M, et al. Preferred reporting items for systematic review and meta-analysis protocols (PRISMA-P) 2015 statement. *Syst Rev* 2015; 4: 1.
 33. Whiting PF, Rutjes AW, Westwood ME, et al. QUADAS-2: a revised tool for the quality assessment of diagnostic accuracy studies. *Ann Intern Med* 2011; 155: 529-36.
 34. Kumar V, Abbas AK, Aster JC. *Robbins and Contran pathologic basis of disease*. 9th ed. Philadelphia: Saunders-Elsevier, 2015; 1014-8.
 35. MedCalc. Statistical software version 15.8 [Internet]. Ostend: MedCalc Software bvba, 2015 [cited 2020 Dec 10]. Available from: <https://www.medcalc.org>.
 36. Riley RD, Higgins JP, Deeks JJ. Interpretation of random effects meta-analyses. *BMJ* 2011; 342: d549.
 37. Higgins JP, Thompson SG, Deeks JJ, Altman DG. Measuring inconsistency in meta-analyses. *BMJ* 2003; 327: 557-60.
 38. Sterne JA, Sutton AJ, Ioannidis JP, et al. Recommendations for examining and interpreting funnel plot asymmetry in meta-analyses of randomised controlled trials. *BMJ* 2011; 343: d4002.
 39. Ryan NA, Glaire MA, Blake D, Cabrera-Dandy M, Evans DG, Crosbie EJ. The proportion of endometrial cancers associated with Lynch syndrome: a systematic review of the literature and meta-analysis. *Genet Med* 2019; 21: 2167-80.
 40. Lorenzi M, Amonkar M, Zhang J, Mehta S, Law KL. Epidemiology of microsatellite instability high (MSI-H) and deficient mismatch repair (dMMR) in solid tumors: a structured literature review. *J Oncol* 2020; 2020: 1807929.
 41. Ryan NAJ, Blake D, Cabrera-Dandy M, Glaire MA, Evans DG, Crosbie EJ. The prevalence of Lynch syndrome in women with endometrial cancer: a systematic review protocol. *Syst Rev* 2018; 7: 121.
 42. Jerzak KJ, Duska L, MacKay HJ. Endocrine therapy in endometrial cancer: an old dog with new tricks. *Gynecol Oncol* 2019; 153: 175-83.
 43. Ashley CW, Da Cruz Paula A, Kumar R, et al. Analysis of mutational signatures in primary and metastatic endometrial cancer reveals distinct patterns of DNA repair defects and shifts during tumor progression. *Gynecol Oncol* 2019; 152: 11-9.
 44. Sargent DJ, Marsoni S, Monges G, et al. Defective mismatch repair as a predictive marker for lack of efficacy of fluorouracil-based adjuvant therapy in colon cancer. *J Clin Oncol* 2010; 28: 3219-26.
 45. Fujiyoshi K, Yamamoto G, Takenoya T, et al. Metastatic pattern of stage IV colorectal cancer with high-frequency microsatellite instability as a prognostic factor. *Anticancer Res* 2017; 37: 239-47.
 46. Fountzilas E, Kotoula V, Pentheroudakis G, et al. Prognostic implications of mismatch repair deficiency in patients with nonmetastatic colorectal and endometrial cancer. *ESMO Open* 2019; 4: e000474.
 47. Copija A, Waniczek D, Witkos A, Walkiewicz K, Nowakowska-Zajdel E. Clinical significance and prognostic relevance of microsatellite instability in sporadic colorectal cancer patients. *Int J Mol Sci* 2017; 18: 107.

Prognostic role of ALK-1 and h-TERT expression in glioblastoma multiforme: correlation with *ALK* gene alterations

Dalia Elasers¹, Doaa F. Temerik², Alia M. Attia³, A. Hadia⁴, Marwa T. Hussien⁵

¹Department of Pathology, Faculty of Medicine, Assiut University, Assiut; Departments of ²Clinical Pathology, ³Radiation Oncology, ⁴Medical Oncology, and ⁵Oncologic Pathology, South Egypt Cancer Institute, Assiut University, Assiut, Egypt

Background: Anaplastic lymphoma kinase (ALK) is a receptor tyrosine kinase that is expressed in the developing central and peripheral nervous systems during embryogenesis. Human telomerase reverse transcriptase (h-TERT) protein resumption is the main process of preservation of telomeres that maintains DNA integrity. The present study aims to evaluate the prognostic role of ALK-1 and h-TERT protein expression and their correlation with *ALK* gene alterations in glioblastoma multiforme (GBM). **Methods:** The current study is a retrospective study on a cohort of patients with GBM (n=53) that attempted to detect *ALK* gene alterations using fluorescence in situ hybridization. ALK-1 and h-TERT proteins were evaluated using immunohistochemistry. **Results:** Score 3 ALK-1 expression was significantly associated with male sex, tumor multiplicity, Ki labeling index (Ki LI), and type of therapeutic modality. Score 3 h-TERT expression exhibited a significant association with Ki LI. *ALK* gene amplifications (ALK-A) were significantly associated with increased Ki LI and therapeutic modalities. Score 3 ALK-1 protein expression, score 3 h-TERT protein expression, and ALK-A were associated with poor overall survival (OS) and progression-free survival (PFS). Multivariate analysis for OS revealed that *ALK* gene alterations were an independent prognostic factor for OS and PFS. **Conclusions:** High protein expression of both ALK-1 and h-TERT, as well as ALK-A had a poor impact on the prognosis of GBM. Further studies are needed to establish the underlying mechanisms.

Key Words: ALK-1; h-TERT; *ALK* gene; Glioblastoma multiforme; Prognosis

Received: February 1, 2021 **Revised:** March 14, 2021 **Accepted:** March 15, 2021

Corresponding Author: Marwa T. Hussien, MD, PhD, Department of Oncologic Pathology, South Egypt Cancer Institute, Assiut University, Assiut 171516, Egypt
 Tel: +20-88-208671, Fax: +20-88-2087709, E-mail: marwat.hussien@aun.edu.eg

Glioblastoma multiforme (GBM) is a grade IV glioma and is considered the most common and lethal malignant central nervous system (CNS) neoplasm in adults. The incidence rate of GBM is three cases per 100,000 persons in the adult population, with a median survival of 15 months. CNS tumor diagnoses should consist of a histopathological name based on genetic features [1]. According to the recent World Health Organization classification of CNS tumors, GBM that lacks the isocitrate dehydrogenase (IDH) mutation is termed GBM, IDH-wild type, while tumors that harbor an IDH mutation are termed GBM, IDH-mutant type. Tumors that lack any diagnostic mutation are categorized as GBM, not otherwise specified [2]. GBM necessitates robust diagnostic and management strategies [1].

The anaplastic lymphoma kinase (ALK) is a member of the insulin receptor superfamily of receptor tyrosine kinases. The genomic locus that codes the *ALK* gene is located at human chro-

mosome 2p23. The ALK protein has restricted expression in some tissues such as pericytes, endothelial, and neural cells in the brain, and is also found in some types of lymphoma, lung carcinoma, neuroblastomas, and GBMs [3]. Some studies showed that negative ALK-1 expression in GBM predicted better overall survival (OS) [4]. Other studies revealed no significant impact on OS with different ALK expression levels in GBM [5].

ALK gene rearrangements are mostly linked to subcellular changes in the ALK protein, which can be assessed by immunohistochemistry (IHC) and can likewise be evaluated with the fluorescence in situ hybridization (FISH) technique with higher sensitivity and specificity [5]. Both tests use an in vitro diagnostic assay that the Food and Drug Administration (FDA) approved for crizotinib response prediction. FISH is a qualitative test that detects *ALK* gene rearrangements with all potential fusion partners. Other methods of molecular testing such as real-time poly-

merase chain reaction targeted only the fusion site. Therefore, other probable clinically important fusion sites will not be detected. *ALK* gene analysis using FISH helps to detect a specific type of gene aberration, such as gene rearrangement and amplifications [6]. *ALK* gene amplification (*ALK-A*) has been recognized in several types of cancer as anaplastic large cell lymphoma (ALCL), hepatocellular carcinoma (HCC), esophageal squamous cell carcinoma, and GBM [7].

Telomerase is composed of a reverse transcriptase catalytic subunit human telomerase reverse transcriptase (h-TERT) and an RNA template, the human telomerase RNA component (hTERC). The h-TERT coded by the *TERT* gene is an active catalytic protein subset located at chromosome 5p15.33. The other subset of telomere is hTERC or hTR, coded by the human telomerase RNA component (*TERC* gene), which positioned at chromosome 3q26. In cancer cells, the resumption of h-TERT protein is the chief process of telomere preservation [8]. The expression of h-TERT is an important determinant of telomere activity. Generally, h-TERT is not expressed in normal tissues, which has been attributed to strict h-TERT regulation. However, h-TERT was highly expressed in malignant tumors including breast cancer, HCC, thyroid cancer and gliomas [9]. Some studies on GBM patients documented that patients with absent h-TERT expression had significantly longer OS than patients with strong h-TERT expression [10]. However, another study revealed no significant effect of h-TERT expression on survival [11].

The standard treatment for newly diagnosed GBM is maximum safe resection followed by concurrent temozolomide (TMZ) and radiotherapy with adjuvant TMZ for six cycles. This study reported a median OS of 14.6 months after median follow-up duration of 28 months [12]. Despite multimodal treatment of GBM, patient outcomes are still non-satisfying for neuro-oncologists. Molecular characterization of GBM with clinical concern is still under research for emerging targeted therapy. A novel targeted *ALK* inhibitor therapy as crizotinib, which is an FDA-approved treatment for lung cancer, is currently used in clinical trials for *ALK*-positive ALCL and in a few GBM patients [13]. However, emerging resistance to treatment with *ALK* inhibitors in patients remains a major concern. A recent study revealed that a subset of patients with *ALK*-positive lung adenocarcinomas harbor additional *TERT* amplification, which leads to unstable genomes with obvious fast relapse and therapeutic failure [14].

To date, there is no data detailing the relationship between *ALK-1* and h-TERT expression in GBM. The present study aimed to assess *ALK-1* and h-TERT protein expression, their correlation with *ALK* gene alterations in GBM prognosis, and

their relationship to conventional therapy for GBM.

MATERIALS AND METHODS

This was a retrospective study that included 53 patients primarily diagnosed with GBM. All were recruited and diagnosed in Pathology Department, Assiut University Hospital and South Egypt Cancer Institute, between April 2014 and April 2018. Patients were followed until May 2020. All patients were eligible at age 20–80 years, if they had no previous diagnosis of cancer and no previous CNS surgery for any cause. The exclusion criteria were patients with primary malignant brain tumors other than GBM or with brain metastasis, and patients with no follow-up records.

With regards to the treatment modalities used in the current research, all patients underwent surgical intervention, which included gross total resection, subtotal resection, or biopsy. Following surgical intervention, fractionated conformal radiation therapy was delivered to Gross tumor volume 1, which included the T2/FLAIR abnormality and the surgical cavity if present for a total dose of 46 Gy in 23 fractions at 2 Gy per fraction, once daily, for five days per week. Gross tumor volume 2 included T1 contrast enhanced abnormality and the surgical cavity if present for a boost dose of 14 Gy in seven fractions with 2 Gy per fraction, once daily, for five days per week. All patients were treated using a megavoltage linear accelerator and photon energies of 6 MV or more. Adjuvant radiotherapy only was given in 12 patients (22.6%) while the remaining patients received chemotherapy as a part of a treatment protocol. Chemotherapy treatment consisted of TMZ, which was given concomitantly with radiotherapy (75 mg/m²/day, started from the first day of radiotherapy until the end of radiation) in 27 patients (50.9%) or given as concurrent chemoradiotherapy (CCRT) and adjuvant (150–200 mg/m²/for 5 days/every 28 days for 6 or 12 cycles) in 14 patients (26.4%).

Follow-up evaluation included history and neurological examination, laboratory investigations, assessment of treatment related toxicity, and magnetic resonance imaging (MRI) or magnetic resonance spectroscopy imaging that were available for review. Patients were evaluated for response using MRI and or magnetic resonance spectroscopy, which were performed within 48 hours of surgery, before the first cycle, after every 3 cycles of adjuvant TMZ, and every three months after termination of treatment.

The GBM specimens used for evaluation of *ALK-1*, h-TERT immunohistochemical protein expression, and *ALK* gene alterations using the FISH technique. Clinicopathological parameters collected from the patient's archives sheets included patient age,

sex, tumor site, presence of tumor calcification, tumor multiplicity, tumor size, and Ki-67 labeling index (Ki LI) with cutoff point of 14% [15].

Immunohistochemistry

Formalin-fixed paraffin-embedded (FFPE) slides from the GBM tissue blocks, were retrieved from pathology lab and included for IHC study. The slides stained with hematoxylin and eosin were reviewed histologically before staining by the two pathologic consultants in this research. The FFPE blocks were cut into 3–4- μ m thickness, and then put on positively charged glass slides (PCS). Sections were de-paraffinized and rehydrated, followed by antigen retrieval, which was done with Tris-EDTA in a water bath at 90°C for 45 minutes. The primary monoclonal mouse anti-Human ALK/CD246 antibody (clone ALK-1), ready-to-use (code IR641, 117498-002, CVR No. 33211317, Dako, Glostrup, Denmark), Ki-67 antibody (clone MIB-1), ready-to-use (code IR626, primary monoclonal mouse, Dako), and a primary rabbit polyclonal anti-Human TERT antibody (catalog #213737, United State Biological 4 Technology, Salem, MA, USA) were applied. Anti-TERT antibody was used at a dilution of 1/75 (optimum dilution according to datasheet). Both incubated for one hour at room temperature in an airtight humid chamber. A universal staining kit “Ultra Vision Detection System Anti-Polyvalent, HRP/DAB (ready-to-use)” (catalog #TP-015-HD, LAB VISION Corp., Fremont, CA, USA) was applied following the manufacturer’s instructions.

Evaluation of ALK-1 and h-TERT IHC expression

ALK-1 positivity was identified as a brown cytoplasmic expression. A four-tier scoring system was used for evaluation of ALK-1 positivity [5]; score 1 was corresponded to weak cytoplasmic expression of ALK-1, moderate cytoplasmic expression was considered as score 2, and strong cytoplasmic expression was considered as score 3 (Fig. 1). Negative staining was scored as 0.

Positive brown nuclear staining of h-TERT was deemed positive. A three-tier evaluation system was used for scoring of h-TERT IHC protein expression [11]. Score 1 corresponded to nuclear expression in < 5% of tumor cells. h-TERT expression in between 5 and 50% tumor cells was scored as 2, and expression in more than 50% of tumor cells was deemed to score 3 (Fig. 2). Positive cytoplasmic staining of ALK-1 protein in anaplastic lymphoma cells was used as a positive control. Positive nuclear staining of h-TERT in melanoma cells were used as positive control. Negative control done using the same protocol of IHC unless the addition of the primary antibody on tissue section of specific

positive controls.

Ki-67 positivity was identified as a brown nuclear expression. KI LI was defined as the percentage of positive tumor nuclei in 1,000 tumor cells with cutoff value of 14% [15].

Fluorescence in situ hybridization

An ALK break-apart probe set (XT ALK BA Dual Color, Break Apart Rearrangement Probe [reference number: D-6001-100-OG], Metasystems, Altussheim, Germany) was used for FISH to detect gene rearrangements and copy number changes. In each case, we examined around 200 nuclei from at least 5–8 areas. We excluded nuclei with apparent overlapping or truncation.

Four-micrometer-thick tissue sections were cut from FFPE GBM tissue and were put on PCS. The unstained slides were placed overnight at 60°C on a hotplate. Then, the slides were immersed 3 times in xylene for 5 minutes and dehydrated twice in 100% ethanol for 5 minutes at room temperature. In sequence, the slides were immersed for 20 minutes in 0.2 N HCl, in purified water for 3 minutes, and in 1 M sodium thiocyanate at 80°C for 30 minutes. The slides were incubated for 30 minutes in Protease Solution previously warmed to 37°C after removal of excess water and washed in purified water for 3 minutes. Then, dehydration of slides in 70%, 80%, and 100% ethanol for one minute each was done and slides were allowed to dry. Then, they were placed in a dark room. Ten microliters of probe mixture were applied to a slide, immediately covered by a coverslip, and sealed with rubber cement. They were placed in a hybridizer instrument (DakoCytomation, Glostrup, Denmark) at 73°C for 3 minutes followed by an overnight hybridization at 37°C. At the end of the hybridization period, we removed the rubber cement from the slides and placed them in 2 \times saline sodium citrate (SSC; post hybridization wash) at 73°C temperature for 2 minutes, then immersed them for 1 minute in 2 \times SSC at room temperature and allowed the slides to dry. Ten microliters of DAPI counterstain was applied to the target area and covered by a coverslip [6].

Analysis of ALK gene alterations using FISH technique

We analyzed the prepared slides under an oil immersion objective (100 \times) with a fluorescence microscope (M1, Carl Zeiss Microscopy GmbH, Gottingen, Germany) equipped with appropriate filters and a charge-coupled device camera using FISH imaging with the capturing software Metafer 5 (a Metafer slide scanning system [Metasystems]). Non-rearranged ALK showed fusion (yellow signals) or very close abutment of the probes adjacent to the 3' (red) and the 5' (green) ends of the gene. Rearranged ALK appeared as splitting of 3' and 5' signals. Tumor tissues

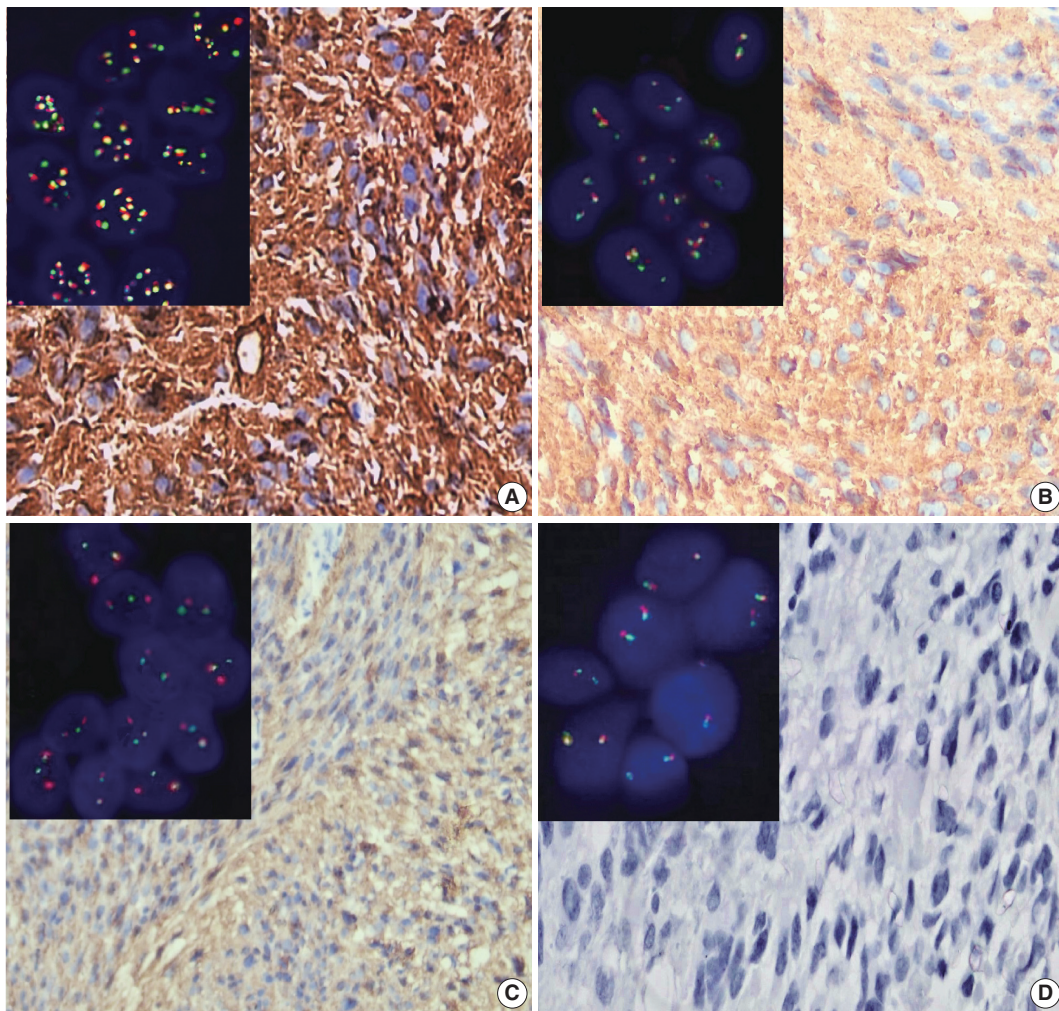


Fig. 1. Expression of anaplastic lymphoma kinase 1 (ALK-1) immunohistochemistry in tumor cells and *ALK* gene alterations in glioblastoma multiforme (GBM). (A) A case of GBM shows strong cytoplasmic expression of ALK-1 in tumor cells (score 3). The inset illustrates *ALK* gene amplification for the same case. (B) A case of GBM shows moderate cytoplasmic staining of ALK-1 in tumor cells. The inset illustrates *ALK* gene gain for the same case. (C) A case of GBM shows weak cytoplasmic expression of ALK-1 in tumor cells (score 1). The inset illustrates *ALK* gene rearrangement for the same case. (D) A case of GBM showed negative expression of ALK-1 (score 0). The inset illustrates that the *ALK* gene was negative for rearrangement with a normal copy number for the same case.

were considered ALK-FISH positive (*ALK*-rearranged) if > 15% tumor cells showed splitting of red and green signals [16]. The mean cutoff copy number of 3 to 5 fusion signals in $\geq 10\%$ of cells represented *ALK*-copy number gain (*ALK*-CNG), while the presence of ≥ 6 copies of *ALK* per cell in $\geq 10\%$ of analyzed cells represented *ALK*-A (Fig. 1) [17].

Statistical analysis

The analysis for this study was done through using the SPSS ver. 21 (IBM Corp., Armonk, NY, USA). Fisher exact test was used to detect the association between ALK protein, TERT protein expression, *ALK* gene alterations, and various clinicopatho-

logical data. Chi-square test was used only when $\leq 20\%$ of the cells had an expected count less than 5. Correlation between *ALK* gene alterations and ALK and TERT IHC protein expression were done via Spearman correlation coefficient test. OS was calculated from the date of surgical resection to the date of death from any cause or last follow-up. Progression-free survival (PFS) was calculated from the date of surgical resection to the date of progression or date of last follow-up or death.

Kaplan-Meier curves were used to analyze OS and PFS. Comparison of survival was determined by log-rank test. Multivariate analysis using Cox proportional hazard model of predictors of outcome variables were applied. The value of significance was

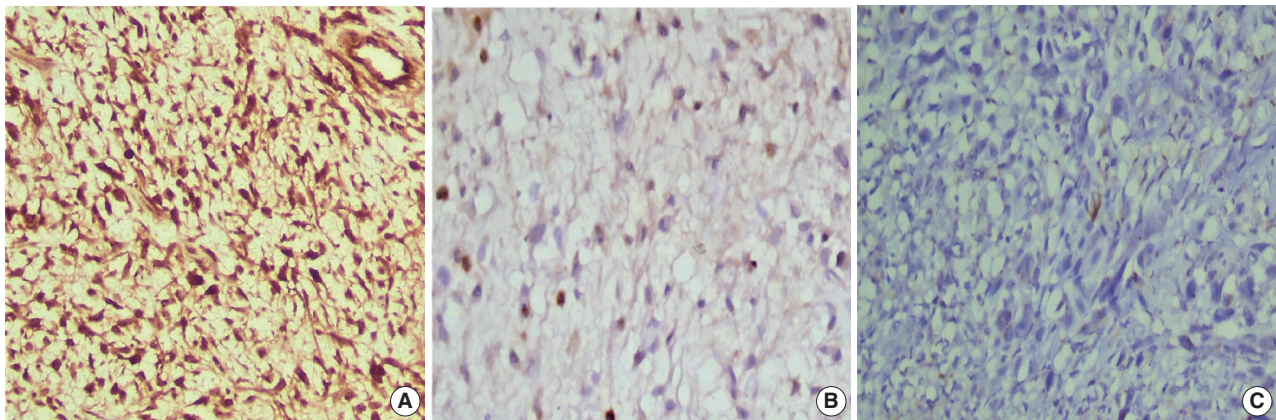


Fig. 2. Expression of human telomerase reverse transcriptase (TERT) immunohistochemistry in tumor cells of glioblastoma multiforme. (A) Strong nuclear expression of TERT in >50% of tumor cells (score 3). (B) Moderate nuclear staining of TERT in 5%–50% of tumor cells (score 2). (C) Weak nuclear expression of TERT in <5% of tumor cells (score 1).

determined as $p < .05$.

RESULTS

The current study included 53 GBM patients. The study included 17 patients (32.1%) who were < 50 years of age, while 36 patients (67.9%) were ≥ 50 years old. Thirty-six cases (67.9%) were males. The most prominent tumor location was at the parieto-occipital region, constituting 28.4% of patients. The median tumor size was 5 cm. Calcification was present in 32 cases (60.4%). There were multiple tumors in six cases (11.3%).

After a median follow-up duration of 12 months (range, 3 to 19 months), 21 out of 53 patients (39.6%) were still alive (Table 1).

Association between ALK-1 IHC protein expression and clinicopathological parameters

ALK-1 expression was detected in 45 cases out of 53 (84.9%). Strong ALK cytoplasmic expression (score 3) was noted in 17 GBM tumors (32.1%). Thirteen cases (24.5%) showed moderate cytoplasmic expression (score 2), while 15 cases (28.3%) showed weak cytoplasmic expression (score 1). Eight cases (15.1%) were negative (score 0).

Score 3 ALK-1 expression showed significant association with male sex ($p = .038$), tumor multiplicity ($p = .046$), and Ki LI ($p \leq .001$). The type of therapeutic modality was positively associated with ALK-1 protein expression ($p = .030$). The clinicopathological associations with ALK-1 protein IHC expression are summarized in Table 2.

Association between h-TERT IHC protein expression and clinicopathological parameters

h-TERT expression was detected in the studied cases with variable percentages and staining intensities. Strong h-TERT nuclear expression in > 50% of tumor cells (score 3) was noted in 29 (54.7%) cases, while moderate expression in 5%–50% of tumor cells (score 2) was present in 16 cases (30.2%) and eight cases (15.1%) showed weak expression in < 5% of tumor cells (score 1).

h-TERT expression showed significant association with the presence of calcifications ($p = .016$). Score 3 h-TERT expression exhibited a significant association with Ki LI ($p = .005$). There was no significant correlation between h-TERT expression and other clinicopathological variables (Table 2).

Association between ALK gene alterations and clinicopathological parameters

Thirty-four cases out of 53 showed ALK gene alterations (64.2%). ALK-A was detected in four cases (7.5%), and all of these cases had strong ALK immunohistochemical expression. ALK-CNG was noted in 12 cases (22.6%), while 18 cases (34.0%) showed ALK gene rearrangement. Nineteen cases (35.9%) were negative. ALK-A was significantly associated with increased Ki LI ($p = .044$). The type of therapeutic modality was positively associated with ALK gene alterations ($p = .027$). There was no significant association between ALK gene alteration and clinicopathological variables (Table 3).

Correlation between ALK gene alterations, ALK-1 and h-TERT IHC protein expression

A strong positive correlation was noted between ALK protein IHC expression and ALK gene alterations ($p = .001$, $r = 0.616$).

Table 1. Clinicopathological characteristics of the patients

Variable	No. (%)
Age (yr)	
<50	17 (32.1)
≥50	36 (67.9)
Sex	
Male	36 (67.9)
Female	17 (32.1)
Site	
CC	4 (7.5)
FP	12 (22.6)
PO	15 (28.4)
TO	7 (13.2)
PS	6 (11.3)
TP	9 (17.0)
Calcification	
Absent	21 (39.6)
Present	32 (60.4)
Multiplicity	
Single	47 (88.7)
Multiple	6 (11.3)
Tumor size	
Median (interquartile range)	5 (4–7)
Type of surgical resection	
GTR	19 (35.0)
STR	25 (47.0)
Biopsy	9 (17.0)
Ki LI (%)	
<14	37 (69.8)
≥14	16 (30.2)
Status	
Living	21 (39.6)
Dead	32 (60.4)
Therapeutic modalities	
RTH only	12 (22.6)
CCRT	14 (26.4)
CCRT and adjuvant TMZ	27 (50.9)

CC, corpus callosum; FP, fronto-parietal; PO, parieto-occipital; TO, temporo-occipital; PS, parasagittal; TP, temporo-parietal; GTR, gross total resection; STR, subtotal resection; Ki LI, Ki labeling index; RTH, radiotherapy; CCRT, concurrent chemoradiotherapy; TMZ, temozolomide.

Moderate correlation was noted between *ALK* gene alterations and TERT IHC ($p = .007$, $r = 0.476$), as (score 2) TERT expression was associated with *ALK* gene rearrangement (56.2%), while (score 3) TERT expression was associated with *ALK*-CNG and *ALK*-A (51.8%). There was a strong positive correlation between *ALK*-1 and TERT IHC protein expression ($p = .002$, $r = 0.602$). The relationships and correlations between *ALK* gene alterations, *ALK*, and TERT IHC protein expression are presented in Tables 3 and 4, respectively.

Outcome analysis

The median follow-up duration of the 53 GBM patients was 12 months (range, 3 to 19 months). During follow-up, 32/53 patients (60.4%) died as a result of tumor progression. According to Kaplan-Meier analysis, the median OS was 12 months (95% confidence interval [CI], 10.449 to 13.551), while the 19-month OS rate was 39.6%. A total of 36/53 patients (67.9%) developed disease progression. The median time to progression was 10 months (range, 2 to 19 months). According to Kaplan-Meier analysis, the median PFS was 10 months (95% CI, 7.860 to 12.140). The PFS rate at 19 months was 32.1%.

ALK-1 protein expression (score 3), h-TERT protein expression (score 3), and *ALK*-A were associated with poor OS and PFS ($p < .001$, $p = .031$, and $p < .001$) and ($p < .001$, $p = .040$, and $p < .001$), respectively. Cases that exhibited high Ki LI had poor OS and short PFS ($p = .016$) and ($p = .022$), respectively (Figs. 3, 4).

Regarding the type of therapeutic modalities, patients treated with adjuvant radiotherapy only had poor OS and PFS compared to those who were treated with CCRT or CCRT and adjuvant TMZ ($p = .002$) and ($p = .004$), respectively (Table 5, Figs. 3E, 4E).

Multivariate analysis for OS and disease-free survival was applied to clinicopathological features that were significant in univariate analysis to adjust for confounders. Our results revealed that *ALK* gene alteration was the only independent prognostic factor for OS and PFS ($p < .001$; hazard ratio [HR], 7.514; 95% CI, 3.292 to 17.155) and ($p < .001$; HR, 4.711; 95% CI, 2.429 to 9.136), respectively (Table 6).

DISCUSSION

GBM exhibits a vast group of modifications, both genetic and epigenetic, which create a great number of mutation subsets, some of which have a proven effect in survival and therapy response [1].

In the present study, high *ALK*-1 expression showed a significant association with male sex, however, no significant relation between *ALK*-1 expression and patient's age. These findings are not matched with the study done by Karagkounis et al. [5], which reported that *ALK* overexpression is more common in older individuals (> 59 years) and that was no association between *ALK* expression and patient's sex. This discrepancy was due to division of their cases into subgroups according to IDH1 protein expression with cutoff median age of 59 years, which was not implemented in the current study.

One persistent debate is whether *ALK*-1 immunohistochemical overexpression was associated with *ALK* gene mutation or amplification in GBM cases. In the current study, we reported that

Table 2. Association between ALK-1, h-TERT IHC protein expression, and clinicopathological parameters

Parameter	ALK-1 IHC				p-value	h-TERT IHC			p-value
	Score 0	Score 1	Score 2	Score 3		Score 1	Score 2	Score 3	
Age (yr)					.236				.123 ^a
<50	2 (11.8)	6 (35.3)	6 (35.3)	3 (17.6)		3 (17.6)	8 (47.1)	6 (35.3)	
≥50	6 (16.7)	9 (25.0)	7 (19.4)	14 (38.9)		5 (13.9)	8 (22.2)	23 (63.9)	
Sex					.038				.267 ^a
Male	7 (19.4)	6 (16.7)	10 (27.8)	13 (36.1)		6 (16.7)	13 (36.1)	17 (47.2)	
Female	1 (5.9)	9 (52.9)	3 (17.6)	4 (23.5)		2 (11.8)	3 (17.6)	12 (70.6)	
Site					.425				.119
CC	2 (50.0)	1 (25.0)	0	1 (25.0)		0	3 (75.0)	1 (25.0)	
FP	1 (8.4)	4 (33.3)	4 (33.3)	3 (25.0)		2 (16.7)	2 (16.7)	8 (66.6)	
PO	2 (13.3)	7 (46.7)	2 (13.3)	4 (26.7)		5 (33.3)	2 (13.3)	8 (53.4)	
TO	2 (28.5)	1 (14.3)	3 (42.9)	1 (14.3)		1 (14.3)	4 (57.1)	2 (28.6)	
PS	0	0	2 (33.3)	4 (66.7)		0	1 (16.6)	5 (83.4)	
TP	1 (11.2)	2 (22.2)	2 (22.2)	4 (44.4)		0	4 (44.4)	5 (55.6)	
Calcification					.315				.016 [*]
Absent	1 (4.8)	6 (28.6)	5 (23.8)	9 (42.8)		3 (14.3)	2 (9.5)	16 (76.2)	
Present	7 (21.9)	9 (28.1)	8 (25.0)	8 (25.0)		5 (15.6)	14 (43.8)	13 (40.6)	
Multiplicity					.046				.501
Single	8 (17.1)	14 (29.8)	13 (27.7)	12 (25.5)		8 (17.0)	15 (31.9)	24 (51.1)	
Multiple	0	1 (16.7)	0	5 (83.3)		0	1 (16.7)	5 (83.3)	
Tumor size					.670				.834
<Median	4 (14.2)	6 (21.4)	9 (32.2)	9 (32.2)		5 (17.8)	7 (25.0)	16 (57.2)	
≥Median	4 (14.2)	9 (32.2)	7 (25.0)	8 (28.6)		3 (12.0)	9 (36.0)	13 (52.0)	
Type of surgical resection					.266				.133
GTR	3 (15.8)	4 (21.1)	6 (31.6)	6 (31.6)		5 (26.3)	3 (15.8)	11 (57.9)	
STR	5 (20.0)	7 (28.0)	7 (28.0)	6 (24.0)		3 (12.0)	11 (44.0)	11 (44.0)	
Biopsy	0	4 (44.4)	0	5 (55.6)		0	2 (22.0)	29 (54.7)	
Ki LI (%)					<.001				.005
<14	8 (21.6)	15 (40.5)	10 (27.1)	4 (10.8)		8 (21.6)	14 (37.8)	15 (40.6)	
≥14	0	0	3 (18.7)	13 (81.3)		0	2 (12.5)	14 (87.5)	
Therapeutic modalities					.030				.287
RTH only	0	3 (25.0)	3 (25.0)	6 (50.0)		1 (8.3)	2 (16.7)	9 (75.0)	
CCRT	5 (35.7)	4 (28.6)	0	5 (35.7)		4 (28.6)	3 (21.4)	7 (50.0)	
CCRT and adjuvant TMZ	3 (11.2)	8 (29.6)	10 (37.0)	6 (22.2)		3 (11.1)	11 (40.7)	13 (48.2)	

Significant at $p < .05$.

ALK-1, anaplastic lymphoma kinase 1; h-TERT, human telomerase reverse transcriptase; IHC, immunohistochemistry; CC, corpus callosum; FP, fronto-parietal; PO, parieto-occipital; TO, temporo-occipital; PS, parasagittal; TP, temporo-parietal; GTR, gross total resection; STR, subtotal resection; Ki LI, Ki labeling index; RTH, radiotherapy; CCRT, concurrent chemoradiotherapy; TMZ, temozolomide.

^aFisher exact test was used in this table except when $\leq 20\%$ of the cells have expected count less than 5 chi-square test was used instead.

ALK-A was detected in four cases out of 17 IHC stains that were strongly positive for ALK-1 expression, and ALK-CNG was noted in 12 cases. This is consistent with two early studies done by Hudson et al. [18] and Kulig et al. [19], which found that 60% and 48.2% of their GBM cases possessed *ALK* gene gain/amplification by FISH, respectively. On the other hand, our results are contrary to those presented by Karagkounis et al. [5] and Chiba et al. [4] with respect to the *ALK* gene via FISH analysis. Karagkounis et al. [5] revealed only one case of GBM showed ALK-A of the 2p domain. Likewise, Chiba et al. [4] revealed no amplification of the *ALK* locus.

A study on non-small lung cancer reported that *ALK* gene non-translocated cancers are commonly related to unstable chromosomes and ALK-CNG, while the *ALK* gene translocated cancers represent a low number of *ALK* gene copies [20]. This may clarify our findings of the association between *ALK* non-rearranged tumors with increased *ALK* gene copies (ALK-A and ALK-CG) and moderate to strong expression of ALK-I IHC, while the *ALK*-rearranged tumors without *ALK* gene extra-copies were associated with negative to weak ALK-I IHC expression. The relationship between *ALK* gene extra-copies (ALK-A and ALK-CG) by FISH and ALK protein expression is still debatable. On one hand, a study

Table 3. Association between *ALK* gene alteration, clinicopathological parameters, and ALK-1 and h-TERT expression

	ALK gene alterations				p-value
	Negative	Rearrangement	Gain	Amplification	
Age (yr)					.430
<50	7 (41.2)	7 (41.2)	3 (17.6)	0	
≥50	12 (33.3)	11 (30.6)	9 (25.0)	4 (11.1)	
Sex					.181
Male	10 (27.8)	12 (33.3)	10 (27.8)	4 (11.1)	
Female	9 (52.9)	6 (35.3)	2 (11.8)	0	
Site					.955
CC	2 (50.0)	1 (20.0)	1 (20.0)	0	
FP	4 (33.3)	3 (25.0)	3 (25.0)	2 (16.7)	
PO	6 (40.0)	5 (33.3)	3 (20.0)	1 (6.7)	
TO	2 (28.6)	3 (42.8)	1 (14.3)	1 (14.3)	
PS	2 (33.3)	1 (16.7)	3 (50.0)	0	
TP	3 (33.3)	5 (55.6)	1 (11.1)	0	
Calcification					.710
Absent	6 (28.6)	7 (33.3)	6 (28.6)	2 (9.5)	
Present	13 (40.6)	11 (34.4)	6 (18.8)	2 (6.2)	
Multiplicity					.162
Single	19 (40.4)	15 (31.9)	10 (21.3)	3 (6.4)	
Multiple	0	3 (50.0)	2 (33.3)	1 (16.7)	
Size					.836
<Median	12 (38.7)	9 (29.0)	7 (22.6)	3 (9.7)	
>Median	7 (31.8)	9 (40.9)	5 (22.7)	1 (4.6)	
Type of surgical resection					.125
GTR	9 (47.4)	3 (15.8)	5 (26.3)	2 (10.5)	
STR	8 (32.0)	9 (36.0)	7 (28.0)	1 (4.0)	
Biopsy	2 (22.2)	6 (66.7)	0	1 (11.1)	
Ki- LI					.044
<14%	15 (40.5)	15 (40.5)	6 (16.2)	1 (2.8)	
≥14%	4 (25.0)	3 (18.8)	6 (37.4)	3 (18.8)	
ALK-1 IHC					.001
Score 0	8 (100)	0	0	0	
Score 1	6 (40.0)	9 (60.0)	0	0	
Score 2	2 (15.4)	5 (38.4)	6 (46.2)	0	
Score 3	3 (17.7)	4 (23.5)	6 (35.3)	4 (23.5)	
h-TERT IHC					.008
Score 1	6 (75.0)	2 (25.0)	0	0	
Score 2	6 (37.5)	9 (56.2)	1 (6.3)	0	
Score 3	7 (24.1)	7 (24.1)	11 (38.0)	4 (13.8)	
Therapeutic modalities					.027
RTH	2 (16.7)	3 (25.0)	3 (25.0)	4 (33.3)	
CCRT & adjuvant TMZ	11 (40.7)	10 (37.0)	6 (22.3)	0	
CCRT	6 (42.9)	5 (35.7)	3 (21.4)	0	

Significant at p < .05.

ALK-1, anaplastic lymphoma kinase 1; h-TERT, human telomerase reverse transcriptase; CC, corpus callosum; FP, fronto-parietal; PO, parieto-occipital; TO, temporo-occipital; PS, parasagittal; TP, temporo-parietal; GTR, gross total resection; STR, subtotal resection; Ki LI, Ki labeling index; IHC, immunohistochemistry; RTH, radiotherapy; CCRT, concurrent chemoradiotherapy; TMZ, temozolomide.

Table 4. Correlation between *ALK* gene alterations, ALK-1, and h-TERT IHC protein expression

	Spearman's rho		
	h-TERT expression	ALK-1 expression	ALK gene alterations
h-TERT expression			
Correlation coefficient	1.000	0.602	0.476
Sig. (2-tailed)		0.002 ^a	0.007 ^a
No.	53	53	53
ALK-1 expression			
Correlation coefficient	0.602	1.000	0.616
Sig. (2-tailed)	0.002 ^a		0.001 ^a
No.	53	53	53
ALK gene alterations			
Correlation coefficient	0.476	0.616	1.000
Sig. (2-tailed)	0.007 ^a	0.001 ^a	
No.	53	53	53

ALK-1, anaplastic lymphoma kinase 1; h-TERT, human telomerase reverse transcriptase; IHC, immunohistochemistry.

^aSignificant; correlation is significant at the 0.01 level (2-tailed).

revealed that *ALK* gene aberrations detected by FISH and *ALK* overexpression by IHC in rhabdomyosarcoma were significantly correlated [21]. On the other hand, other studies found no association between *ALK* gene aberrations detected by FISH and *ALK* expression by IHC in various cancer types such as esophageal squamous cell carcinoma and colorectal carcinoma [22]. Furthermore, a study of a neuroblastoma cell line harboring *ALK-A* was accompanied by reduction of *ALK* levels as a result of N-linked glycosylation inhibition with subsequent inhibition of its phosphorylated downstream molecules such as *AKT* and *STAT3* [23]. This controversy between the relationship between *ALK* gene extra-copies on FISH and *ALK* protein expression may be attributed to either transcriptional or post-transcriptional modifications, or degradation, such as N-linked glycosylation activation or inhibition, which lead to *ALK* activation and reduction, respectively.

Regarding h-TERT immunohistochemical expression, the current work revealed strong h-TERT nuclear expression in about half of the studied cases; this is compatible with the study done by Potharaju et al. [10], which showed that 60% of GBM patients expressed strong h-TERT. In spite of the use of h-TERT IHC as a mirror to detect tumors harboring *TERT*-mutation, h-TERT IHC was not able to identify the differences between *TERT*-mutated GBMs and *TERT*-nonmutant GBMs. h-TERT protein overexpression was noted even among gliomas with wildtype *TERT*. Moreover, h-TERT IHC widely varied through the *TERT*-mutant gliomas such as oligodendrogliomas and GBMs. This indicates that h-TERT IHC expression may be regulated by various mechanisms along with *TERT* promoter mutations [24].

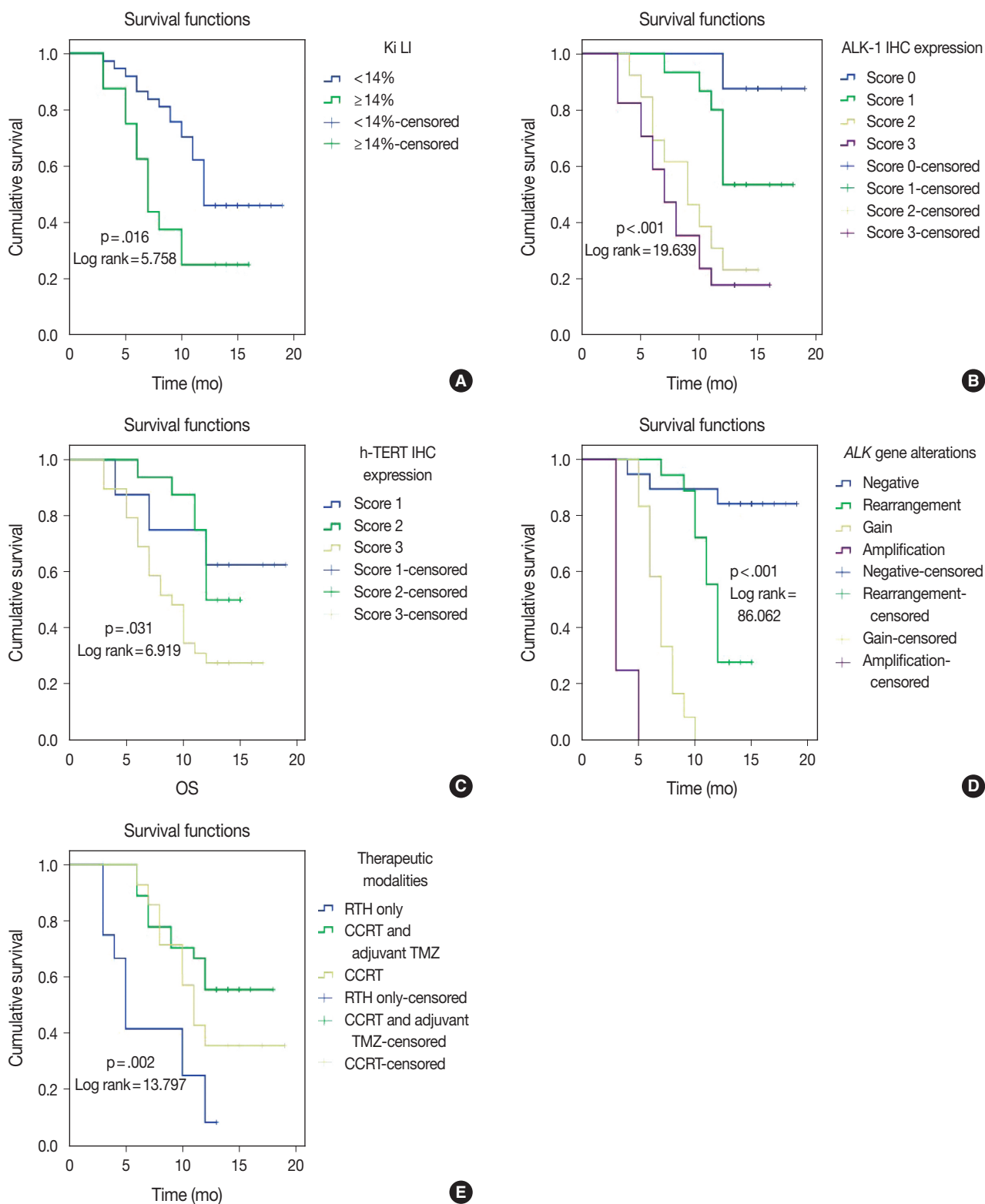


Fig. 3. Overall survival (OS) for anaplastic lymphoma kinase 1 (ALK-1), human telomerase reverse transcriptase (h-TERT) immunohistochemistry (IHC) expression, and ALK gene alterations. (A) High Ki labeling index (Ki LI) is associated with poor OS. (B) ALK-1 score 3 is associated with poor OS. (C) TERT score 3 is associated with poor OS. (D) ALK gene amplification is associated with poor OS. (E) Patients treated with adjuvant radiotherapy only had poor OS compared to those who were treated with concurrent chemoradiotherapy (CCRT) or CCRT and adjuvant temozolomide (TMZ).

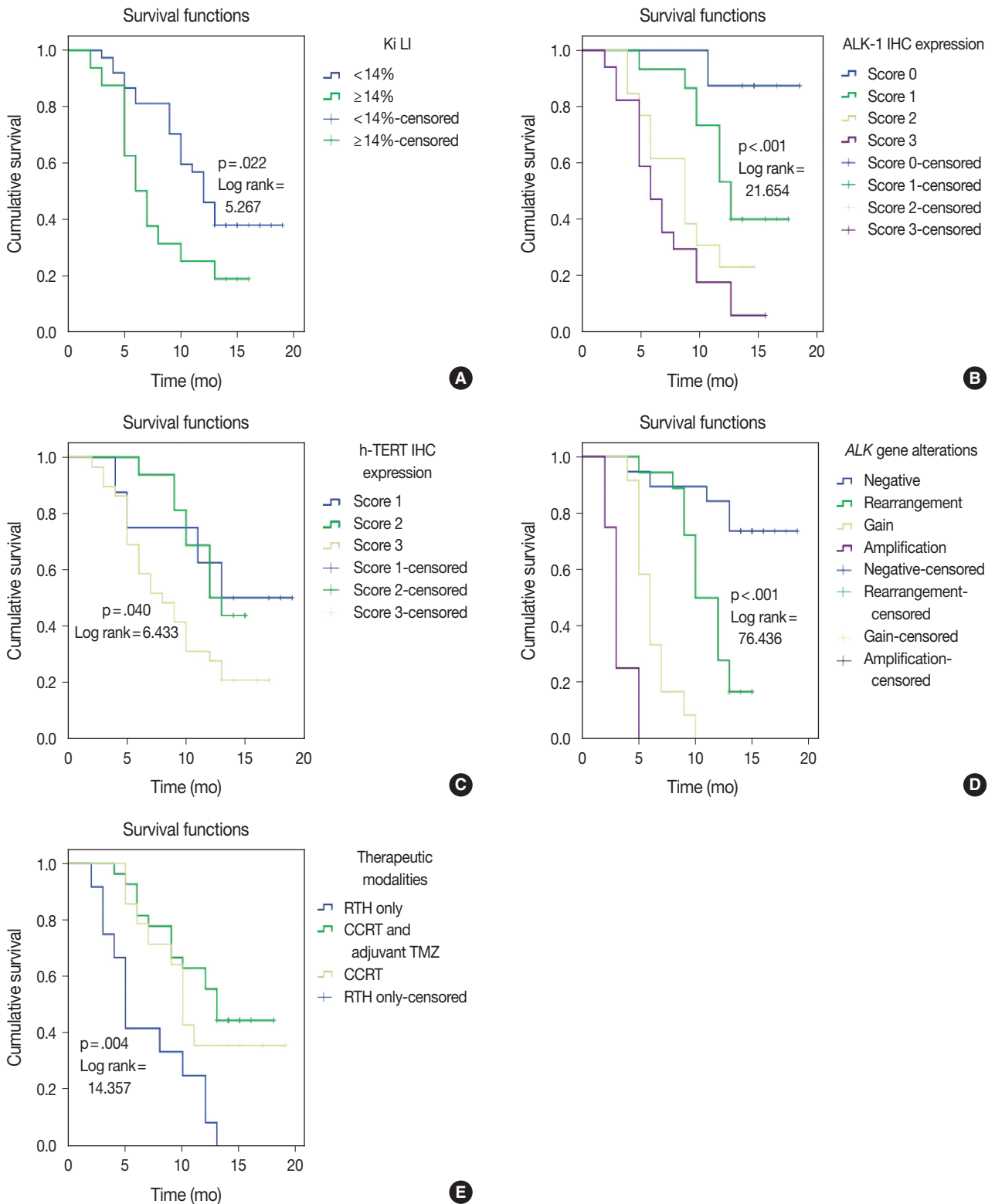


Fig. 4. Progression-free survival (PFS) for anaplastic lymphoma kinase 1 (ALK-1), human telomerase reverse transcriptase (h-TERT) immunohistochemistry (IHC) expression, and *ALK* gene alterations. (A) High Ki labeling index (Ki LI) is associated with short PFS. (B) ALK-1 score 3 is associated with poor PFS. (C) TERT score 3 is associated with poor PFS. (D) *ALK* gene amplification is associated with poor PFS. (E) Patients treated with adjuvant radiotherapy only had poor PFS compared to those who were treated with concurrent chemoradiotherapy (CCRT) or CCRT and adjuvant temozolomide (TMZ).

Table 5. Kaplan-Meier analysis for OS and PFS

Parameter	OS		PFS	
	Log-rank (chi-square)	p-value	Log-rank (chi-square)	p-value
Age (<50 yr vs. ≥50 yr)	3.146	.076	2.419	.120
Sex (male vs. female)	3.326	.119	3.887	.153
Site (CC vs. FP vs. PO vs. TO vs. PS vs. TP)	3.398	.639	4.216	.519
Calcification (absent vs. present)	0.666	.414	0.253	.615
Multiplicity (single vs. multiple)	3.993	.254	3.505	.190
Size (<median vs. >median)	0.010	.921	0.048	.827
Type of surgical resection (GTR vs. STR vs. biopsy)	0.066	.967	0.168	.919
Ki LI (<14% vs. ≥14%)	5.758	.016	5.267	.022
ALK-1 IHC (score 0 vs. score 1 vs. score 2 vs. score 3)	19.639	<.001	21.654	<.001
h-TERT IHC (score 1 vs. score 2 vs. score 3)	6.919	.031	6.433	.040
ALK gene alterations (negative rearrangement vs. gain amplification)	86.062	<.001	76.436	<.001
Therapeutic modalities (RTH only vs. CCRT vs. CCRT and adjuvant TMZ)	13.797	.002	14.357	.004

Significant at $p < 0.5$.

OS, overall survival; PFS, progression-free survival; CC, corpus callosum; FP, fronto-parietal; PO, parieto-occipital; TO, temporo-occipital; PS, parasagittal; TP, temporo-parietal; GTR, gross total resection; STR, subtotal resection; Ki LI, Ki labeling index; ALK-1, anaplastic lymphoma kinase 1; IHC, immunohistochemistry; h-TERT, human telomerase reverse transcriptase; RTH, radiotherapy; CCRT, concurrent chemoradiotherapy; TMZ, temozolomide.

Table 6. Multivariate analysis for significant predictors of OS and PFS

	OS					PFS				
	B	SE	p-value	HR	95 % CI for Exp (B)	B	SE	p-value	HR	95 % CI for Exp (B)
Ki LI	0.125	0.468	.790	1.133	0.453–2.833	-0.001	0.435	.998	0.099	0.426–2.344
ALK-1 protein expression	0.357	0.347	.304	0.429	0.724–2.821	0.505	0.306	.099	1.657	0.909–3.010
h-TERT protein expression	-0.368	0.411	.371	0.692	0.310–1.549	-0.352	0.356	.322	0.703	0.350–1.411
ALK gene alterations	2.017	0.421	<.001	7.514	3.292–17.155	1.550	0.338	<.001	4.711	2.429–9.136
Therapeutic modalities	0.050	0.311	.872	1.052	0.571–1.935	-0.007	0.295	.982	0.993	0.558–1.769

Significant at $p < 0.5$.

OS, overall survival; PFS, progression-free survival; HR, hazards ratio; CI, confident interval; Ki LI, Ki labeling index; ALK-1, anaplastic lymphoma kinase 1; h-TERT, human telomerase reverse transcriptase.

An interesting finding is the presence of a significant association between h-TERT expression and the presence of tumor calcification in the present study, which may be attributed to the hypoxic state in GBM that leads to activation of hypoxia-inducible factor-1 α (HIF-1 α) in response to hypoxic status with subsequent increase in intracellular calcium (Ca²⁺) and promotion of the Ca²⁺ signaling pathway [25]. Furthermore, activation of HIF-1 α enhances h-TERT transcription [26].

Concerning the relationship between Ki LI and ALK-1/h-TERT protein expression, all the aforementioned biomarkers had a reportedly positive association with Ki LI [4]. Persson and Englund [11] discerned that high values of Ki LI were not significantly associated with high h-TERT staining. The current study showed that high Ki LI had a poor impact on OS and PFS. This is in agreement with Persson and Englund [11], and in contrast with other studies, which noted no effect of Ki LI on OS [11,27,28]. The prognostic value of Ki LI in GBM is still uncertain, as the distribution of proliferative index was different in variable areas within the same tumor and different cutoff points are

used in the literature.

Overall, there was a strong positive correlation between ALK-1 and h-TERT IHC protein expression in the current research. All GBM cases displayed necrosis and/or microvascular proliferation, which is essential for their diagnosis [29]. These findings were corresponding to a hypoxic state of the microenvironment. ALK expression was significantly higher in tumor cells in hypervascular lesions as compared to those adjacent to necrotic foci in GBMs, and was positively correlated with the microvascular density as determined by CD34 expression. Overexpression of ALK induced an enhancement of the HIF-1 α /vascular endothelial growth factor-A axis through activation of Stat3 [4]. Furthermore, a study done by Marzec et al. [30] reported that ALK-positive T-cell lymphoma expresses HIF1 α . HIF1 α mRNA expression is induced in ALK-positive T-cell lymphoma by the transcription of nucleophosmin/ALK tyrosine kinase. NPM/ALK activates the HIF1 α gene through the STAT3 transcription factor [30].

GBMs contain considerable hypoxic areas within the tumor.

Potharaju et al. [10] suggested that an intratumoral decrease in oxygen concentration can augment HIF-1 α expression and enhance h-TERT transcription and telomerase, which in turn lead to proliferation of cancer stem cells [26]. Consequently, both ALK-1 and h-TERT expression are highly expressed in the hypervascular area of GBM, depending on HIF-1 α activation. This may explain the close relationship between ALK and h-TERT expression in GBM.

Regarding OS, high ALK-1 expression, high h-TERT expression, and ALK-A were associated with poor OS in the studied cases. This result was in congruent with a study [4] showing that loss of ALK expression had improved OS in contrast to the ALK-positive cases and another report [10] showing that patients with absent or weak h-TERT expression had significantly longer OS than patients with strong h-TERT expression. However, the current findings are inconsistent with those of Karagkounis et al. [5] and Persson and Englund [11], which noted no significant impact of ALK-1 and h-TERT expression on OS, respectively.

Interestingly, we found that *ALK* gene alteration was an independent prognostic factor for OS. This is in agreement with a previous observation, which revealed that patients who had ALK-A died within one month from diagnosis [5].

In the current study, the type of therapeutic modality was positively associated with both ALK-1 protein expression and *ALK* gene alterations. Patients who were treated with adjuvant radiotherapy only had poor survival outcomes compared to those who were treated with CCRT or CCRT and maintenance TMZ. The best survival outcome was among patients who were treated with adjuvant CCRT and maintenance TMZ. A potential therapeutic application in patients harboring ALK-A was noted in in vitro studies that applied specific ALK inhibitors to cell lines with ALK-A [7]. Furthermore, Le Rhun et al. [13] suggested that GBM patients with ALK protein expression and ALK-CNG could benefit from novel targeted ALK inhibitors (crizotinib). Therefore, ALK-targeting therapy may be used for treatment of GBM patients with *ALK* gene alterations, taking into consideration the h-TERT mutation.

The limitation of this research is that it lacks application of IDH-1 IHC for subdivision of GBM into molecular subtypes according to IDH status and for correlation with ALK-1 and h-TERT IHC, which will add to the research. This point is recommended in future studies.

In summary, Break-Apart ALK FISH is a reliable diagnostic technique that can be applied with ease on FFPE tissue whenever the exact fusion partners are indefinite. Furthermore, *ALK* gene alterations have a significant prognostic impact on GBM

patients. Subsequent studies with a larger number of GBM cases are recommended for better evaluation of the role of ALK-1, h-TERT, and *ALK* gene alterations in tumor progression and related mechanisms.

The current work concluded that high protein expression of ALK-1, h-TERT, and ALK-A had poor impact on the prognosis of GBM. Accordingly, ALK-1 protein expression, h-TERT protein expression, and *ALK* gene alteration detection could be used as valuable prognostic markers in GBM patients. The type of therapeutic modality was positively associated with *ALK* gene alterations. The use of ALK-targeting therapy as part of treatment plan for GBM patients with *ALK* gene alterations is the goal, and requires further studies with a larger sample size.

Ethics Statement

The research was approved by the Committee of Medical Ethics, Faculty of Medicine, Assiut University IRB. No. 17300482. A written informed consent for participation and publication was obtained from each participant after receiving information about the details of the study. Confidentiality of patients' records was assured and maintained throughout the study.

Availability of Data and Material

The datasets generated or analyzed during the current study are available from the corresponding author on reasonable request.

Code Availability

Not applicable.

ORCID

Marwa T. Hussien <https://orcid.org/0000-0001-8561-8501>

Author Contributions

Conceptualization: DE, MTH. Data curation: DE, MTH, DFT. Formal analysis: DE, MTH. Methodology: DE, MTH, DFT. Resources: DE, MTH, DFT. Writing—original draft: DE, MTH. Writing—review & editing: AMA, AH. Approval of final manuscript: all authors.

Conflicts of Interest

The authors declare that they have no potential conflicts of interest.

Funding Statement

No funding to declare.

References

1. Stoyanov GS, Dzhenkov D, Ghenev P, Iliev B, Enchev Y, Tonchev AB. Cell biology of glioblastoma multiforme: from basic science to diagnosis and treatment. *Med Oncol* 2018; 35: 27.
2. Louis DN, Perry A, Reifenberger G, et al. The 2016 World Health Organization classification of tumors of the central nervous system: a summary. *Acta Neuropathol* 2016; 131: 803-20.
3. Chiarle R, Voena C, Ambrogio C, Piva R, Inghirami G. The anaplastic lymphoma kinase in the pathogenesis of cancer. *Nat Rev Cancer* 2008; 8: 11-23.
4. Chiba R, Akiya M, Hashimura M, et al. ALK signaling cascade con-

- fers multiple advantages to glioblastoma cells through neovascularization and cell proliferation. *PLoS One* 2017; 12: e0183516.
5. Karagkounis G, Stranjalis G, Argyrakos T, et al. Anaplastic lymphoma kinase expression and gene alterations in glioblastoma: correlations with clinical outcome. *J Clin Pathol* 2017; 70: 593-9.
 6. Wojas-Krawczyk K, Krawczyk PA, Ramlau RA, et al. The analysis of *ALK* gene rearrangement by fluorescence in situ hybridization in non-small cell lung cancer patients. *Contemp Oncol (Pozn)* 2013; 17: 484-92.
 7. Zito Marino F, Botti G, Aquino G, et al. Unproductive effects of *ALK* gene amplification and copy number gain in non-small-cell lung cancer: *ALK* gene amplification and copy gain in NSCLC. *Int J Mol Sci* 2020; 21: 4927.
 8. Hafezi F, Perez Bercoff D. The solo play of *TERT* promoter mutations. *Cells* 2020; 9: 749.
 9. Leao R, Apolonio JD, Lee D, Figueiredo A, Tabori U, Castelo-Branco P. Mechanisms of human telomerase reverse transcriptase (hTERT) regulation: clinical impacts in cancer. *J Biomed Sci* 2018; 25: 22.
 10. Potharaju M, Mathavan A, Mangaleswaran B, et al. Clinicopathological analysis of HIF-1alpha and TERT on survival outcome in glioblastoma patients: a prospective, single institution study. *J Cancer* 2019; 10: 2397-406.
 11. Persson A, Englund E. Different assessments of immunohistochemically stained Ki-67 and hTERT in glioblastoma multiforme yield variable results: a study with reference to survival prognosis. *Clin Neuropathol* 2008; 27: 224-33.
 12. Stupp R, Mason WP, van den Bent MJ, et al. Radiotherapy plus concomitant and adjuvant temozolomide for glioblastoma. *N Engl J Med* 2005; 352: 987-96.
 13. Le Rhun E, Chamberlain MC, Zairi F, et al. Patterns of response to crizotinib in recurrent glioblastoma according to *ALK* and *MET* molecular profile in two patients. *CNS Oncol* 2015; 4: 381-6.
 14. Alidousty C, Duerbaum N, Wagener-Rydzek S, et al. Prevalence and potential biological role of *TERT* amplifications in *ALK* translocated adenocarcinoma of the lung. *Histopathology* 2021; 78: 578-85.
 15. Saha R, Chatterjee U, Mandal S, Saha K, Chatterjee S, Ghosh SN. Expression of phosphatase and tensin homolog, epidermal growth factor receptor, and Ki-67 in astrocytoma: a prospective study in a tertiary care hospital. *Indian J Med Paediatr Oncol* 2014; 35: 149-55.
 16. McLeer-Florin A, Moro-Sibilot D, Melis A, et al. Dual IHC and FISH testing for *ALK* gene rearrangement in lung adenocarcinomas in a routine practice: a French study. *J Thorac Oncol* 2012; 7: 348-54.
 17. Salido M, Pijuan L, Martinez-Aviles L, et al. Increased *ALK* gene copy number and amplification are frequent in non-small cell lung cancer. *J Thorac Oncol* 2011; 6: 21-7.
 18. Hudson L, Kulig K, Young D, McLendon R, Abemethy A. *ALK* and *cMET* expression in glioblastoma multiforme: implications for therapeutic targeting. *Mol Cancer Ther* 2011; 10(11 Suppl): A42.
 19. Kulig K, McLendon RE, Locke SC, et al. *MET* and *ALK* in glioblastoma multiforme (GBM): comparison of IHC and FISH. *J Clin Oncol* 2012; 30(15 Suppl): 2021.
 20. Peretti U, Ferrara R, Pilotto S, et al. *ALK* gene copy number gains in non-small-cell lung cancer: prognostic impact and clinico-pathological correlations. *Respir Res* 2016; 17: 105.
 21. Lee JS, Lim SM, Rha SY, et al. Prognostic implications of anaplastic lymphoma kinase gene aberrations in rhabdomyosarcoma; an immunohistochemical and fluorescence in situ hybridisation study. *J Clin Pathol* 2014; 67: 33-9.
 22. Schoppmann SF, Streubel B, Birner P. Amplification but not translocation of anaplastic lymphoma kinase is a frequent event in oesophageal cancer. *Eur J Cancer* 2013; 49: 1876-81.
 23. Del Grosso F, De Mariano M, Passoni L, Luksch R, Tonini GP, Longo L. Inhibition of N-linked glycosylation impairs *ALK* phosphorylation and disrupts pro-survival signaling in neuroblastoma cell lines. *BMC Cancer* 2011; 11: 525.
 24. Masui K, Komori T, Kato Y, et al. Elevated *TERT* expression in *TERT*-wildtype adult diffuse gliomas: histological evaluation with a novel *TERT*-specific antibody. *Biomed Res Int* 2018; 2018: 7945845.
 25. Leclerc C, Haeich J, Aulestia FJ, et al. Calcium signaling orchestrates glioblastoma development: facts and conjunctures. *Biochim Biophys Acta* 2016; 1863: 1447-59.
 26. Nishi H, Nakada T, Kyo S, Inoue M, Shay JW, Isaka K. Hypoxia-inducible factor 1 mediates upregulation of telomerase (hTERT). *Mol Cell Biol* 2004; 24: 6076-83.
 27. Alkhaibary A, Alassiri AH, AlSufiani F, Alharbi MA. Ki-67 labeling index in glioblastoma; does it really matter? *Hematol Oncol Stem Cell Ther* 2019; 12: 82-8.
 28. Tsidulko AY, Kazanskaya GM, Kostromskaya DV, et al. Prognostic relevance of NG2/CSPG4, CD44 and Ki-67 in patients with glioblastoma. *Tumour Biol* 2017; 39: 1010428317724282.
 29. Abdelzaher E. Glioblastoma multiforme, NOS [Internet]. Bingham Farms: PathologyOutlines.com, 2020 [cited 2020 May 27]. Available from: <https://www.pathologyoutlines.com/topic/cnstumorglioblastomagiantcell.html>.
 30. Marzec M, Liu X, Wong W, et al. Oncogenic kinase NPM/*ALK* induces expression of HIF1alpha mRNA. *Oncogene* 2011; 30: 1372-8.

Spindle cell oncocytoma of the sella turcica with anaplastic features and rapid progression in short-term follow-up: a case report with proposal of distinctive radiologic features

Dong Ja Kim¹, SangHan Lee², Mee-seon Kim³, Jeong-Hyun Hwang⁴, Myong Hun Hahm⁵

¹Department of Forensic Medicine, School of Medicine, Kyungpook National University, Daegu;

²Department of Forensic Medicine, Defense Institute of Forensic Science, Seoul;

³Department of Pathology, Kyungpook National University Hospital, Daegu;

Departments of ⁴Neurosurgery and ⁵Radiology, School of Medicine, Kyungpook National University, Daegu, Korea

We present a rare case of spindle cell oncocytoma (SCO) of the sella turcica with malignant histologic features and rapid progression. A 42-year-old woman experienced bilateral blurred vision and was preoperatively misdiagnosed as having a pituitary macroadenoma on magnetic resonance imaging. After surgery, SCO was diagnosed by the histopathologic features of interlacing fascicles of spindle tumor cells with finely granular, eosinophilic cytoplasm. Focal anaplastic changes and necrosis were present. Immunohistochemically, the tumor cells were positive for vimentin, epithelial membrane antigen, S-100, galectin-3, and thyroid transcription factor 1. Four months later, the tumor had progressed, and second surgery with adjuvant radiotherapy was performed; the patients remains under observation. In this report, we proposed distinctive radiologic features for differential diagnosis between SCO and other pituitary tumors.

Key Words: Oncocytoma; Sella turcica; Neoplasms; Progression; Radiology

Received: December 1, 2020 **Revised:** January 14, 2021 **Accepted:** January 26, 2021

Corresponding Author: Myong Hun Hahm, Department of Radiology, School of Medicine, Kyungpook National University, 680 Gukchaebosang-ro, Jung-gu, Daegu 41944, Korea

Tel: +82-53-200-3376/3380, Fax: +82-53-200-3349/3969, E-mail: hammh7@gmail.com

In 2002, Roncaroli et al. [1] initially described spindle cell oncocytoma (SCO) of the sella turcica, which has been characterized as World Health Organization (WHO) grade I non-endocrine neoplasm of the sella turcica [2]. From 2002 to 2019, < 50 cases of SCO of the sella turcica had been reported in the literature as case reports or case series [1,3,4]. Histologically, this tumor is composed of fascicles of spindle cells with eosinophilic oncocytic cytoplasm. The tumor cells lack immunoreactivity for neuroendocrine markers and pituitary hormones. Mitoses are rare in most cases, and SCO was initially described with a benign clinical course [1]. However, subsequent cases with multiple recurrences have been reported; therefore, differential radiologic diagnosis from other benign pituitary neoplasm is important.

Herein, we present a preoperatively misdiagnosed case of SCO of the sella turcica with focal anaplastic histologic features and rapid progression in the short-term follow-up period, suggesting a malignant clinical course. Moreover, we retrospectively proposed

a distinctive radiologic finding of SCO on preoperative magnetic resonance imaging (MRI).

CASE REPORT

A 42-year-old woman presented with complaints of bilateral blurred vision for 3 months. Bitemporal hemianopsia was observed on ophthalmological examination. A 22-mm-sized sella/suprasellar mass was found on brain MRI. The mass had well-circumscribed margin, compression at the optic chiasm, and intense enhancement without gross hemorrhage, calcification, and necrosis. As will be described later in the Discussion, proposed characteristic findings of SCO of the sella turcica, which were different from those of pituitary adenoma, were observed in dynamic contrast enhanced T1-weighted imaging (DCE-T1WI) as follows: (1) spoke-wheel pattern of early arterial enhancement in periphery and (2) late central stellate enhancement (Fig. 1).

On preoperative evaluation, there was no abnormality in other organs. The patient had been taking medication for hypothyroidism and adrenal insufficiency before visiting our hospital. Preoperative laboratory tests in our hospital revealed normal range of thyroid, cortisol, and adrenocorticotropic hormone; T3, 0.74 ng/mL (0.6–1.9); free T4, 1.47 ng/dL (0.89–1.8); cortisol, 9.19 ng/dL (2.47–19.5); and adrenocorticotropic hormone, 29.44 pg/mL (0–60). Abnormal results of hormonal test included low thyroid-stimulating hormone level at 0.07 μ IU/mL (0.3–0.4), elevated prolactin level at 48.85 ng/mL (4.79–23.3), and low luteinizing hormone level at 0.38 mIU/mL (0.56–89.09).

She was initially misdiagnosed as having pituitary adenoma or craniopharyngioma and underwent endoscopic transnasal trans-

sphenoidal resection. The neurosurgeon described the tumor as highly vascular and causing significant intraoperative bleeding. Therefore, total resection was not possible, and residual solid lesion was observed in the superior part of the mass on immediate postoperative MRI (Fig. 2).

Grossly, the tumor mass was pale-yellow and solid with focal hemorrhage. Histologically, the tumor was mainly composed of interlacing fascicles of plump spindle cells with eosinophilic and oncocytic cytoplasm and intervening thin blood vessels. Mild to moderate nuclear atypia was identified, and focal pleomorphic tumor cells were noted. Mitoses were frequent (3–4 counts/10 high-power field), and focal coagulative necrosis was seen (Fig. 3A–C). The immunohistochemical study revealed a lack of re-

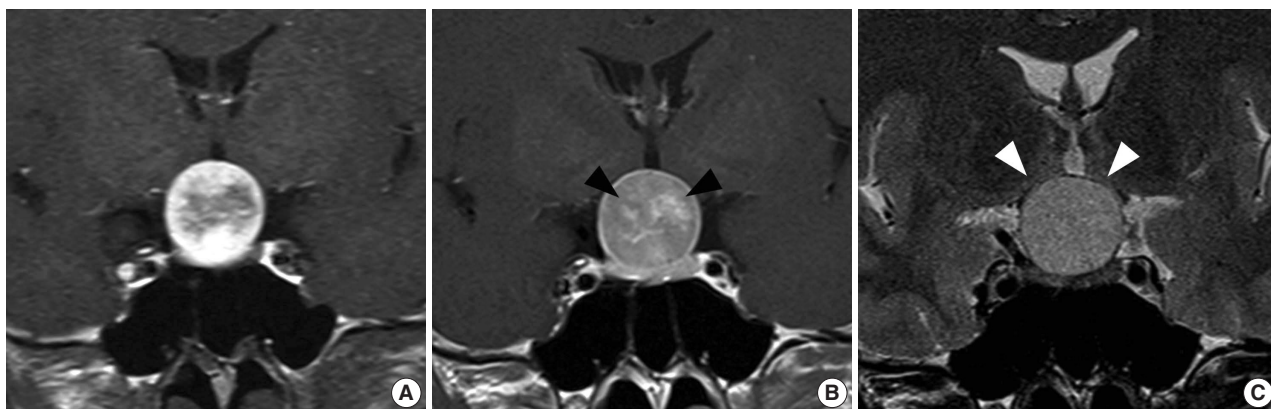


Fig. 1. Preoperative magnetic resonance imaging. Coronal dynamic contrast enhanced T1-weighted imaging, early arterial phase (A), delayed phase (B), and coronal T2-weighted imaging (C). Note the late central stellate enhancement (black arrowheads). White arrowheads indicate the paper-thin compressed optic chiasm.

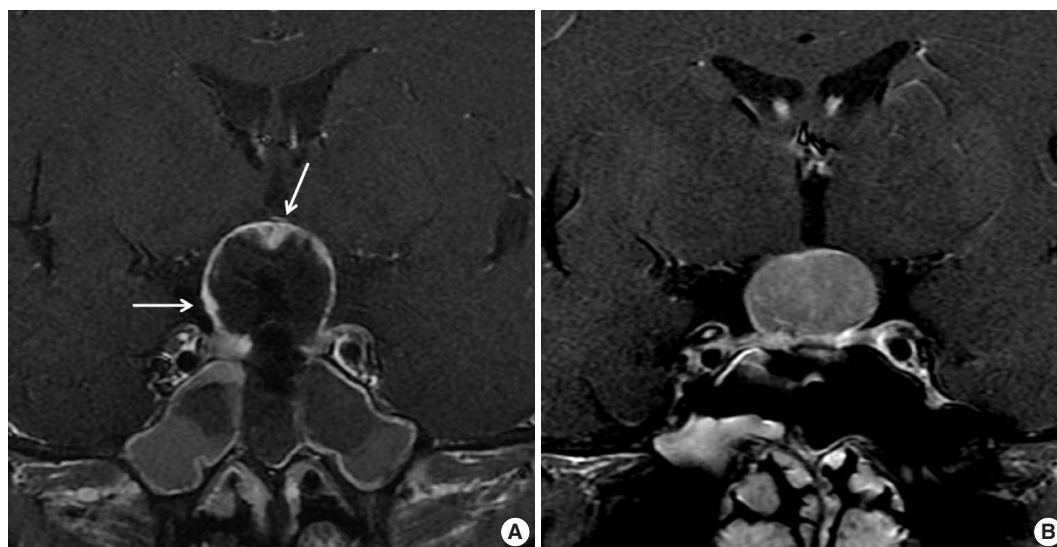


Fig. 2. Immediate postoperative contrast-enhanced magnetic resonance imaging (MRI) (A) and 4-month follow-up MRI (B). Note the residual solid lesion including the superior part of the mass on immediate postoperative MRI (arrows) and rapid progression of the mass refilling the operation cavity.

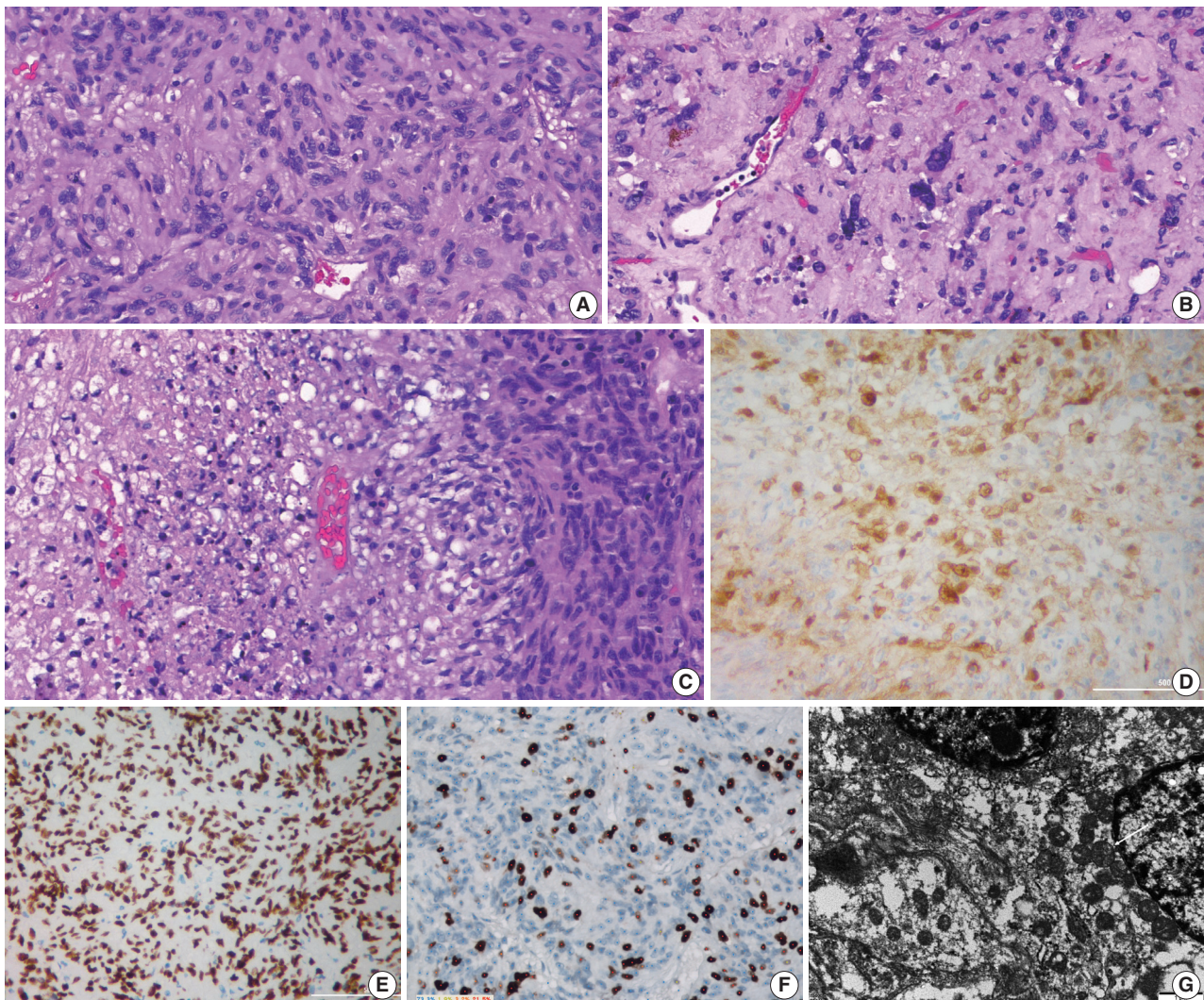


Fig. 3. Histopathologic findings. (A) The tumor is composed of interlacing fascicles of spindle cells with abundant eosinophilic cytoplasm. (B) Focal nuclear pleomorphism and hyalinized stroma are seen. (C) Focal coagulative tumor necrosis is present. The tumor cells show immunoreactivity for galectin-3 (D) and thyroid transcription factor 1 (E). (F) The Ki-67 index was 26.7%. (G) Ultrastructural examination using paraffin-embedded tissue block show numerous mitochondria (white arrow) in tumor cell.

activity for neuroendocrine markers and pituitary hormones. The tumor cells were immunoreactive for vimentin, epithelial membrane antigen (EMA), S-100 protein, thyroid transcription factor 1 (TTF-1), and galectin-3 (Fig. 3D, E) and negative for glial fibrillary acidic protein. The Ki-67 index was 26.7% (Fig. 3F). The tumor was diagnosed as SCO based on the characteristics of histopathology and immunohistochemical results. On ultrastructural findings using paraffin-embedded tissues, the neoplastic cells contained numerous mitochondria with lamellar cristae. The neoplastic cells were linked by intermediate junctions and desmosomes (Fig. 3G).

Four months after initial operation, the patient complained of headache and aggravating blurred vision of the left eye. Fol-

low-up MRI revealed a regrown tumor mass (Fig. 2B), and the patient underwent a second surgery. Histologic sections of the materials from the second operation revealed similar pathologic features, and the Ki-67 index was 20.5%. Postoperative adjuvant radiotherapy has been performed, and the patient is under observation.

DISCUSSION

SCO is a rare nonfunctioning tumor of the sella turcica and accounts for approximately 0.1% to 0.4% of all sellar regions tumors [1,5,6]. Previously, this tumor was suspected to be derived from folliculostellate cells of the anterior pituitary gland, which

are sustentacular cells of adenohypophysis [1]. However, subsequent studies reported that pituicytes are suggested as their cells of origin. Owing to the same or similar immunohistochemical characteristics, Mete et al. [7] believed that SCO is a variant of pituicytoma. The term “pituicytoma” has been used to describe a number of tumors in the region of the sella turcica, such as pilocytic astrocytomas, granular cell tumors, and even pituitary adenoma. Nontumorous pituicytes, SCOs, and granular cell tumors are positive for TTF-1, but folliculostellate cells and adenohypophysis are negative for TTF-1, which indicates that SCO is a common lineage of pituicytes [7].

Clinically, the tumor is often misdiagnosed as a nonfunctioning pituitary adenoma. Because of the compressive effect on the optic chiasm and pituitary gland, the common symptoms include visual disturbances, headache, and panhypopituitarism. Histologically, the tumor is composed of spindle cells arranged in interlacing fascicular structures with intervening blood vessels and should be differentiated with null cell adenoma with oncocyctic change, meningioma, schwannoma, granular cell tumor, solitary fibrous tumor, and paraganglioma [8]. Immunohistochemically, SCO is negative for neuroendocrine markers such as synaptophysin and chromogranin, pituitary hormones, cytokeratin, desmin, and smooth muscle actin and typically positive for TTF-1, EMA, vimentin, and galectin-3 [1,3-6]. The ultrastructural characteristics of SCO include cytoplasmic accumulation of numerous mitochondria and several cell-cell junctions, mainly short desmosomes [9].

Many authors have described the radiologic features of SCO of the sella turcica as nonspecific and generally not differentiable from pituitary adenoma. However, Hasiloglu et al. recently described new radiologic signs in diagnosis of SCO of the sella turcica in three cases: (1) millimetric hypointense foci and linear signal void areas in T2-weighted imaging and (2) hypervascular features of the tumor such as early intense contrast enhancement in DCE-T1WI [10]. Reported findings of SCO of the sella turcica are distinguishable from those of a typical pituitary adenoma characterized by later enhancement than a normal pituitary gland. However, these are less specific findings for SCO.

Interestingly, our case showed a common enhancement pattern of so-called segmental enhancement inversion. This is a spoke-wheel pattern of early arterial enhancement in the periphery and late central stellate enhancement and is typically observed in renal oncocytoma with a critical size, as summarized by Woo et al. [11]. Early arterial spoke-wheel-like enhancement is observed by peripheral parenchymal tissues composed of compactly arranged tumor cells with scarcely intervening stroma, and delayed

central enhancement is attributed to a central fibrous stellate scar [11,12]. This radiopathologic evidence of a central fibrous stellate scar were reported in adrenal oncocytoma and thyroid oncocyctic (Hurthle cell) tumor [13,14].

In our case, radiopathologic correlation was not possible because of piecemeal resection owing to a surgical procedure, but peculiar radiologic findings were identified. Therefore, we propose that the central fibrous stellate scar causing segmental enhancement inversion is shared by oncocytoma and might be a highly specific finding for SCO of the sella turcica. Conclusively, we suggest that SCO could be diagnosed preoperatively.

Discrimination can be difficult even if distinctive MRI findings are recognized because SCO is a very rare tumor in the sella turcica. However, early arterial enhancement and signal void are predictors of high bleeding risk during surgery, regardless of histopathologic diagnosis. Therefore, considering the possibility of tumor other than benign adenoma, we should have discussed the option of preoperative embolization and should have attempted complete resection.

Fewer than 50 cases had been reported in the English literature. Giantini Larsen et al. [3] retrospectively reviewed 40 cases of SCO of the pituitary glands from 2002 to 2018 and additionally presented six cases in 2018. In 2019, Yip et al. [4] reported a case of SCO presenting as pituitary apoplexy. The ages of patients varied from 24 to 88 years. Because the preoperative diagnosis was suggestive of pituitary adenoma, the patients were often managed by transsphenoidal approach. When Roncaroli et al. [1] described five cases of SCOs in 2002, no recurrence was noted in any case within 2–68 months of follow-up. They suggested a benign nature of SCO based on the absence of cellular anaplasia, mitoses, and necrosis along with a low Ki-67 proliferation labeling index. In contrast to the initially described benign behavior, many authors have reported several cases of recurrent SCO. In their retrospective review, Giantini Larsen et al. [3] reported that 39% were recurrent at the time of surgery and recurred postoperatively after resection. However, SCO is retained as a grade I tumor in the recent updated 2017 WHO classification [2]. We believe that it is important to reevaluate the clinical outcome of this tumor in a large-scale study and to identify the histopathologic factors to predict aggressive behavior of this tumor. The Ki-67 proliferation index was low in most cases, with a range of 1% to 8% [3]. Kong et al. [15] reported a case of malignant SCO with repeating recurrence and a continuously increasing Ki-67 index up to 45%. In the present case, increased mitotic figures, nuclear atypia, necrosis, and high MIB-1 index are possible contributory factors for patient prognosis.

The tumor progressed within 4 months after the operation, and the time interval from initial operation and tumor progression was very short. Thus, SCO is more clinically aggressive and should be classified as malignancy compared with other tumors of the sellar region. Although SCO of the sella turcica can have malignant behavior, no radiologic malignant features of SCO such as gross hemorrhage, necrosis, or invasion into the adjacent tissue was identified in our case. Hence, radiologically, SCO should be considered preoperatively with segmental enhancement inversion, and postoperative close follow-up is necessary.

The pathogenesis and prognosis of SCOs remain uncertain, and the behavior of this tumor needs to be further studied. Classification of SCO of the pituitary gland will establish more biologically and clinically uniform groups of tumors. This will allow pathologists and radiologists to better diagnose these tumors and predict clinical outcomes for the patients.

Ethics Statement

Formal written informed consent was not required with a waiver by the appropriate IRB/Ethics Committee (KNUH IRB No. 2020-09-029).

Availability of Data and Material

The datasets generated or analyzed during the study are available from the corresponding author on reasonable request.

Code Availability

Not applicable.

ORCID

Dong Ja Kim <https://orcid.org/0000-0001-8462-3173>
 SangHan Lee <https://orcid.org/0000-0003-0390-3494>
 Mee-seon Kim <https://orcid.org/0000-0002-4244-1985>
 Jeong-Hyun Hwang <https://orcid.org/0000-0002-5306-6922>
 Myong Hun Hahm <https://orcid.org/0000-0001-9165-6117>

Author Contributions

Conceptualization: Kim DJ, Lee S, Data curation: Kim DJ, Hahm MH. Formal analysis: Kim DJ, Lee S. Investigation: Kim MS. Methodology: Kim DJ, Hahm MH. Software: Kim DJ. Validation: Hahm MH. Visualization: Kim MS. Writing—original draft: Kim DJ, Hahm MH. Writing—review & editing: Kim DJ, Hwang JH, Hahm MH.

Conflicts of Interest

The authors declare that they have no potential conflicts of interest.

Funding Statement

No funding to declare.

Acknowledgments

The authors thank Professor Sung-Hye Park, Department of Pathology, Seoul National University College of Medicine, for her diagnostic assistance with this study.

References

- Roncaroli F, Scheithauer BW, Cenacchi G, et al. 'Spindle cell oncocytoma' of the adenohypophysis: a tumor of folliculostellate cells? *Am J Surg Pathol* 2002; 26: 1048-55.
- Lopes MB. The 2017 World Health Organization classification of tumors of the pituitary gland: a summary. *Acta Neuropathol* 2017; 134: 521-35.
- Giantini Larsen AM, Cote DJ, Zaidi HA, et al. Spindle cell oncocytoma of the pituitary gland. *J Neurosurg* 2018; 131: 517-25.
- Yip CM, Lee HP, Hsieh PP. Pituitary spindle cell oncocytoma presented as pituitary apoplexy. *J Surg Case Rep* 2019; 2019: rjz179.
- Kloub O, Perry A, Tu PH, Lipper M, Lopes MB. Spindle cell oncocytoma of the adenohypophysis: report of two recurrent cases. *Am J Surg Pathol* 2005; 29: 247-53.
- Matyja E, Maksymowicz M, Grajkowska W, Olszewski W, Zielinski G, Bonicki W. Spindle cell oncocytoma of the adenohypophysis: a clinicopathological and ultrastructural study of two cases. *Folia Neuropathol* 2010; 48: 175-84.
- Mete O, Lopes MB, Asa SL. Spindle cell oncocytomas and granular cell tumors of the pituitary are variants of pituitary tumor. *Am J Surg Pathol* 2013; 37: 1694-9.
- Sali A, Epari S, Tampi C, Goel A. Spindle cell oncocytoma of adenohypophysis: Review of literature and report of another recurrent case. *Neuropathology* 2017; 37: 535-43.
- Guadagno E, Cervasio M, Di Somma A, Califano M, Solari D, Del Basso De Caro M. Essential role of ultrastructural examination for spindle cell oncocytoma: case report of a rare neoplasm and review of the literature. *Ultrastruct Pathol* 2016; 40: 121-4.
- Hasiloglu ZI, Ure E, Comunoglu N, et al. New radiological clues in the diagnosis of spindle cell oncocytoma of the adenohypophysis. *Clin Radiol* 2016; 71: 937.
- Woo S, Cho JY, Kim SH, et al. Segmental enhancement inversion of small renal oncocytoma: differences in prevalence according to tumor size. *AJR Am J Roentgenol* 2013; 200: 1054-9.
- Monk IP, Lahiri R, Sivaprakasam R, Malhotra S, Praseedom RK, Jah A. Adrenocortical oncocytoma: review of imaging and histopathological implications. *Int J Surg Case Rep* 2010; 1: 30-2.
- Coppola M, Romeo V, Verde F, et al. Integrated imaging of adrenal oncocytoma: a case of diagnostic challenge. *Quant Imaging Med Surg* 2019; 9: 1896-901.
- Deng D, Chen X, Wang H, Wu H. Typical manifestations of Hurthle cell adenoma of the thyroid on contrast-enhanced CT: a case report. *Medicine (Baltimore)* 2019; 98: e15866.
- Kong X, Li D, Kong Y, Zhong D. Malignant adenohypophysis spindle cell oncocytoma with repeating recurrences and a high Ki-67 index. *Medicine (Baltimore)* 2017; 96: e5657.

Hepatoid thymic carcinoma: a case report of a rare subtype of thymic carcinoma

Ji-Seon Jeong^{1*}, Hyo Jeong Kang^{1*}, Uiree Jo¹, Min Jeong Song², Soon Yeol Nam³, Joon Seon Song¹

¹Department of Pathology, Asan Medical Center, University of Ulsan College of Medicine, Seoul;

²Department of Pathology, Kyung Hee University Hospital at Gangdong, Kyung Hee University College of Medicine, Seoul;

³Department of Otolaryngology, Asan Medical Center, University of Ulsan College of medicine, Seoul, Korea

Hepatoid thymic carcinoma is an extremely rare subtype of primary thymus tumor resembling “pure” hepatoid adenocarcinomas with hepatocyte paraffin 1 (Hep-Par-1) expression. A 53-year-old man presented with voice change and a neck mass. Multiple masses involving the thyroid, cervical and mediastinal lymph nodes, and lung were detected on computed tomography. Papillary thyroid carcinoma was confirmed by biopsy, and the patient underwent neoadjuvant chemoradiation therapy. However, the anterior mediastinal mass was enlarged after the treatment whereas the multiple masses in the thyroid and neck decreased in size. Microscopically, polygonal tumor cells formed solid sheets or trabeculae resembling hepatocytes and infiltrated remnant thymus. The tumor cells showed immunopositivity for cytokeratin 7, cytokeratin 19, and Hep-Par-1 and negativity for α -fetoprotein. Possibilities of germ cell tumor, squamous cell carcinoma, and metastasis of thyroid papillary carcinoma were excluded by immunohistochemistry. This report on the new subtype of thymic carcinoma is the third in English literature thus far.

Key Words: Hepatoid carcinoma; Thymus; α -Fetoprotein; Hep-Par-1

Received: November 17, 2020 **Accepted:** March 10, 2021

Corresponding Author: Joon Seon Song, MD, PhD, Department of Pathology, Asan Medical Center, University of Ulsan College of Medicine, 88 Olympic-ro 43-gil, Songpa-gu, Seoul 05505, Korea

Tel: +82-2-3010-4548, Fax: +82-2-472-7898, E-mail: songjs@amc.seoul.kr

*These authors contributed equally to this work.

Hepatoid thymic carcinoma (HTC) is a rare subtype of thymic carcinoma and has been inserted in the 4th edition *WHO classification of tumors of the lung, pleura, thymus and heart* in 2015 [1]. It was first described by Franke et al. [2] in 2004 and only two cases have been reported until now [2,3]. This tumor was defined as a thymic carcinoma morphologically resembling hepatocellular carcinoma with immunoreactivity for hepatocyte paraffin 1 (Hep-Par-1) but immunonegativity for α -fetoprotein (AFP), differentiating from hepatoid adenocarcinoma (HAC) of other organs [2]. Herein, we report an additional case of HTC.

CASE REPORT

A previously healthy 53-year-old man presented with voice change and a neck mass. On the neck computed tomography (CT) and chest CT, multiple masses involving bilateral lobes of the thyroid gland, cervical lymph nodes and left mediastinum

were detected (Fig. 1). Papillary thyroid carcinoma with metastases to neck lymph nodes were confirmed by core needle biopsies, and the mediastinal mass showed poorly differentiated carcinoma. The patient underwent neoadjuvant chemoradiation therapy (radiation therapy, 70 Gy/35 fractions; cisplatin based chemotherapy for 3 cycles) under the impression of long lasting papillary thyroid carcinoma with anaplastic change. However, the anterior mediastinal mass was enlarged after the treatment whereas the thyroid and neck masses decreased in size. The patient underwent total thyroidectomy with radical neck dissection and mediastinal mass excision. Both thyroid masses were severely calcified, and the histologic features were those of classic papillary thyroid carcinoma. An ill-demarcated anterior mediastinal mass measured 6 cm and showed heterogeneous, tan colored, and firm cut surface (Fig. 2A). Microscopically, polygonal tumor cells formed solid sheets or trabeculae resembling hepatocytes and infiltrated remnant thymus. The tumor cells often

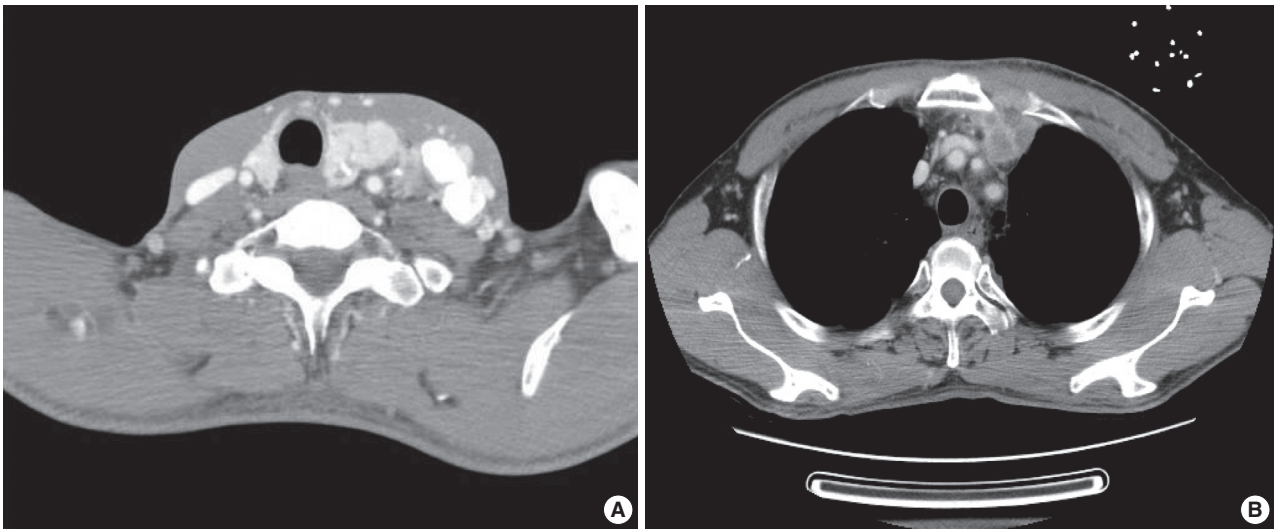


Fig. 1. Radiologic findings. (A) Neck computed tomography (CT) shows a large infiltrating mass with calcification in left thyroid lobe and multiple hypervascular masses in the left level II–VI, left supraclavicular area and right lower neck. (B) The chest CT shows anterior mediastinal mass, measuring 6 cm.

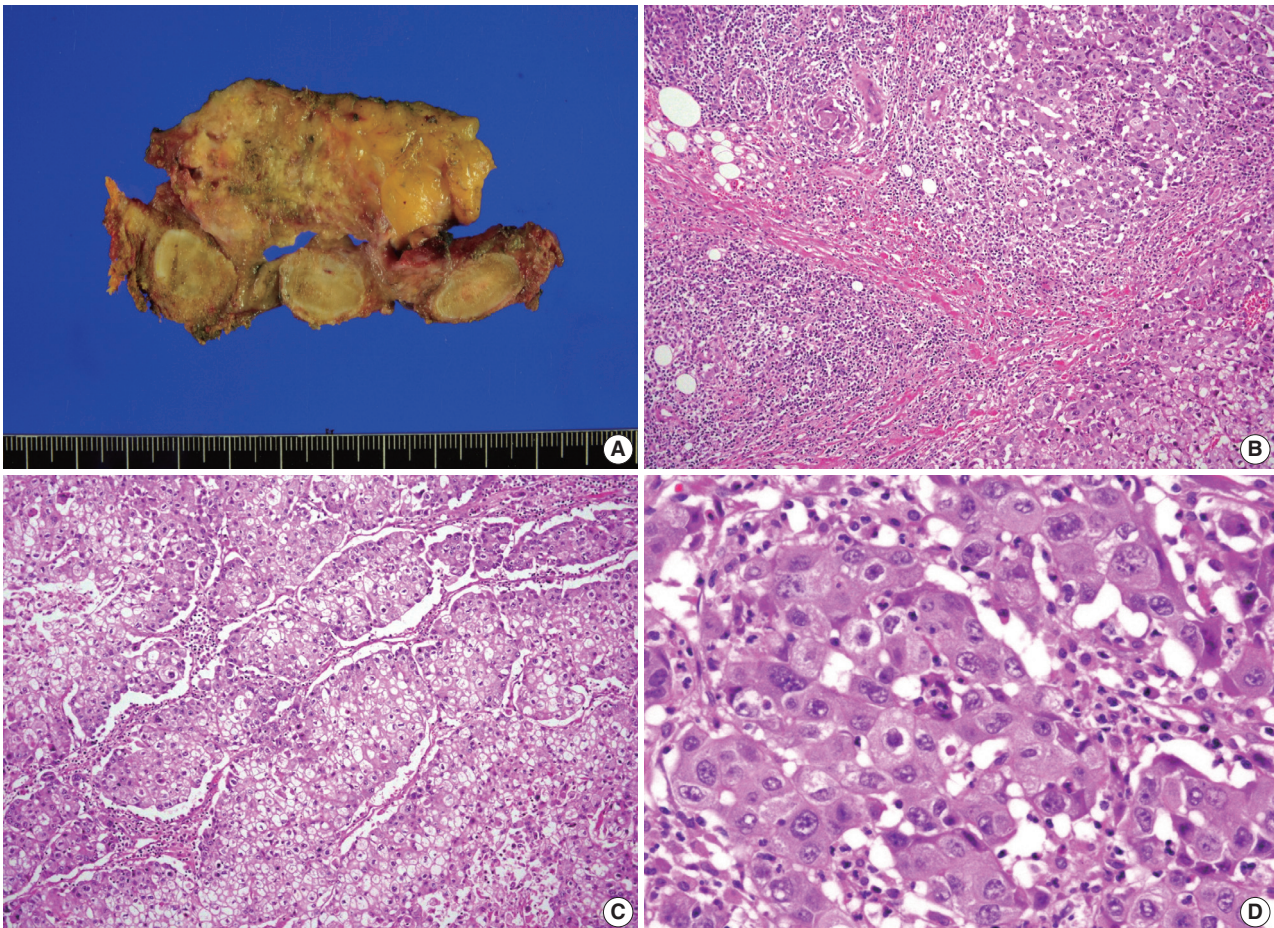


Fig. 2. Pathologic findings. (A) Grossly, an ill-demarcated anterior mediastinal mass, measuring 6 cm shows a heterogeneous, tan colored, firm cut surface. (B, C) Microscopically, the polygonal tumor cells formed solid sheet or trabeculae resembling hepatocytes and infiltrated remnant thymus. Part of the tumor shows clear cytoplasm. (D) The tumor cells show distinct cell borders, abundant eosinophilic cytoplasm, and pleomorphic vesicular nuclei.

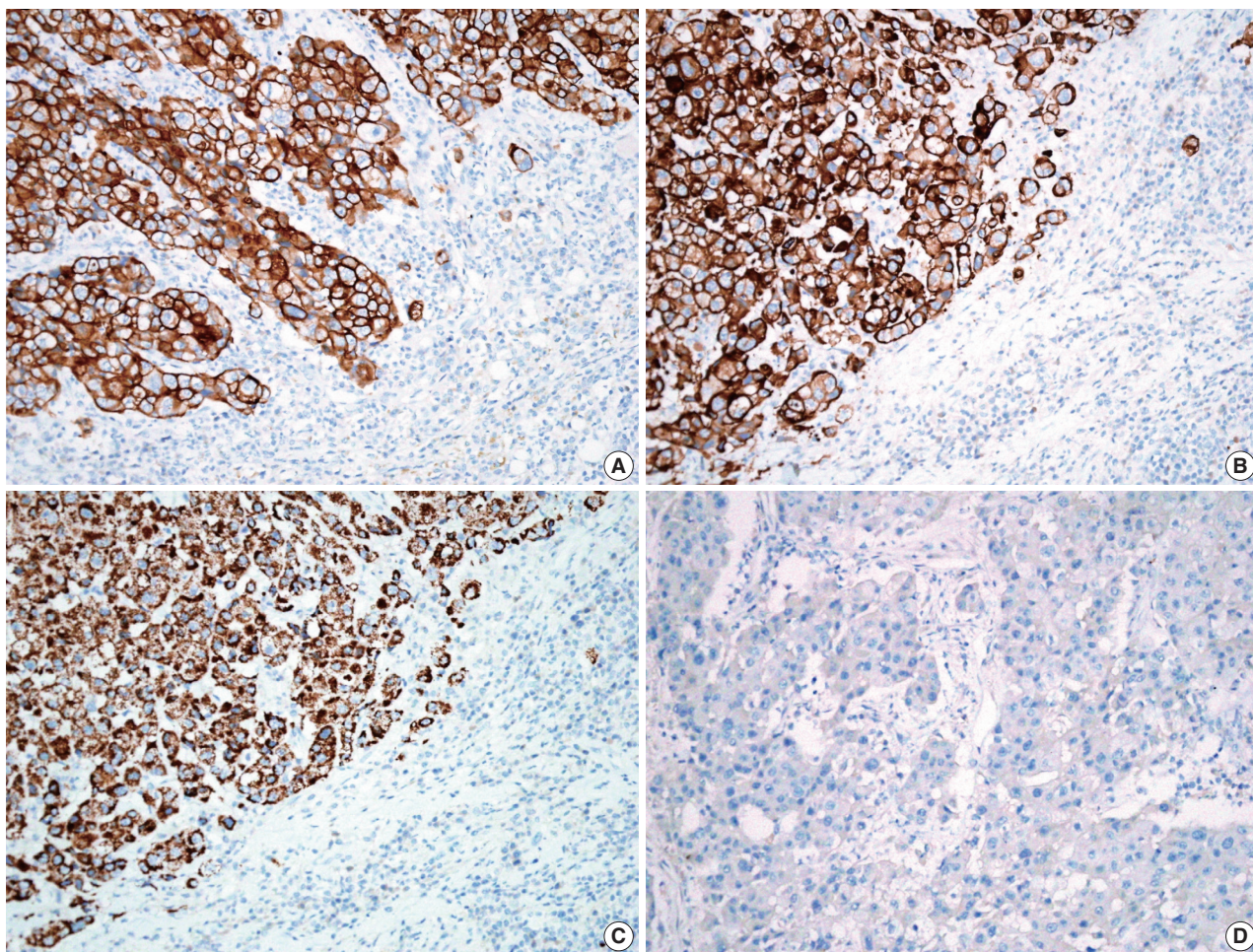


Fig. 3. Representative image of immunohistochemistry. The tumor cells show immune-positivity for cytokeratin 7 (A), cytokeratin 19 (B), and Hep-Par-1 (hepatocyte, C) and negativity for α -fetoprotein (D) by immunohistochemistry.

showed clear cytoplasmic change (Fig. 2B–D), and immunopositivity for cytokeratin (CK) 7, CK 19 and Hep-Par-1 and negativity for AFP (Fig. 3). Possibilities of metastatic hepatocellular carcinoma, germ cell tumor, squamous cell carcinoma, anaplastic thyroid carcinoma, and NUT carcinoma were excluded by immunohistochemistry (IHC). The results of IHC are summarized in Table 1. The patient has been lost to follow-up after 6-month follow-up.

DISCUSSION

HTC is extremely rare and only two cases have been published in English literature thus far [2,3]. In brief, the patients were 70-year-old female and 34-year-old male. The sizes measured 18 cm and 6.6 cm. The patients underwent surgery with adjuvant chemoradiation therapy. The outcomes were not informative due to short follow-up periods or failure to follow-up.

The results of IHC staining showed similar profiles in all cases as follows: CK 7 (+), CK 19 (+/-), Hep-Par-1 (+), and AFP (-) (Table 2).

To exclude the possibility of anaplastic transformation of papillary thyroid carcinoma or poorly differentiated thyroid carcinoma, we performed IHC. Based on the results of IHC (paired box 8 [PAX-8] [-], thyroid transcription factor-1 [-], thyroglobulin [-]), we thought that this case was not of thyroid origin. It has been reported that immunoreactivity for PAX-8 in anaplastic thyroid carcinoma was 79% [4]. Histologic features, adjacent involved thymic tissue and immunoreactivity for Hep-Par-1 supported the diagnosis of HTC.

HAC has been reported in many other organs including the stomach, gallbladder, lung, uterus, and urinary bladder, etc. [5]. HTCs show distinct immunoprofiles that differentiate them from HAC. While 91.6% of HAC express AFP and 38.1% of HAC express Hep-Par-1, all HTCs are negative for AFP protein

and positive for Hep-Par-1 although the cases are extremely rare. Hep-Par-1 is recognized as a mitochondrial antigen of hepatocyte and it is normally expressed in small intestinal epithelium and hepatocytes. Thus, it is highly sensitive (92%) in diagnosing hepatocellular carcinoma [6]. However, our case had no hepatic mass, no evidence of hepatitis B and C, and was immunoreactive for CK 7 and CK 19, excluding the possibility of metastatic hepatocellular carcinoma.

HAC is a very aggressive neoplasm with metastasis at the time of diagnosis in a high proportion of patients and has a worse prognosis than more common types of tumors [7]. More than

half of patients died within the first 12 months [5]. The 5-year survival rate of gastric HAC has been known to be significantly lower than that of conventional gastric cancer (9% vs. 44%, $p = .001$) [7]. The 5-year survival rate of thymic carcinoma ranges from 30% to 70%, depending on the initial stage of disease [8]. HTC is also thought to have a poor prognosis, judging from the cases of HAC; however, it is hard to say definitively due to the small number of cases.

Histogenesis of this tumor is still unclear and the previous authors favored an endodermal origin rather than a germ cell origin [2,3], based on the hypothesis of endodermal origin of gastric and pulmonary hepatoid neoplasms [9,10]. Further study including genetic analysis is required to determine the histogenesis of this tumor.

In conclusion, we report this rare subtype of thymic carcinoma having peculiar characteristics of morphology and immunohistochemical features. In addition, being aware of this entity will contribute to collecting an adequate number of cases to lay the groundwork for identifying pathophysiology and establishing treatment in the near future.

Table 1. The results of immunohistochemical staining

Antibody	Clone	Dilution	Results
Cytokeratin 7	Dako, Denmark	1:400	Positive
Cytokeratin 19	Cell Marque, USA	1:100	Positive
Hepatocyte	Dako, Denmark	1:200	Positive
α -Fetoprotein	Neomarkers, USA	1:200	Negative
TTF-1	Novo, UK	1:200	Negative
Thyroglobulin	Dako, Denmark	1:2,000	Negative
Galectin-3	Novo, UK	1:200	Negative
PAX-8	Cell Marque, USA	1:50	Negative
SALL 4	Biocare, USA	1:100	Negative
Oct 3/4	Novo, UK	1:100	Negative
PLAP	Dako, Denmark	1:100	Negative
β -hCG	Cell Marque, USA	1:1,000	Negative
CD10	Novo, UK	1:25	Negative
p63	Novo, UK	1:20	Negative
HMB45	DAKO, Denmark	1:50	Negative
TFE3	Cell Marque, USA	1:50	Positive
Calretinin	Zymed, USA	1:400	Negative
WT1	Dako, Denmark	1:100	Negative
Chymotrypsin	Chemicon (Millipore), USA	1:16,000	Negative
α 1 antitrypsin	Santa Cruz, Germany	1:400	Negative
CD56	NOVO, UK	1:25	Negative
CD30	Dako, Denmark	1:25	Negative
CD5	Novo, UK	1:200	Negative
NUT	Cell signaling, USA	1:100	Negative
c-erb2	Dako, Denmark	1:500	Negative

TTF-1, thyroid transcription factor-1; PAX-8, paired box 8; SALL4, Sal-like protein 4; Oct 3/4, octamer-binding transcription factor 3/4; PLAP, placental alkaline phosphatase; β -hCG, beta-subunit of human chorionic gonadotropin; TFE3, transcription factor binding to IGHM enhancer 3; WT1, Wilms' tumour 1.

Ethics Statement

This case was deemed exempt by the Asan Medical Center Institutional Review Board (IRB #2020-1567). Informed consent was obtained from individual participant included in this study.

Availability of Data and Material

All data generated or analyzed during the study are included in this published article.

Code Availability

Not applicable.

ORCID

Ji-Seon Jeong <https://orcid.org/0000-0002-4596-3658>
 Hyo Jeong Kang <https://orcid.org/0000-0002-5285-8282>
 Uiree Jo <https://orcid.org/0000-0001-6783-4016>
 Min Jeong Song <https://orcid.org/0000-0002-5891-4329>
 Soon Yeol Nam <https://orcid.org/0000-0002-8299-3573>
 Joon Seon Song <https://orcid.org/0000-0002-7429-4254>

Author Contributions

Conceptualization: JSS, JSJ, HJK. Data curation: JSJ, HJK, UJ, MJS, SYN.

Table 2. Summary of hepatoid thymic carcinoma reported in the English literature

Study	Age (yr)/Sex	Size (cm)	Location	Treatment	Outcome	Immunohistochemistry
Franke et al. [2]	70/F	18	Thymus	Surgery+adjuvant RTx	AWD (22 mo)	CK7(+), CK19(+), HepPar-1(+), AFP(-)
Lee et al. [3]	34/M	6.6	Thymus	Surgery+adjuvant CCRTx	FU loss (2 yr, AWD)	CK7(+), CK19(-), HepPar-1(+), AFP(-)
Present case	53/M	6.0	Mediastinum	Neoadjuvant CCRTx+surgery	FU loss (6 mo, AWD)	CK7(+), CK19(+), HepPar-1(+), AFP(-)

F, female; RTx, radiation therapy; AWD, alive with disease; CK, cytokeratin; HepPar-1, hepatocyte paraffin 1; AFP, α -fetoprotein; M, male; CCRTx, chemoradiation therapy; FU, follow-up.

Methodology: JSS, JSJ. Project administration: JSS. Writing—original draft: JSS, JSJ. Writing—review & editing: JSS, HJK. Approval of final manuscript: all authors.

Conflicts of Interest

JSS, a contributing editor of the *Journal of Pathology and Translational Medicine*, was not involved in the editorial evaluation or decision to publish this article. All remaining authors have declared no conflicts of interest.

Funding Statement

No funding to declare.

References

1. Travis WD, Brambilla E, Burke AP, Marx A, Nicholson AG. WHO classification of tumours of the lung, pleura, thymus and heart. 4th ed. Lyon: IARC Press, 2015.
2. Franke A, Strobel P, Fackeldey V, et al. Hepatoid thymic carcinoma: report of a case. *Am J Surg Pathol* 2004; 28: 250-6.
3. Lee JH, Kim H, Chae YS, Won NH, Choi JS, Kim CH. Hepatoid thymic carcinoma: a case report. *Korean J Pathol* 2009; 43: 562-5.
4. Nonaka D, Tang Y, Chiriboga L, Rivera M, Ghossein R. Diagnostic utility of thyroid transcription factors Pax8 and TTF-2 (FoxE1) in

thyroid epithelial neoplasms. *Mod Pathol* 2008; 21: 192-200.

5. Su JS, Chen YT, Wang RC, Wu CY, Lee SW, Lee TY. Clinicopathological characteristics in the differential diagnosis of hepatoid adenocarcinoma: a literature review. *World J Gastroenterol* 2013; 19: 321-7.
6. Chu PG, Ishizawa S, Wu E, Weiss LM. Hepatocyte antigen as a marker of hepatocellular carcinoma: an immunohistochemical comparison to carcinoembryonic antigen, CD10, and alpha-fetoprotein. *Am J Surg Pathol* 2002; 26: 978-88.
7. Liu X, Cheng Y, Sheng W, et al. Analysis of clinicopathologic features and prognostic factors in hepatoid adenocarcinoma of the stomach. *Am J Surg Pathol* 2010; 34: 1465-71.
8. Engels EA. Epidemiology of thymoma and associated malignancies. *J Thorac Oncol* 2010; 5(10 Suppl 4): S260-5.
9. Ishikura H, Kirimoto K, Shamoto M, et al. Hepatoid adenocarcinomas of the stomach: an analysis of seven cases. *Cancer* 1986; 58: 119-26.
10. Ishikura H, Kanda M, Ito M, Nosaka K, Mizuno K. Hepatoid adenocarcinoma: a distinctive histological subtype of alpha-fetoprotein-producing lung carcinoma. *Virchows Arch A Pathol Anat Histo-pathol* 1990; 417: 73-80.

Histologic subtyping of ampullary carcinoma for targeted therapy

Seung-Mo Hong

Department of Pathology, Asan Medical Center, University of Ulsan College of Medicine, Seoul, Korea

Carcinomas of the ampulla of Vater, or ampullary carcinomas, are a rare form of gastrointestinal tract cancer in Korea. Of the many histologic subtypes of ampullary carcinomas, the vast majority are tubular adenocarcinomas of the intestinal type, pancreaticobiliary type, or mixed type. There are no well-established adjuvant chemotherapy protocols for treating advanced-stage ampullary cancer, and most of the currently used chemotherapeutic regimens are either extrapolated from pancreatic, biliary, and colorectal cancers or derived from retrospective studies from high-volume institutions [1].

In this issue of the *Journal of Pathology and Translational Medicine*, Kumari et al. [2] report the whole-exome sequencing results of ampullary carcinomas. Their observations confirmed the commonly mutated genes identified by next-generation sequencing of ampullary carcinomas, which included *KRAS*, *TP53*, *APC*, *ELF3*, *SMAD4*, *CTNNB1*, *MUC4*, *ERBB2*, and *CDKN2A* [3-6]. The authors also found that the mutation patterns of several genes were different according to the histologic subtype: *KRAS*, *TP53*, and *CDH10* mutations were more frequently found in the pancreaticobiliary type, which shares mutations commonly observed in pancreatic ductal adenocarcinomas. In contrast, *APC*, *ACVR2A*, *SOX9*, and *EPHA6* genes were more frequently mutated in the intestinal type ampullary carcinomas, which were commonly mutated in colorectal cancers [3-5]. This suggests that gemcitabine-based regimens could be particularly useful in patients with pancreaticobiliary type ampullary carcinomas, and 5-fluorouracil-based regimens could be beneficial for those with intestinal type ampullary carcinomas. Therefore, providing information regarding the histologic subtypes in surgical pathologic reports

could be helpful for the selection of chemotherapeutic regimens in patients with surgically resected ampullary carcinomas.

Ethics Statement

Not applicable.

Availability of Data and Material

Data sharing not applicable to this article as no datasets were generated or analyzed during the study.

Code Availability

Not applicable.

ORCID

Seung-Mo Hong <https://orcid.org/0000-0002-8888-6007>

Conflicts of Interest

The authors declare that they have no potential conflicts of interest.

Funding Statement

No funding to declare.

References

1. Regalla DK, Jacob R, Manne A, Paluri RK. Therapeutic options for ampullary carcinomas: a review. *Oncol Rev* 2019; 13: 440.
2. Kumari N, Singh RK, Mishra SK, Krishnani N, Mohindra S, L R. Identification of PI3K-AKT signaling as the dominant altered pathway in intestinal type ampullary cancers through whole-exome sequencing. *J Pathol Tansl Med* 2021; 55: 192-201.
3. Hechtman JE, Liu W, Sadowska J, et al. Sequencing of 279 cancer genes in ampullary carcinoma reveals trends relating to histologic subtypes and frequent amplification and overexpression of ERBB2 (HER2). *Mod Pathol* 2015; 28: 1123-9.
4. Gingras MC, Covington KR, Chang DK, et al. Ampullary cancers harbor ELF3 tumor suppressor gene mutations and exhibit frequent WNT dysregulation. *Cell Rep* 2016; 14: 907-19.
5. Yachida S, Wood LD, Suzuki M, et al. Genomic sequencing identifies ELF3 as a driver of ampullary carcinoma. *Cancer Cell* 2016; 29: 229-40.
6. Kwon MJ, Kim JW, Jung JB, et al. Low incidence of *KRAS*, *BRAF*, and *PIK3CA* mutations in adenocarcinomas of the ampulla of Vater and their prognostic value. *Hum Pathol* 2016; 50: 90-100.

Received: April 28, 2021 Accepted: April 29, 2021

Corresponding Author: Seung-Mo Hong, MD, PhD

Department of Pathology, Asan Medical Center, University of Ulsan College of Medicine, 88 Olympic-ro 43-gil, Songpa-gu, Seoul 05505, Korea
 Tel: +82-2-3010-4558, Fax: +82-2-472-7898, E-mail: smhong28@gmail.com

Prognostic and predictive markers in glioblastoma and ALK overexpression

Jang-Hee Kim

Departments of Pathology, Ajou University School of Medicine, Suwon, Korea

Glioblastoma (GBM) is the most common primary malignant brain tumor with a lethal clinical course [1]. Due to recent advances in medical knowledge and treatment modalities, survival of cancer patients has significantly improved. However, prognosis of patients with GBM remains dismal and less than 5% survive more than 5 years despite aggressive surgical resection and concurrent and adjuvant chemoradiation therapy [1-3]. This is the reason why new therapeutic approaches are urgently needed.

In this issue, Elsens et al. [4] reported anaplastic lymphoma kinase (ALK) and telomerase reverse transcriptase (TERT) expression in GBM and their clinical significance. The authors found ALK overexpression significantly correlated with ALK gene alterations and TERT expression. In addition, ALK and TERT overexpression and ALK gene alterations were associated with poor overall survival (OS) and progression-free survival (PFS), indicating that ALK overexpression could be an additional prognostic marker of GBM.

In GBM patients, age, performance status, extent of surgery, and histologic grade are generally considered prognostic factors [1]. With recent advances in the understanding of molecular pathogenesis of gliomas, certain molecular characteristics of gliomas have been included as prognostic markers [2,5]. Among those molecular alterations, isocitrate dehydrogenase (*IDH*) mutation status is considered as an important prognostic marker for GBM [1,2,5]. *IDH* mutation is typically identified in secondary GBM, which develops from a pre-existing glioma through malignant transformation. Patients with *IDH*-mutant GBM are younger and have a significantly longer survival than patients

with *IDH*-wild type GBM [1,2]. *IDH* is an enzyme involved in the tricarboxylic acid cycle. *IDH* mutations alter enzymatic activity resulting in production of the oncometabolite, 2-hydroxyglutamate, which can cause tumor-driving epigenetic changes [6]. To date, a target agent for mutant *IDH* is not available. However, the development of therapies specific for *IDH* mutations will lead to a fundamental change in the treatment of GBM [5].

The blood brain barrier (BBB) is a major obstacle in the development of new drugs for brain tumors. Most chemotherapeutic drugs cannot penetrate the BBB and only a limited number of drugs can be used in treatment of GBM [3,5]. Temozolomide, an alkylating agent that can penetrate the BBB, is currently included in the standard GBM therapy [1,3,5]. Temozolomide induces alkylation or methylation of DNA frequently at the N⁷- or O⁶-position of guanine residues, which causes cytotoxicity and death of tumor cells. However, tumor cells with O⁶-methylguanine-DNA methyltransferase (MGMT) can remove the DNA alkyl group induced by temozolomide, rendering tumor cells resistant to temozolomide [3]. Therefore, MGMT activity status in GBM is considered an important predictive marker of therapeutic effects caused by alkylating agents. Methylation in the promoter region of MGMT can abolish MGMT activity; therefore, analysis of the methylation status in the promoter region of MGMT is currently performed in GBM patients to predict the response to temozolomide [1-3,5].

ALK is a protein with tyrosine kinase activity and encoded by the ALK gene located on chromosome 2 [7]. ALK gene alterations can promote carcinogenesis [8] and have been reported in various tumors, including anaplastic large cell lymphoma [9], melanoma [8], neuroblastoma [10], and a subset of non-small cell lung carcinoma [11]. The most frequent ALK-related genetic aberrations are translocations [12]. In recent studies, ALK overexpression in GBM reportedly ranged from 30%–70% [4,12,13].

Received: April 27, 2021 Accepted: April 29, 2021

Corresponding Author: Jang-Hee Kim, MD
Department of Pathology, Ajou University School of Medicine, 206 World cup-ro,
Yeongtong-gu, Suwon 16499, Korea
Tel: +82-31-219-5925, Fax: +82-31-219-5934, E-mail: drjhk@ajou.ac.kr

Chiba et al. [14] suggested a possible biological role of ALK in stimulating proliferation and neovascularization in GBM. Dalia et al. [4] showed that ALK overexpression in GBM was significantly associated with proliferation of tumor cells, poor OS, and PFS, indicating a prognostic role in GBM. However, data on the prognostic role of ALK in GBM are very limited and remain controversial [4,12,13]. To properly evaluate the prognostic role of ALK in GBM, further investigative studies with large cohorts are needed.

Chemotherapeutic agents targeting *ALK* genetic alterations (e.g., *EML4-ALK* gene fusion) have been used in clinical practice for treatment of ALK-positive lung cancer and patients showed improved OS and PFS [15]. In GBM, pre-clinical and in vivo studies showed positive outcomes with application of ALK inhibitors in GBM [16-19]. To date, no clinical trials of ALK inhibitors for the treatment of GBM have shown a significant effect on the survival of GBM patients, probably due to low BBB penetration of ALK inhibitors and difficulties in achieving adequate therapeutic concentration in the brain [13,16-19]. However, development of new ALK inhibitors that can penetrate the BBB is ongoing, and if ALK overexpression can predict sensitivity to new ALK inhibitors, ALK overexpression will be an additional important predictive marker in the treatment of GBM.

Ethics Statement

Not applicable.

Availability of Data and Material

Data sharing not applicable to this article as no datasets were generated or analyzed during the study.

Code Availability

Not applicable.

ORCID

Jang-Hee Kim <https://orcid.org/0000-0001-5825-1361>

Conflicts of Interest

J.-H.K., a contributing editor of the *Journal of Pathology and Translational Medicine*, was not involved in the editorial evaluation or decision to publish this article.

Funding Statement

No funding to declare.

References

1. Louis DN, Ohgaki H, Wiestler OD, Cavenee WK. WHO classification of tumours of the central nervous system. Revised 4th ed. Lyon: IARC Press, 2016; 28-56.
2. Eckel-Passow JE, Lachance DH, Molinaro AM, et al. Glioma groups

- based on 1p/19q, *IDH*, and *TERT* promoter mutations in tumors. *N Engl J Med* 2015; 372: 2499-508.
3. Hegi ME, Diserens AC, Gorlia T, et al. *MGMT* gene silencing and benefit from temozolomide in glioblastoma. *N Engl J Med* 2005; 352: 997-1003.
 4. Elsen D, Temerik DF, Attia AM, Hadia A, Hussien MT. Prognostic role of ALK-1 and h-TERT expression in glioblastoma multiforme: correlation with *ALK* gene alterations. *J Pathol Transl Med* 2021; 55: 212-224.
 5. Aldape K, Zadeh G, Mansouri S, Reifenberger G, von Deimling A. Glioblastoma: pathology, molecular mechanisms and markers. *Acta Neuropathol* 2015; 129: 829-48.
 6. Gross S, Cairns RA, Minden MD, et al. Cancer-associated metabolite 2-hydroxyglutarate accumulates in acute myelogenous leukemia with isocitrate dehydrogenase 1 and 2 mutations. *J Exp Med* 2010; 207: 339-44.
 7. Morris SW, Naeve C, Mathew P, et al. ALK, the chromosome 2 gene locus altered by the t(2;5) in non-Hodgkin's lymphoma, encodes a novel neural receptor tyrosine kinase that is highly related to leukocyte tyrosine kinase (LTK). *Oncogene* 1997; 14: 2175-88.
 8. Wiesner T, Lee W, Obenauf AC, et al. Alternative transcription initiation leads to expression of a novel ALK isoform in cancer. *Nature* 2015; 526: 453-7.
 9. Yu R, Chen G, Zhou C, et al. Extra copies of ALK gene locus is a recurrent genetic aberration and favorable prognostic factor in both ALK-positive and ALK-negative anaplastic large cell lymphomas. *Leuk Res* 2012; 36: 1141-6.
 10. Janoueix-Lerosey I, Lopez-Delisle L, Delattre O, Rohrer H. The ALK receptor in sympathetic neuron development and neuroblastoma. *Cell Tissue Res* 2018; 372: 325-37.
 11. Wu SG, Kuo YW, Chang YL, et al. *EML4-ALK* translocation predicts better outcome in lung adenocarcinoma patients with wild-type EGFR. *J Thorac Oncol* 2012; 7: 98-104.
 12. Karagkounis G, Stranjalis G, Argyrakos T, et al. Anaplastic lymphoma kinase expression and gene alterations in glioblastoma: correlations with clinical outcome. *J Clin Pathol* 2017; 70: 593-9.
 13. Franceschi E, De Biase D, Di Nunno V, et al. The clinical and prognostic role of ALK in glioblastoma. *Pathol Res Pract* 2021; 221: 153447.
 14. Chiba R, Akiya M, Hashimura M, et al. ALK signaling cascade confers multiple advantages to glioblastoma cells through neovascularization and cell proliferation. *PLoS One* 2017; 12: e0183516.
 15. Shaw AT, Bauer TM, de Marinis F, et al. First-line lorlatinib or crizotinib in advanced ALK-positive lung cancer. *N Engl J Med* 2020; 383: 2018-29.
 16. Goodwin CR, Rath P, Oyinlade O, et al. Crizotinib and erlotinib inhibits growth of c-Met(+)/EGFRvIII(+) primary human glioblastoma xenografts. *Clin Neurol Neurosurg* 2018; 171: 26-33.
 17. Greish K, Jasim A, Parayath N, et al. Micellar formulations of crizotinib and dasatinib in the management of glioblastoma multiforme. *J Drug Target* 2018; 26: 692-708.
 18. Das A, Cheng RR, Hilbert ML, et al. Synergistic effects of crizotinib and temozolomide in experimental FIG-ROS1 fusion-positive glioblastoma. *Cancer Growth Metastasis* 2015; 8: 51-60.
 19. Le Rhun E, Chamberlain MC, Zairi F, et al. Patterns of response to crizotinib in recurrent glioblastoma according to ALK and MET molecular profile in two patients. *CNS Oncol* 2015; 4: 381-6.

